AN ABSTRACT OF THE THESIS OF

Jeffrey J. Pashak for the degree of Master of Science in Chemical Engineering presented on April 26, 1990.

Title: Design of a Heat Exchanger Network to Challenge Controller Design Methods

Abstract approved: Redacted for Privacy

Dr. Keith L. Levien

A simple heat exchanger network has been studied as an example of a dynamically interactive process. The process is relatively simple, requiring only temperature measurements and flow rate manipulations. Equations are presented for the design of a physical process having a specified steady-state Relative Gain Array and specified dynamic characteristics. Although the physical process is simple, it is shown to be a challenging control problem.

The design equations were used to fit data from existing equipment and to design a simpler configuration which has significant dynamic interactions but only small steady-state interactions. This simple configuration was simulated and the performances of two Proportional-Integral controllers or an Internal Model Controller were compared. Only the IMC controller showed satisfactory control of the process.

Design of a Heat Exchanger Network to Challenge Controller Design Methods

by

Jeffrey J. Pashak

A THESIS

Submitted to

Oregon State University

in partial fulfillment of
the requirements for the
degree of

Master of Science

Completed April 26, 1990

Commencement June 1990

APPROVED:

Redacted for Privacy

Assistant Professor of Chemical Engineering, in charge of major

Redacted for Privacy

Head of Department of Chemical Engineering

Redacted for Privacy

Dean of Graduate School

Date thesis is presented April 26, 1990

ACKNOWLEDGEMENT

I would like to thank Dr. Robert Mrazek for his assistance and guidance through my undergraduate and graduate years in Chemical Engineering. He was always there and ready to give advice on life.

I would like to thank Dr. Keith Levien for his patience and assistance in the completion of this thesis and for his insight as my graduate advisor. I would also like to thank Dr. Gregory Rorrer for sitting on my defense committee at the last minute, Dr. Peter Nelson (Environmental Engineering) and Dr. Chris Biermann (Forest Products) for taking the time to be on my defense committee.

My parents and friends in Shekinah Class deserve many thanks, as they have been supportive in my years in graduate school.

I would especially like to thank the Chemical Engineering Department as a whole for their financial support, without which none of this would have been possible.

TABLE OF CONTENTS

LIST OF FIGURES

LIST OF TABLES

NOMENCLATURE

A1 - heat transfer area of the cold side of the recycle heat exchanger, m^2
A2 - heat transfer area of the hot side of the recycle heat exchanger, m^2
A3 - heat transfer area of the process side of the steam heat exchanger, m^2
Cp - heat capacity, J/kg K
F - full process flow rate, m^3/s
g_{ij} - individual transfer functions
IMC - Internal Model Control
IRC - impulse response coefficient
K - $\frac{\text{steady-state output}}{\text{steady-state input}}$
K_c - PI controller gain
K_u - ultimate gain for Ziegler-Nichols tuning
M - imput suppression parameter for IMC tuning
N - number of impulse response coefficients used for IMC tuning
ODE - ordinary differential equation
P - optimization horizon for IMC tuning
PI - Proportional-Integral
P_u - ultimate period for Ziegler-Nichols tuning
R1-8 - RTS ratios numbers 1-8, Table 36
RGA - Relative Gain Array
RPZ - slowest pole to most significant zero ratio
RTS - gain ratio of the transfer functions with manipulated variable TS, g_{22}/g_{12}
RX - gain ratio of the transfer functions with manipulated variable X, g_{21}/g_{11}
T - sampling time for IMC tuning
T1 - temperature of the fluid leaving the cold side of the recycle heat exchanger, °C
T2 - temperature of the fluid leaving the hot side of the recycle heat exchanger, °C
TAU - time delay for IMC tuning
t_d - elapsed time befor system response for Cohen-Coon tuning
TF - temperature of the product stream, °C
TF/X - transfer function of temperature TF for a change in X
TF/TS- transfer function of temperature TF for a change in TS
TH - temperature of the process fluid leaving the steam heat exchanger, °C
TH/X - transfer function of temperature TH for a change in X
TH/TS- transfer function of temperature TH for a change in TS

TI - temperature of the inlet stream, °C
TS - temperature of the steam, °C
u - input variable vector
U1 - recycle heat exchanger overall heat transfer coefficient, W/m^2 K
U2 - recycle heat exchanger overall heat transfer coefficient, W/m^2 K
U3 - steam heat exchanger overall heat transfer coefficient, W/m^2 K
V1 - volume of the cold side of the recycle heat exchanger, m^3
V2 - volume of the hot side of the recycle heat exchanger, m^3
V3 - volume of the process side of the steam heat exchanger, m^3
X - fraction of process flow to the recycle heat exchanger
y - output variable vector
Y - lumped parameter for the steam heat exchanger comprised of U3 * A3 / (ρ * Cp), m^3/s
z - state variable vector
Z - lumped parameter for the recycle heat exchanger comprised of U1 * A1 / (ρ * Cp), m^3/s
β_i - input penalty parameter matrix for IMC tuning
γ_i - output penalty parameter for IMC tuning
λ_{11} - (1,1) element of the Relative Gain Array
ρ - fluid density, kg/m^3
τ - time constant for Cohen-Coon tuning
τ_i - integral time constant

DESIGN OF A HEAT EXCHANGER NETWORK TO CHALLENGE CONTROLLER DESIGN METHODS

CHAPTER 1 - INTRODUCTION

The current industrial climate of demanding environmental and economic constraints has resulted in dynamically interacting control loops and difficult process control design problems. In general, tighter control on a process leads to more dynamic interactions, particularly in coupled heat and mass transfer operations with recycled streams. Because interactions are so prevalent in industry, experiments in the control of a process with significant dynamic interactions should be included in undergraduate laboratories for chemical engineers.

The most commonly discussed dynamically interactive process model in the chemical engineering literature has been the distillation column. Some reasons for its popularity are that it is used frequently in industry and has complex dynamics. These complexities include coupled heat and mass transfer, nonlinear behavior, time varying parameters and high order dynamics, and make modeling very difficult. However, due to its slow dynamics, high cost and complexities of operation, few departments operate a pilot plant scale distillation column as a process control experiment.

The simplest process model that can have dynamic interactions is one with two inputs and two outputs. Although steady-state theory may indicate little interaction exists in a process, recent studies suggest that dynamic interactions are also important and must be considered (Jensen et al, 1986; Economou and Morari, 1986; Grosdidier and Morari, 1986 and Mijares et al, 1986).

The main goal of this thesis is to show that it is possible to design an interactive process, consisting of physically simple heat exchangers (Figure 1), that is difficult to control using traditional control algorithms. A concurrent goal is to show that this simple process, in which only temperatures are measured and flow rates are manipulated, can be designed to have strong dynamic interactions even though its Relative Gain Array (RGA) shows little steady-state interactions.

Throughout this thesis the term "process" is used to refer to the nonlinear model of the physical equipment and the term "system" is used to refer to the linear transfer function description of the process, i.e. gains, poles and zeros. Usually a process control project begins with the description of a process, the system parameters are determined and finally a control scheme which yields adequate performance is found. Relationships derived here make it possible to start

HEAT EXCHANGER NETWORK

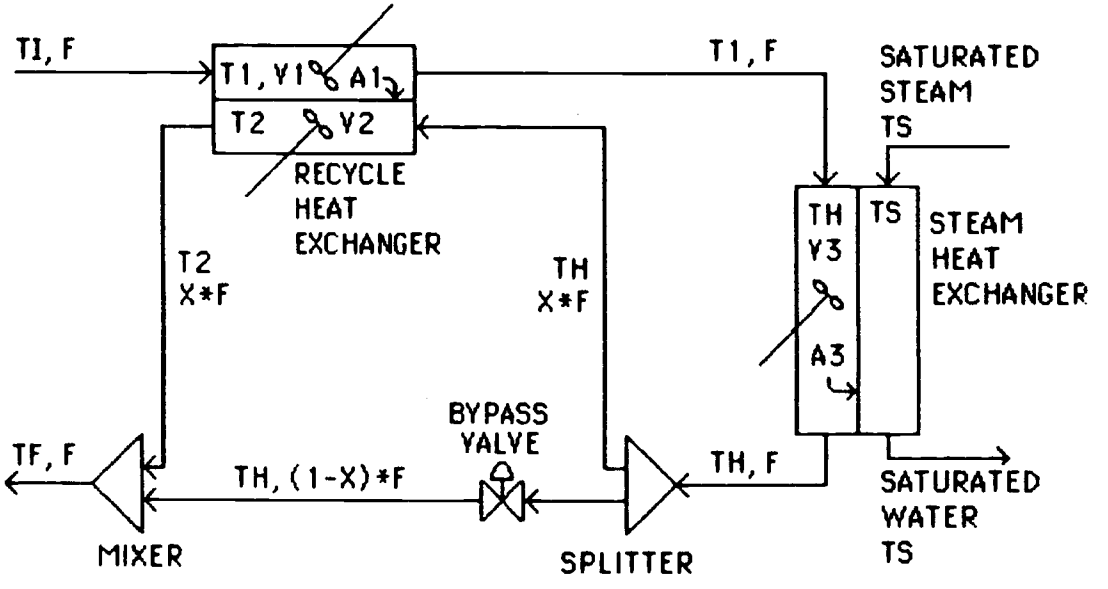

Fig. 1. Heat exchanger network

with the desired system parameters and determine a set of required process parameters to obtain a desired transfer function (Figure 2).

This thesis is organized into four chapters followed by conclusions:

1) Derivation of a fundamental transfer function model for a simple process
2) Application of the fundamental model to published dynamic data from a similar process (Lee & Levien, 1986)
3) Determination of a "reasonable" laboratory scale design to exhibit small steady-state interactions and large dynamic interactions
4) Comparison of the closed loop performance of two PI controllers with that obtained by using a multivariable Internal Model Controller.

Sensitivity of the system parameters to the process design is shown in Appendix A.

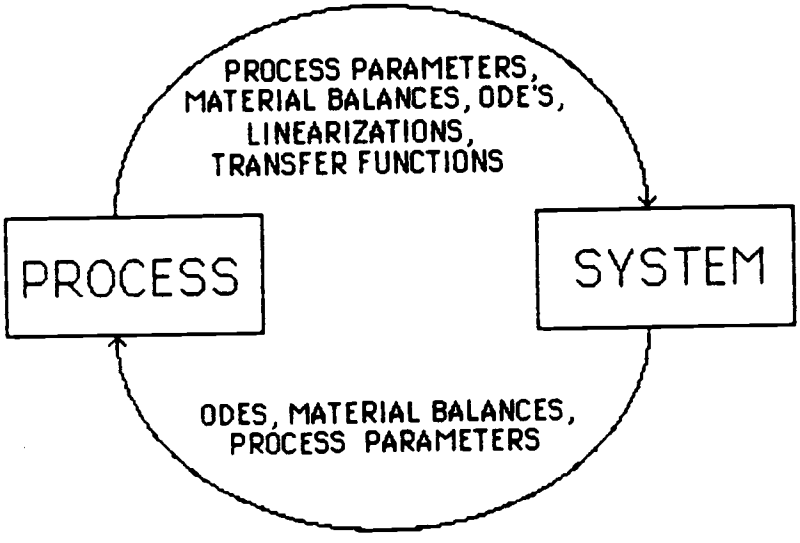

Fig. 2. Process and system diagram

CHAPTER 2 - DERIVATION OF A FUNDAMENTAL TRANSFER FUNCTION MODEL

This chapter describes the process diagram (Figure 1) and the fundamental model in terms of the process parameters (Table 1). The process dynamics were simplified for this study by replacing the countercurrent and plate heat exchangers used by Callaghan, Lee and Newell (1988) with stirred tank heat exchangers and by neglecting dead time so the model is made up of ordinary differential equations (ODEs).

At this point it may be helpful to trace the flow of fluid through the process diagram (Figure 1). The process fluid enters at the top left of the diagram and passes through the cold side of the recycle heat exchanger, where it is warmed by the fluid which has been recycled to the hot side of this heat exchanger. The process fluid continues through the process side of the steam heat exchanger where it is further heated. After leaving the steam heat exchanger, the fluid is split and a fraction of the flow is sent to the hot side of the recycle heat exchanger while the rest of the flow passes through the bypass line. The two streams are mixed and form the product stream, which leaves the process at the bottom left of the diagram. It is important to realize that the only source of external

Table 1. The nineteen original process parameters and variables

Note: Control volumes are shown in Figure 3

Fluid Parameters -	ρ	- fluid density
	Cp	- fluid heat capacity
Heat Exchanger Parameters -	U1	- heat transfer coefficient for control volume 1
	U2	- heat transfer coefficient for control volume 2
	U3	- heat transfer coefficient for control volume 3
	A1	- heat transfer area for control volume 1
	A2	- heat transfer area for control volume 2
	A3	- heat transfer area for control volume 3
	V1	- volume of heat exchanger in control volume 1
	V2	- volume of heat exchanger in control volume 2
	V3	- volume of heat exchanger in control volume 3
Constant Inlet Flow Parameters -	F	- full process flow rate
	TI	- inlet temperature of the process fluid
State Variables -	T1	- process fluid temperature out of the full process flow side of the recycle heat exchanger
	T2	- process fluid temperature out of the recycle process flow side of the recycle heat exchanger
Manipulated Variables -	X	- fraction of process flow recycled to the recycle heat exchanger
	TS	- temperature of saturated steam in the steam heat exchanger
Output Variables -	TF	- final temperature out of process
	TH	- process side temperature in the steam heat exchanger

energy to the process is from the steam heat exchanger and the bypass valve simply redistributes the heat within the process.

The heat exchanger network model contains 19 process parameters and variables which can be arranged into six groups: fluid parameters, heat exchanger parameters, constant inlet flow parameters, state variables, manipulated variables and output variables (Table 1). In order to make a comparison with previous modeling, Lee and Levien (1986), the manipulated variables of the process were chosen to be the fraction of hot fluid recycled through the recycle heat exchanger (X) and the temperature of the steam into the steam heat exchanger (TS). These correspond to manipulating the bypass valve and the steam valve, respectively, in Lee and Levien. The outputs of the process were the same as the Lee and Levien process: the product temperature of the process (TF) and the temperature of the process side of the steam heat exchanger (TH). The states were chosen to be the temperature of the process flow side (cold) of the recycle heat exchanger (T1), the temperature of the recycle process flow side (hot) of the recycle heat exchanger (T2) and the temperature of the process side of the steam heat exchanger (TH, also one of the outputs).

Because relatively small temperature changes occur

within this process with water as the process fluid, fluid density was assumed to be constant. The fundamental model consists of four ODEs (Table 2) which represent material and energy balances around four control volumes (Figure 3) defined for the process. The first control volume contains the full process flow (cold) side of the recycle heat exchanger and results in the first equation in Table 2. The second control volume contains the recycle process flow (hot) side of the recycle heat exchanger and results in the second equation in Table 2. The third equation in Table 2 represents the third control volume which contains the process side of the steam heat exchanger. The fourth control volume contains the mixing point which produces the product stream and is represented by the fourth equation in Table 2. Since transportation lags can be designed to be negligible, no dead time appears in the equations in Table 2. This may not always be the case and transportation lags can be readily determined by knowing the flow rate through the pipe and the pipe dimensions. The effects of including dead times in the transfer functions remains a topic for future study.

The number of parameters can be decreased from 19 to 13 (Table 3) by appropriate combinations to produce the new parameters Z and Y and because A1 = A2 and U1 = U2. Parameters Z and Y can be used because each

Table 2. Ordinary differential equations from material and energy balances

From control volume 1:

1. $$V1\,\rho\,Cp\,\frac{dT1}{dt} = F\,\rho\,Cp\,TI + U1\,A1\,(T2 - T1) - F\,\rho\,Cp\,T1$$

From control volume 2:

2. $$V2\,\rho\,Cp\,\frac{dT2}{dt} = F\,X\,\rho\,Cp\,TH - U1\,A1\,(T2 - T1) - F\,X\,\rho\,Cp\,T2$$

From control volume 3:

3. $$V3\,\rho\,Cp\,\frac{dTH}{dt} = F\,\rho\,Cp\,T1 + U3\,A3\,(TS - TH) - F\,\rho\,Cp\,TH$$

From control volume 4:

4. $$F\,\rho\,Cp\,TF = F\,X\,\rho\,Cp\,T2 + F\,(1 - X)\,\rho\,Cp\,TH$$

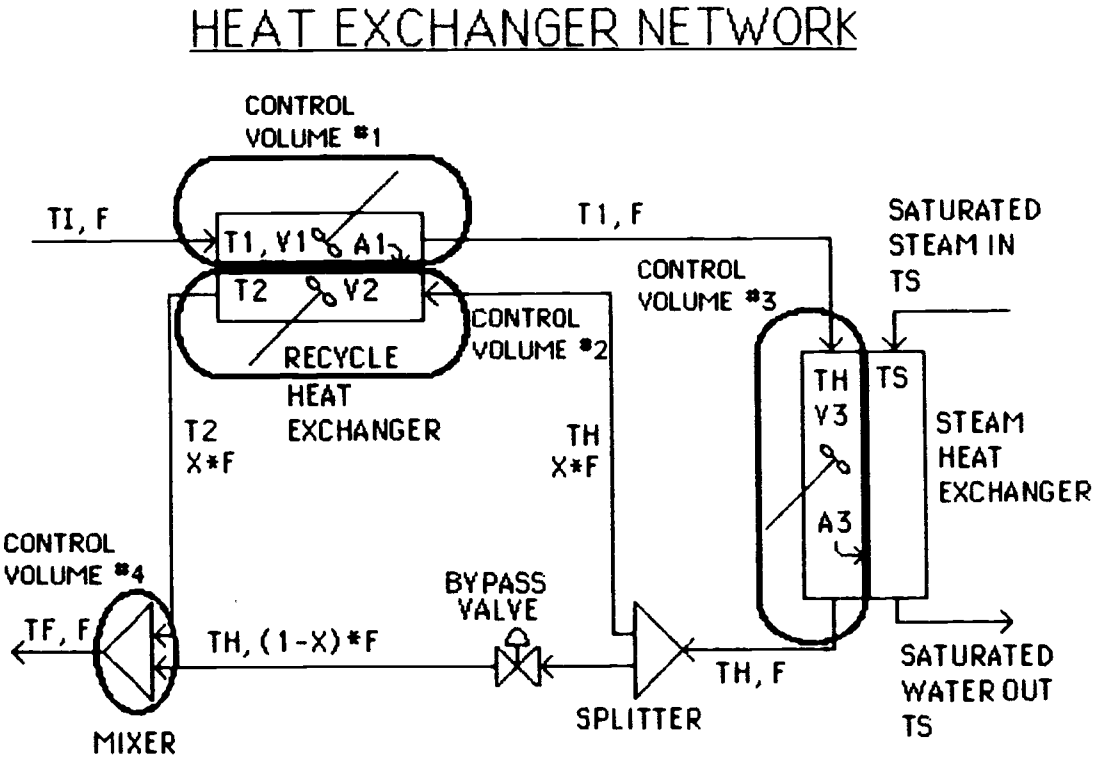

Fig. 3. Control volumes for material and energy balances

Table 3. The thirteen required process parameters and variables

Note: Control volumes are shown in Figure 3.

Heat Exchanger Parameters -

- Z - lumped parameter for recycle heat exchanger $Z = \frac{U1\ A1}{\rho\ Cp}$
- Y - lumped parameter for steam heat exchanger $Y = \frac{U3\ A3}{\rho\ Cp}$
- V1 - volume of heat exchanger in control volume 1
- V2 - volume of heat exchanger in control volume 2
- V3 - volume of heat exchanger in control volume 3

Note: A1 and A2 describe the same heat transfer area and U1 and U2 describe the same heat transfer resistance.

Constant Inlet Flow Parameters -

- F - full process flow rate
- TI - inlet temperature of the process fluid

State Variables -

- T1 - process fluid temperature out of the full process flow side of the recycle heat exchanger
- T2 - process fluid temperature out of the recycle process flow side of the recycle heat exchanger

Manipulated Variables -

- X - fraction of process flow recycled to the recycle heat exchanger
- TS - temperature of saturated steam in the steam heat exchanger

Output Variables -

- TF - final temperature out of process
- TH - process side temperature of the steam heat exchanger

of these combinations of variables appear in the equations as a group. After substitution, two of the resulting ODEs are nonlinear and must be linearized to obtain transfer function models. The nonlinearity is of the product form, that is, the product of an input (X) and a state (TH or T2). The four equations are written in deviation variable form and then Laplace transformed.

Equations 1 through 3 can be manipulated into an explicit form for the state derivative as a function of the other variables (Table 4). Equation 4 is algebraic and can be arranged as an expression for TF (Table 4). Substitutions (Table 5) were performed to further simplify manipulations to obtain the transfer functions of Table 6.

Equations 1 and 2 of Table 6 were set into the matrix form

$$Az = Bu + Cy \tag{1}$$

where z, u and y are the vectors of intermediate variables, input variables and output variables, respectively. Solving for z yields (Table 7a)

$$z = A^{-1}Bu + A^{-1}Cy. \tag{2}$$

Equations 3 and 4 of Table 6 were set into the

Table 4. Linearized Laplace equations

1. $$\overline{T1} = \frac{\frac{Z}{F + Z}}{\left(\frac{V1}{F + Z}\right)s + 1}\overline{T2}$$

2. $$\overline{T2} = \frac{\frac{F\,X}{F\,X + Z}}{\left(\frac{V2}{F\,X + Z}\right)s + 1}\overline{TH} + \frac{\frac{F\,(TH - T2)}{F\,X + Z}}{\left(\frac{V2}{F\,X + Z}\right)s + 1}\bar{X}$$

$$+ \frac{\frac{Z}{F\,X + Z}}{\left(\frac{V2}{F\,X + Z}\right)s + 1}\overline{T1}$$

3. $$\overline{TH} = \frac{\frac{F}{F + Y}}{\left(\frac{V3}{F + Y}\right)s + 1}\overline{T1} + \frac{\frac{Y}{F + Y}}{\left(\frac{V3}{F + Y}\right)s + 1}\overline{TS}$$

4. $$\overline{TF} = X\,\overline{T2} + (T2 - TH)\,\bar{X} + (1 - X)\,\overline{TH}$$

Table 5. Substitutions for linearized Laplace equations

$$h1 = \frac{\frac{Z}{F + Z}}{\left(\frac{V1}{F + Z}\right)s + 1}$$

$$h2 = \frac{\frac{F\,X}{F\,X + Z}}{\left(\frac{V2}{F\,X + Z}\right)s + 1}$$

$$h3 = \frac{\frac{F\,(TH - T2)}{F\,X + Z}}{\left(\frac{V2}{F\,X + Z}\right)s + 1}$$

$$h4 = \frac{\frac{Z}{F\,X + Z}}{\left(\frac{V2}{F\,X + Z}\right)s + 1}$$

$$h5 = \frac{\frac{F}{F + Y}}{\left(\frac{V3}{F + Y}\right)s + 1}$$

$$h6 = \frac{\frac{Y}{F + Y}}{\left(\frac{V3}{F + Y}\right)s + 1}$$

$$h7 = X$$

$$h8 = (T2 - TH)$$

$$h9 = (1 - X)$$

Table 6. Laplace equations after substitution

1. $\overline{T1} = h1\ \overline{T2}$

2. $\overline{T2} = h2\ \overline{TH} + h3\ \overline{X} + h4\ \overline{T1}$

3. $\overline{TH} = h5\ \overline{T1} + h6\ \overline{TS}$

4. $\overline{TF} = h7\ \overline{T2} + h8\ \overline{X} + h9\ \overline{TH}$

Table 7a. State equation in matrix form

$$\begin{bmatrix} \overline{T1} \\ \overline{T2} \end{bmatrix} = \frac{\begin{bmatrix} h1\ h3 & 0 \\ h3 & 0 \end{bmatrix}}{1 - h1\ h4} \begin{bmatrix} \overline{X} \\ \overline{TS} \end{bmatrix} + \frac{\begin{bmatrix} h1\ h2 & 0 \\ h2 & 0 \end{bmatrix}}{1 - h1\ h4} \begin{bmatrix} \overline{TH} \\ \overline{TF} \end{bmatrix}$$

Table 7b. Output equation in matrix form

$$\begin{bmatrix} \overline{TH} \\ \overline{TF} \end{bmatrix} = \begin{bmatrix} h5 & 0 \\ h5\ h9 & h7 \end{bmatrix} \begin{bmatrix} \overline{T1} \\ \overline{T2} \end{bmatrix} + \begin{bmatrix} 0 & h6 \\ h8 & h6\ h9 \end{bmatrix} \begin{bmatrix} \overline{X} \\ \overline{TS} \end{bmatrix}$$

Table 7c. Final output equation in matrix form

$$\begin{bmatrix} \overline{TF} \\ \overline{TH} \end{bmatrix} = \begin{bmatrix} g_{11} & g_{12} \\ g_{21} & g_{22} \end{bmatrix} \begin{bmatrix} \overline{X} \\ \overline{TS} \end{bmatrix}$$

where

$$g_{11} = \frac{h8 - h1\ h4\ h8 - h1\ h2\ h5\ h8 + h1\ h3\ h5\ h9 + h3\ h7}{1 - h1\ h4 - h1\ h2\ h5}$$

$$g_{12} = \frac{h6\ h9 + h2\ h6\ h7 - h1\ h4\ h6\ h9}{1 - h1\ h4 - h1\ h2\ h5}$$

$$g_{21} = \frac{h1\ h3\ h5}{1 - h1\ h4 - h1\ h2\ h5}$$

$$g_{22} = \frac{h6 - h1\ h4\ h6}{1 - h1\ h4 - h1\ h2\ h5}$$

matrix form

$$C'y = B'u + A'z \tag{3}$$

where z, u and y are the vectors of intermediate variables, input variables and output variables, respectively. Solving for y yields (Table 7b)

$$y = C'^{-1}B'u + C'^{-1}A'z. \tag{4}$$

Substituting equation (2) into (4) yields

$$y = C'^{-1}B'u + C'^{-1}A'(A^{-1}Bu + A^{-1}Cy) \tag{5}$$

$$= (C'^{-1}B' + C'^{-1}A'A^{-1}B)u + C'^{-1}A'A^{-1}Cy. \tag{6}$$

Therefore,

$$y = (I - C'^{-1}A'A^{-1}C)^{-1}(C'^{-1}B' + C'^{-1}A'A^{-1}B)u \tag{7}$$

is the transfer function matrix between the outputs and the inputs (Table 7c). The individual transfer functions can be obtained from the matrix form to find the response of a single output given a change in one of the inputs. After back substitution of the process parameters into the transfer functions and simplification, it is possible to see the effect each of the individual process parameters has on the transfer functions (Tables 8a and 8b).

Table 9 shows the transfer functions of Lee and Levien. In Tables 8a and 9 the transfer functions TH/X

Table 8a. Transfer functions with process parameters and variables

For the matrix form

$$\begin{bmatrix} \overline{TF} \\ \overline{TH} \end{bmatrix} = \begin{bmatrix} g_{11} & g_{12} \\ g_{21} & g_{22} \end{bmatrix} \begin{bmatrix} \overline{X} \\ \overline{TS} \end{bmatrix}$$

The transfer functions are of the general form

$$g_{i,j} = \frac{C4\ [C3\ s^3 + C2\ s^2 + C1\ s + C0]}{D3\ s^3 + D2\ s^2 + D1\ s + D0}$$

For i = 1, j = 1

$C4 = -(TH - T2)$

$C3 = V1\ V2\ V3$

$C2 = V1\ V2\ (F + Y) + V1\ V3\ Z + V2\ V3\ (F + Z)$

$C1 = V1\ Z\ (F + Y) + V2\ (F + Z)\ (F + Y) + V3\ F\ Z$

$C0 = F\ Z\ Y$

For i = 1, j = 2

$C4 = C3 = 0$

$C2 = (1 - X)\ Y\ V1\ V2$

$C1 = V1\ Y\ (F\ X + Z - ZX) + V2\ Y\ (F + Z)\ (1-X)$

$C0 = F^2\ X\ Y + F\ Z\ Y$

For all i,j

$D3 = V1\ V2\ V3$

$D2 = V1\ V2\ (F + Y) + V1\ V3\ (F\ X + Z) + V2\ V3\ (F + Z)$

$D1 = V1\ (F\ X + Z)\ (F + Y) + V2\ (F + Z)\ (F + Y) + V3\ [F^2\ X + F\ Z\ (1 + X)]$

$D0 = F^3\ X + F^2\ (X\ Y + Z) + F\ Z\ Y\ (1 + X)$

* parameters defined in Table 3

Table 8b. Transfer functions with process parameters and variables (cont.)

For the matrix form

$$\begin{bmatrix} \overline{TF} \\ \overline{TH} \end{bmatrix} = \begin{bmatrix} g_{11} & g_{12} \\ g_{21} & g_{22} \end{bmatrix} \begin{bmatrix} \overline{X} \\ \overline{TS} \end{bmatrix}$$

The transfer functions are of the general form

$$g_{i,j} = \frac{C4\ [C3\ s^3 + C2\ s^2 + C1\ s + C0]}{D3\ s^3 + D2\ s^2 + D1\ s + D0}$$

For i = 2, j = 1

$$C4 = C3 = C2 = C1 = 0$$

$$C0 = (TH - T2)\ F^2\ Z$$

For i = 2, j = 2

$$C4 = C3 = 0$$

$$C2 = V1\ V2\ Y$$

$$C1 = V1\ Y\ (F\ X + Z) + V2\ Y\ (F + Z)$$

$$C0 = F^2\ X\ Y + F\ Z\ Y\ (1 + X)$$

For all i,j

$$D3 = V1\ V2\ V3$$

$$D2 = V1\ V2\ (F + Y) + V1\ V3\ (F\ X + Z) + V2\ V3\ (F + Z)$$

$$D1 = V1\ (F\ X + Z)\ (F + Y) + V2\ (F + Z)\ (F + Y) + V3\ [F^2\ X + F\ Z\ (1 + X)]$$

$$D0 = F^3\ X + F^2\ (X\ Y + Z) + F\ Z\ Y\ (1 + X)$$

* parameters defined in Table 3

Table 9. Lee and Levien transfer functions based on a 5 second sample time

For the matrix form

$$\begin{bmatrix} \overline{TF} \\ \overline{TH} \end{bmatrix} = \begin{bmatrix} g_{11} & g_{12} \\ g_{21} & g_{22} \end{bmatrix} \begin{bmatrix} \overline{X} \\ \overline{TS} \end{bmatrix}$$

The transfer functions are of the general form

$$g_{i,j} = \frac{e^{-ds}(C1\ s + C0)}{D2\ s^2 + D1\ s + D0}$$

For i = 1, j = 1

d = 2.4	D2 = 14.5
C1 = 68.53	D1 = 9.4
C0 = 0.89	D0 = 1

For i = 1, j = 2

d = 2.8	D2 = 0
C1 = 0	D1 = 12.3
C0 = 6.8	D0 = 1

For i = 2, j = 1

d = 5.1	D2 = 0
C1 = 0	D1 = 6.7
C0 = -7.2	D0 = 1

For i = 2, j = 2

d = 2.9	D2 = 62.2
C1 = 91.91	D1 = 23
C0 = 9.1	D0 = 1

and TF/X occur with opposite signs. However, Table 8a shows the negative sign on the TF/X transfer function while Table 9 shows the negative sign on the TH/X transfer function. In the fundamental model, increasing the X signal results in an increased fraction of the total flow to the recycle process flow side of the recycle heat exchanger. In the Lee and Levien paper, an increase in the physical X signal results in a decrease in this flow. The important thing to notice is that the transfer functions for TH/X and TF/X have opposite signs in both the fundamental model and the Lee and Levien model.

The fact that the signs must be opposite can be seen by looking at Figure 4 for two limiting cases. At steady state, the maximum heat transferred to the process, and therefore the greatest final output temperature, TF, will occur when the temperature differential across the steam heat exchanger is the greatest. For any given steam temperature, this occurs when there is no flow to the recycle heat exchanger, that is X = 0. By examination of Figures 1 and 4, with no recycle temperature TF will be equal to temperature TH. This is the lowest possible value for temperature TH, as the temperature into the steam heat exchanger, T1, will be at its minimum temperature, i.e., the inlet temperature, TI. When the entire process flow is

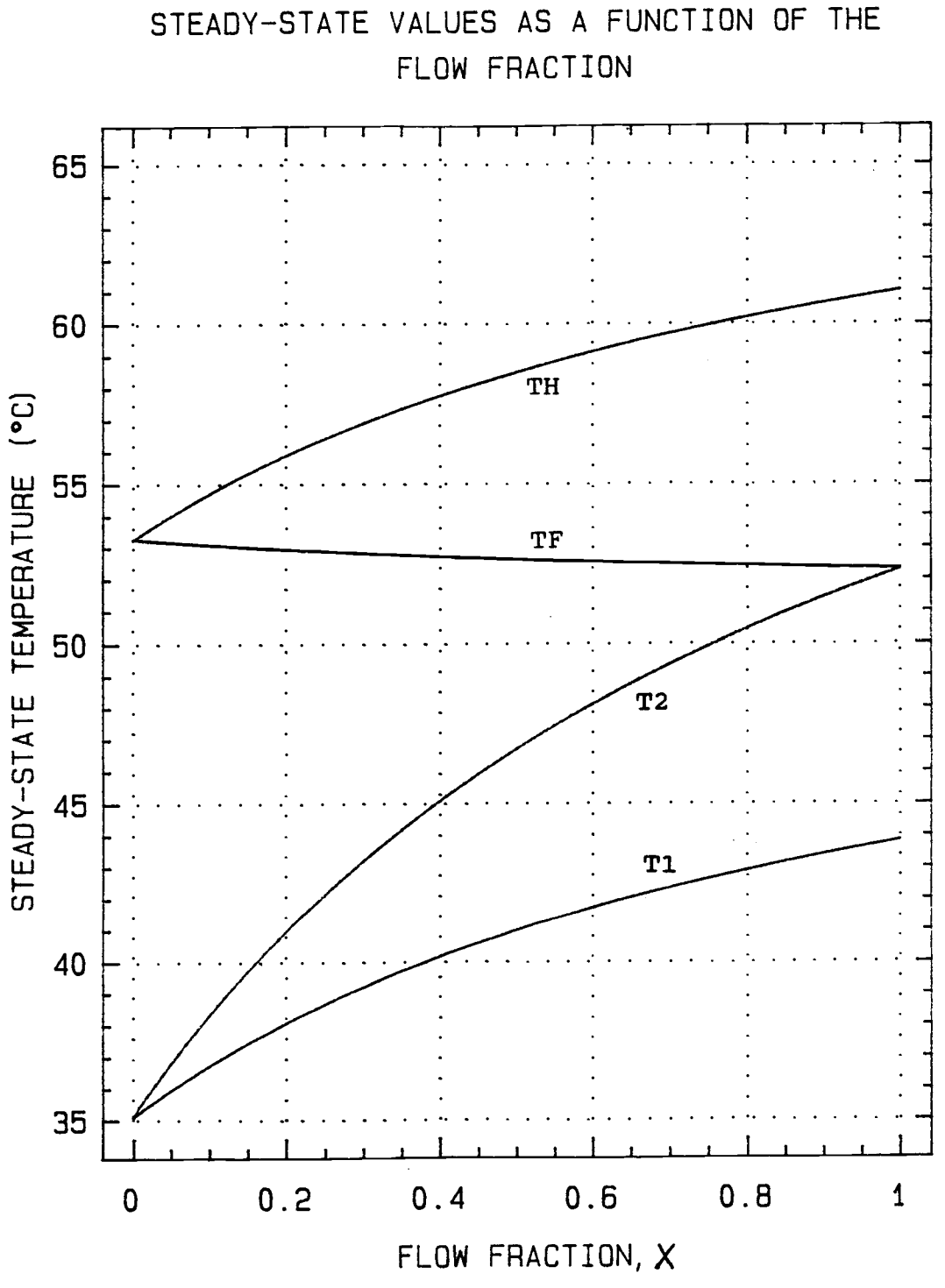

Fig. 4. Steady-state design temperatures as a function of the flow fraction

recycled, that is X = 1, Figure 4 shows the result is the minimum value of the final output temperature, TF, and the maximum value of temperature TH. This occurs because all of the process fluid is passed through the recycle heat exchanger and has transferred the maximum amount of heat to the cold inlet fluid preheating temperature T1 to its maximum value, resulting in the greatest possible temperature TH. To summarize, as the recycle flow fraction (X) increases, temperature TF decreases while temperature TH increases, thus explaining the opposite signs on the transfer functions.

REMARKS

1. The overall energy input to the process comes only from the steam heat exchanger and the bypass valve serves to simply redistribute the heat within the process.

2. The transfer function gains of TF/X and TH/X must have opposite signs because of the opposite effects of an increase in the recycle flow fraction on temperatures TF and TH.

3. For the fundamental model, all four of the transfer functions have the same third order denominator and thus all have the same poles. Therefore, any differences in responses are caused by the different

gains and zeros. The lower order experimental transfer functions of Lee and Levien have four different denominators which were determined by fitting the equations to the data.

4. The large overshoot of the response of TF to X makes this process interesting. The steady-state change is only a fraction of the maximum change which occurs. This large initial deviation of the response was found to be sensitive to process design parameters and forms the basis for creating a complex controller problem.

CHAPTER 3 - MATCHING THE FUNDAMENTAL TRANSFER FUNCTION TO THE EXPERIMENTAL TRANSFER FUNCTION

The purpose of this chapter is to see if dynamic step responses similar to those of the Lee and Levien experimental data (Figure 5) could be obtained from the fundamental model. Certain process parameter values and steady-state conditions (Table 10a) were kept as close as possible to the values reported by Lee and Levien. When process parameters were unknown, "reasonable" values were chosen (Table 10b). Reasonable is a relative term: here it is taken as meaning values which lead to positive heat transfer areas and/or areas that are viable for a given volume. When any process parameter was found to be infeasible for the fundamental model, adjustments to all parameters were made by trial and error to find a complete set of reasonable process parameters.

The fitting process was organized in three phases:

Phase 1) attempt to match the Lee and Levien process parameters - this phase yielded negative heat transfer areas and/or negative process temperatures

Phase 2a) match the experimental RGA and therefore the ratio of the transfer function gains

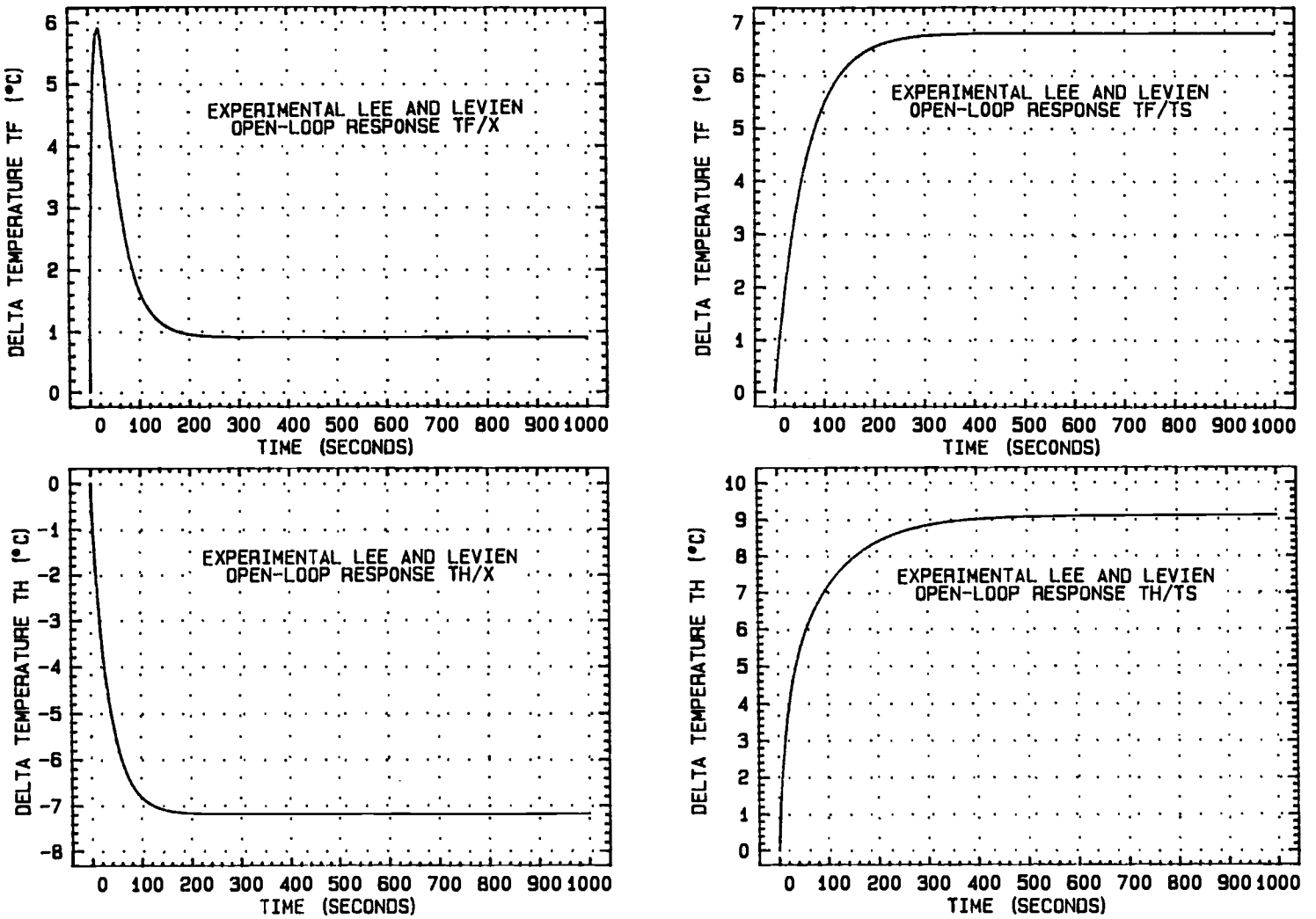

Fig. 5. Experimental transfer function open-loop responses to unit step changes in the manipulated variables

Table 10a. Table of known (fixed) process parameters and conditions from Lee and Levien

T1 = 35 °C	A3 = 0.099 m^2
TH = 68 °C	ρ = 1000 Kg / m^3
TF = 59 °C	Cp = 4186 J / Kg K
TS = 186 °C	X = 0.5
V1 = V2 = 0.04 m^3	V3 = 0.00973 m^3

Table 10b. Table of fitted process parameters and conditions

T1 = 28 °C	A3 = 0.099 m^2
TH = 75 °C	ρ = 1000 Kg / m^3
TF = 59.114 °C	Cp = 4186 J / Kg K
TS = 455.183 °C	X = 0.5
V1 = V2 = 0.04 m^3	V3 = 0.00973 m^3

Phase 2b) maintain the general shape of the experimental response curves (ignoring dead time in the data)

Phase 3) approach the experimental ratio of the slowest pole to the most significant zero in the TF/X transfer function.

The original process parameters and variables (Table 1) were used in the fitting process. There were four steady-state temperatures known from the Lee and Levien paper. These "target" temperatures were T1, TH, TF and TS (Table 10a). The heat transfer area of the countercurrent steam heat exchanger (A3) was also known. The fluid was known to be water for which the density and heat capacity were easily estimated (Welty, et al.). These temperatures and the heat transfer area yielded negative heat transfer areas, negative process temperatures, temperatures out of the recycle heat exchanger lower than the process inlet temperature or heat transfer areas too large for a given heat exchanger volume when applied to the steady-state material and energy balances (Tables 11a and 11b).

The individual transfer function gains of the Lee and Levien paper could not be matched due to unknown conversions between the voltage signals to the control valves and the steam temperature or the flow rate of fluid bypassing the recycle heat exchanger. The

Table 11a. Steady-state mass and energy balance equations for the heat exchanger network

1. $TI - T1 + \frac{U1\ A1}{F\ \rho\ CP} (T2 - T1) = 0$

2. $TH - T2 = \frac{U1\ A1}{F\ X\ \rho\ CP} (T2 - T1)$

3. $T1 - TH + \frac{U2\ A2}{F\ \rho\ CP} (TS - TH) = 0$

4. $TF = X\ T2 + (1 - X)\ TH$

Table 11b. Revised steady-state mass and energy balance equations with the combined parameters for the heat exchanger network

1. $TI - T1 + \frac{Z}{F} (T2 - T1) = 0$

2. $TH - T2 = \frac{Z}{F\ X} (T2 - T1)$

3. $T1 - TH + \frac{Y}{F} (TS - TH) = 0$

4. $TF = X\ T2 + (1 - X)\ TH$

experimental transfer functions are in units of degrees per volt while the fundamental transfer functions derived in this work are in degrees per fraction of flow recycled and degrees per degree for X and TS, respectively. Although the effects of input changes, measured in volts, on both the flow control valve and steam control valve were unknown, it was decided to maintain the ratio of the two gains, which is dimensionless, for each manipulated variable. Although this procedure ignores process dynamics introduced by the control valve transducers, the unknown conversion from volts to valve opening or volts to steam temperature cancel out. Using these ratios is shown to be acceptable as they are included in the equation for the (1,1) element of the Relative Gain Array (RGA) below. Although this procedure does not allow a direct comparison of individual gains, the RGA for the experimental and fundamental model can be made to be the same since the (1,1) element of the RGA can be written

$$\lambda_{11} = \frac{1}{1 - \frac{(g_{21})}{(g_{11})} * \frac{(g_{12})}{(g_{22})}} = \frac{1}{1 - \frac{RX}{RTS}} \qquad (8)$$

where RX is defined as g_{21}/g_{11} and RTS is defined as g_{22}/g_{12}. Therefore, two 2 X 2 systems having the same gain ratios and/or ratio of gain ratios will have the

same RGA.

Since phase 1 of the fitting process yielded infeasible process parameters, a spreadsheet was used to investigate perturbations of the target steady-state temperatures (T1, TH, TF and TS) while maintaining the gain ratios. The initial (experimental) and final values for the target temperatures and other known process parameters are shown in Table 10b. These gain ratios were found to be -8.089 and 1.338 for the flow fraction (RX) and steam temperature (RTS), respectively. The gain ratios were also found to be only a function of the four target temperatures, as shown in Table 12. Once these four temperatures were determined it was possible to calculate the inlet temperature, TI, using equation 1 of Table 13. Also from the four target temperatures and the steam heat exchanger area (A3), the ratio of overall heat transfer coefficient to flow rate (U3/F) was fixed using equation 2 of Table 13. The range of overall heat transfer coefficients for different types of heat exchangers was found from Welty, et al (1976). The average values of the range for steam to water (2800 W / m^2 K) and water to water (1250 W / m^2 K) heat exchangers were used. The nominal operating value of the fraction of flow to the recycle heat exchanger, X, was chosen to be in the middle of the operating range (0.5). These values allowed the

Table 12. Equations for the transfer function gain ratios

$$\text{Steam temperature ratio} = RTS = \frac{2\,TH - T1 - TF}{TH - T1}$$

$$\text{Flow fraction ratio} = RX = \frac{-(TS - TH)}{(TH - T1)}$$

Table 13. Equations used to fit the various process parameters

1. The inlet temperature into the network.

$$TI = T1 + TF - TH$$

2. The steam heat exchanger heat transfer coefficient to flow rate ratio.

$$\frac{U3}{F} = \frac{\rho\, CP\, (TH - T1)}{A3\, (TS - TH)}$$

3. The temperature out of the hot side of the recycle heat exchanger.

$$T2 = \frac{TF - (1 - X)\, TH}{X}$$

4. The overall flow rate into the network.

$$F = \frac{U3\, A3\, (TS - TH)}{\rho\, CP\, (TH - T1)}$$

5. The combined recycle heat exchanger heat transfer parameter.

$$Z = \frac{F\, X\, (TH - T2)}{(T2 - T1)}$$

calculation of the temperature out of the hot side of the recycle heat exchanger (T2) using equation 3 of Table 13, the process flow rate through the network (F) using equation 4 of Table 13, and the lumped parameter for the recycle heat exchanger, Z, using equation 5 of Table 13. From these thirteen values, all of the model transfer function gains can be calculated and the gain ratios can be compared to the experimental ratios.

The remaining parameters, the heat exchanger volumes V1, V2 and V3, determine the dynamic parts of the transfer functions, i.e., the system poles and zeros. Volume V3 was fixed at the experimental countercurrent heat exchanger volume. Volumes V1 and V2 were used to adjust the slowest pole to most significant zero ratio of the TF/X transfer function in order to form similar response curves to the experimental data. Both the linear and nonlinear response curves were compared in each case.

All of the above parameters were calculated through the use of DTXFCN, a program written for this thesis. DTXFCN was used to calculate the poles and zeros of the exact (non-strictly proper) transfer function and approximate (strictly proper, for use with some simulation packages) transfer function equations. The strictly proper transfer functions were generated by adding a relatively fast and insignificant pole at

S = -1 to each exact transfer function. In addition, DTXFCN calculated the lumped heat transfer parameters, temperatures TI and T2 and the slowest pole to most significant zero ratio, RPZ. The exact and strictly proper transfer functions are shown in Tables 14a and 14b.

The nonlinear open-loop response is calculated using the program DTHES2 written for this purpose which used EPISODE (Byrne and Hindmarsh, 1975), an ordinary differential equation solver.

The linear response is simulated by the subroutine SMXPO of the CONSYD (Morari and Ray, 1986) software package using the matrix exponential method for computation. SMXPO requires a strictly proper transfer function so those of Table 14a are used. In order to qualitatively compare the shape of the responses, the nonlinear, linear and experimental (without dead time) open-loop responses have been normalized by dividing the individual responses by their steady-state value and by diving the time by the time it takes to reach at least 99.9 % steady-state value. Thus the value 1 represents the steady-state value of the temperature and the time the response reaches steady state. These normalized responses are shown in Figures 6a and 6b.

The FORTRAN code of both programs DTXFCN and DTHES2 along with an example run of each program are in

Table 14a. Exact transfer functions for the heat exchanger network

$$\frac{\overline{TF}}{X} = \frac{-0.49463E\text{-}3\ s^3 - 0.5104E\text{-}4\ s^2 - 0.13572E\text{-}5\ s - 0.62978E\text{-}9}{0.15568E\text{-}4\ s^3 + 0.17107E\text{-}5\ s^2 + 0.52016E\text{-}7\ s + 0.27642E\text{-}9}$$

$$\frac{\overline{TF}}{TS} = \frac{0.52977E\text{-}7\ s^2 + 0.28991E\text{-}8\ s + 0.29322E\text{-}10}{0.15568E\text{-}4\ s^3 + 0.17107E\text{-}5\ s^2 + 0.52016E\text{-}7\ s + 0.27642E\text{-}9}$$

$$\frac{\overline{TH}}{X} = \frac{0.50943E\text{-}8}{0.15568E\text{-}4\ s^3 + 0.17107E\text{-}5\ s^2 + 0.52016E\text{-}7\ s + 0.27642E\text{-}9}$$

$$\frac{\overline{TH}}{TS} = \frac{0.10595E\text{-}6\ s^2 + 0.50887E\text{-}8\ s + 0.38283E\text{-}10}{0.15568E\text{-}4\ s^3 + 0.17107E\text{-}5\ s^2 + 0.52016E\text{-}7\ s + 0.27642E\text{-}9}$$

Table 14b. Strictly proper transfer functions for the heat exchanger network

$$\frac{\overline{TF}}{X} = \frac{-0.49463E\text{-}3\ s^3 - 0.5104E\text{-}4\ s^2 - 0.13572E\text{-}5\ s - 0.62978E\text{-}9}{0.15568E\text{-}4\ s^4 + 0.17279E\text{-}4\ s^3 + 0.17627E\text{-}5\ s^2 + 0.52292E\text{-}7\ s + 0.27642E\text{-}9}$$

$$\frac{\overline{TF}}{TS} = \frac{0.52977E\text{-}7\ s^2 + 0.28991E\text{-}8\ s + 0.29322E\text{-}10}{0.15568E\text{-}4\ s^4 + 0.17279E\text{-}4\ s^3 + 0.17627E\text{-}5\ s^2 + 0.52292E\text{-}7\ s + 0.27642E\text{-}9}$$

$$\frac{\overline{TH}}{X} = \frac{0.50943E\text{-}8}{0.15568E\text{-}4\ s^4 + 0.17279E\text{-}4\ s^3 + 0.17627E\text{-}5\ s^2 + 0.52292E\text{-}7\ s + 0.27642E\text{-}9}$$

$$\frac{\overline{TH}}{TS} = \frac{0.10595E\text{-}6\ s^2 + 0.50887E\text{-}8\ s + 0.392833E\text{-}10}{0.15568E\text{-}4\ s^4 + 0.17279E\text{-}4\ s^3 + 0.17627E\text{-}5\ s^2 + 0.52292E\text{-}7\ s + 0.27642E\text{-}9}$$

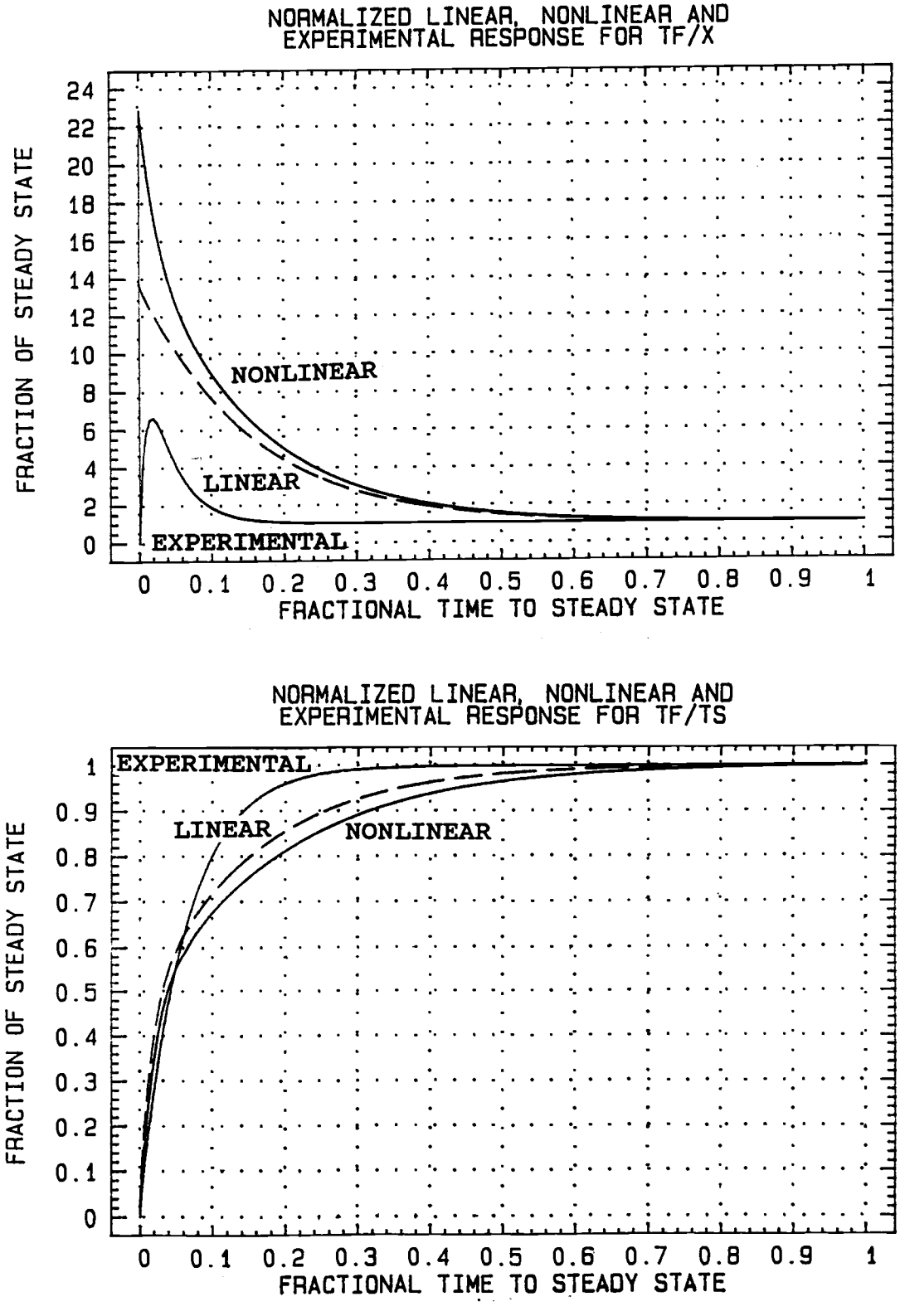

Fig. 6a. Normalized linear, nonlinear and experimental TF responses to unit step changes in the manipulated variables

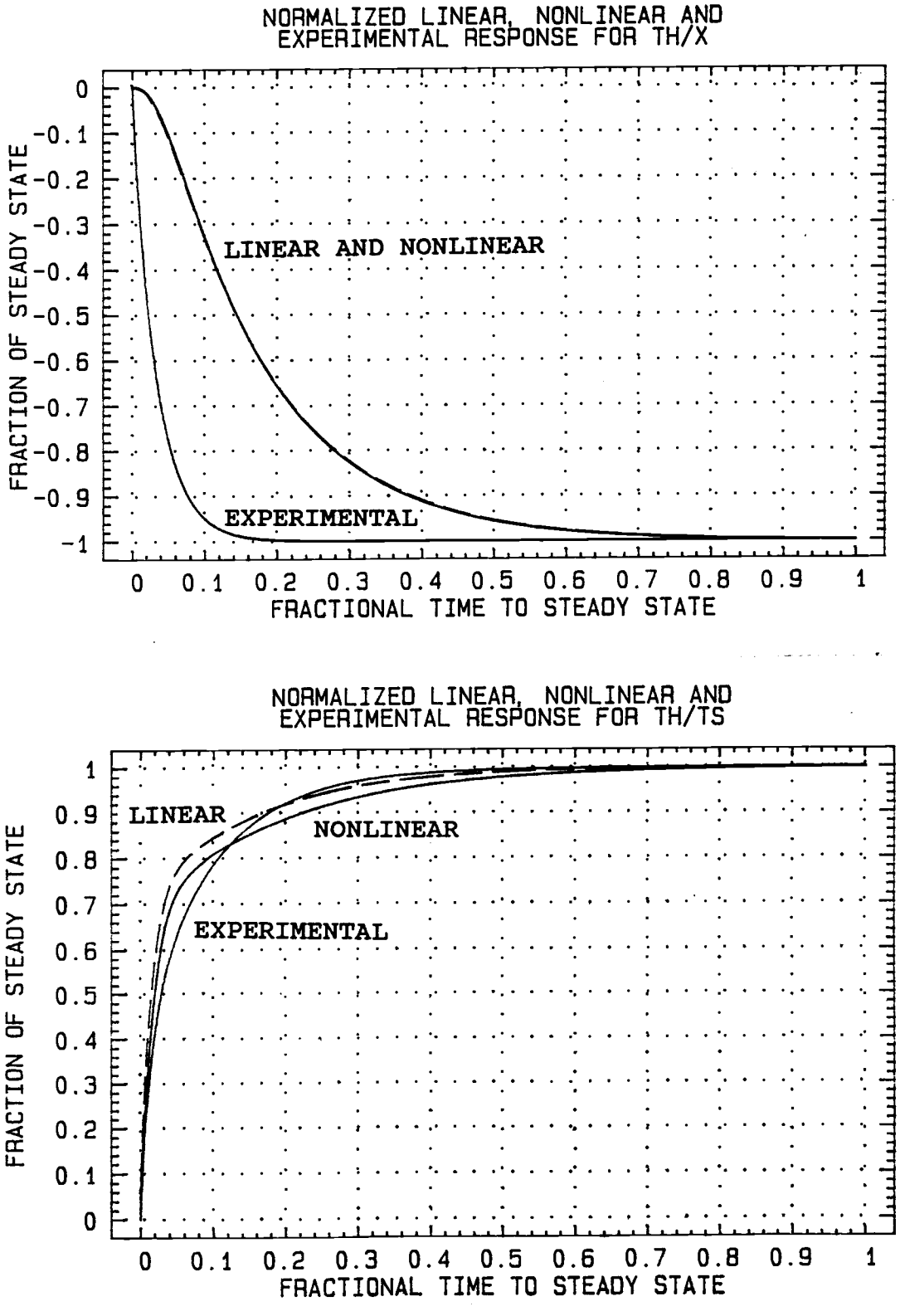

Fig. 6b. Normalized linear, nonlinear and experimental TH responses to unit step changes in the manipulated variables

Appendices B and C.

REMARKS

1. It was necessary to perturb the known temperature data in order to fit the experimental data with the simplified heat transfer process model of Chapter 1, while matching the transfer function gain ratios for each manipulated variable.

2. The fundamental model's transfer function gain ratios were found to be functions only of the four target temperatures, TS, T1, TH and TF. These ratios also fix the RGA, allowing other physical parameters to be varied while the RGA remains constant.

3. The transfer functions can be completely specified by thirteen of the original nineteen process parameters and variables. The thirteen essential parameters are the four target temperatures, RHO, CP, A3, U3, X, V1, V2, V3 and either U1 or A1. The two redundant variables are U2 (= U1) and A2 (= A1). The other four dependent values are TI, T2, F and either A1 or U1, whichever was not chosen above.

4. The fitted inlet temperature (TI) is not a function of the fraction of flow through the recycle heat exchanger. The reason for this can be seen from the mass and energy balance for the control volume shown

in Figure 7, which shows the variables necessary to calculate TI.

5. The shapes of the open-loop step response curves are very dependent on the heat exchanger volumes. The larger the volumes the slower the changes in the step response curve. This agrees with intuition since there would be more water to heat up with a larger volume given a constant heat transfer area.

6. The difficult steps of fitting the data are to make sure the heat transfer area is viable for the given heat exchanger volume and that the process temperatures do not require a negative heat transfer area.

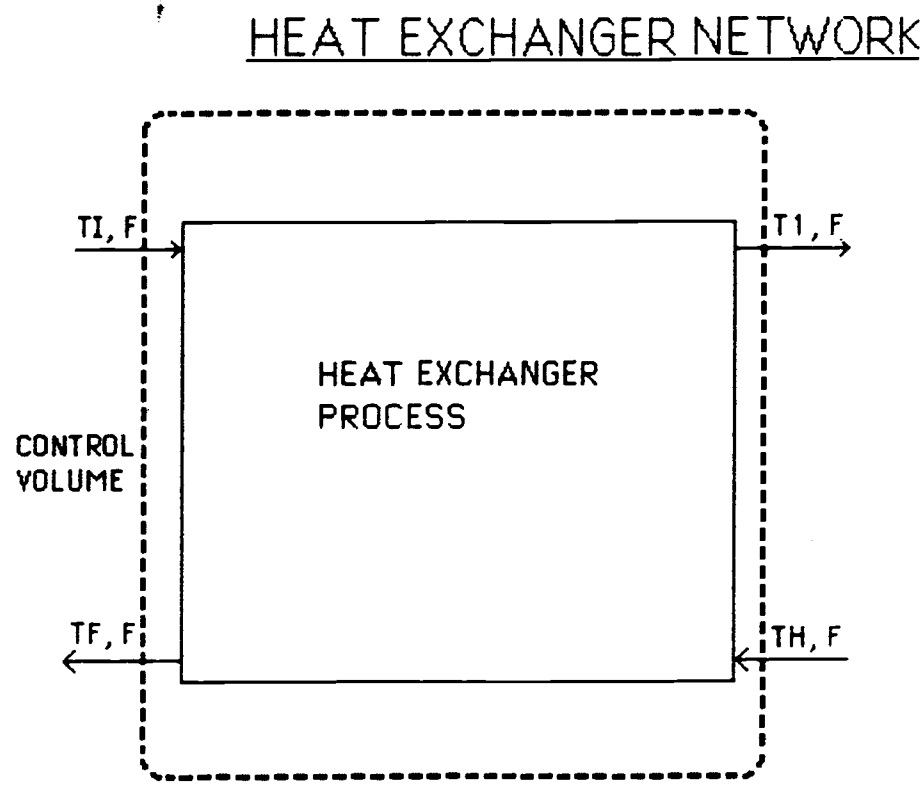

Fig. 7. Control volume showing values necessary to calculate the inlet temperature TI

CHAPTER 4 - DESIGN OF A SIMPLE HEAT EXCHANGER NETWORK FOR A PROCESS CONTROL LAB

This chapter describes the design of a process to be used in advanced real-time control experiments. The major objective is to design a multi-variable process with significant dynamic interactions to be used in an undergraduate process control laboratory. Efficient heat transfer is not the objective of this network. The design criteria includes time to reach a new steady state of less than 30 minutes, a network size small enough to fit within a 3 meter square area, simple heat exchangers (to simplify mass and energy balance equations and the construction of the network), steam temperatures readily available in a control lab and small flow rates to conserve energy and water. The final design presented here is based on the available resources at Oregon State University. Other designs could be made using the programs developed in this study, see Appendix A. As in Chapter 2, efforts were made to create a design which matched as many of the experimental parameter values as possible. This included both the process and system parameters with the RGA being fixed at the experimental value.

The required list of process parameters and variables (Table 3) was used in determining the final

design. The lumped parameters were later separated to verify the possibility of a specific heat exchanger design which would fit the design criteria.

The method of determining the final design was similar to the method used in Chapter 2. The first step was to determine the design temperatures T1, TH, TF and TS given the constraint of matching the gain ratios (Table 12) of 1.338 and -8.089 for the steam temperature, RTS and the flow fraction manipulated variables, RX, respectively. In addition, a steady-state steam temperature of 200 °C was chosen as a readily available steam temperature in our laboratory. From these four temperatures and the steam heat exchanger area, A3, the inlet temperature TI and the ratio of overall heat transfer coefficient for the steam heat exchanger to flow rate (U3/F) were found. Again, from Welty, et al (1976), the average overall heat transfer coefficients for steam to water (2800 W / m^2 K) and water to water (1250 W / m^2 K) heat exchangers were used. The fraction of flow to the recycle heat exchanger, X, was chosen to be 0.5, again to be in the middle of the operating range. These values allowed the calculation of the temperature out of the hot side of the recycle heat exchanger, T2, the overall flow rate through the network, F, and the lumped parameter for the recycle heat exchanger, Z (Table 13). These ten values

and the gain ratios allowed the individual transfer function gains (Table 15) and the RGA to be calculated (Table 16a). Since the RGA was fixed at the experimental value of 0.1419 this calculation was used as a check of the results to this point.

The heat exchanger volumes V1, V2 and V3, necessary for determining the system parameters, were chosen through a process of trial and error. The volume of the steam heat exchanger, V3, was fixed at the experimental value. It was found that, the maximum ratio of slowest pole to most significant zero was obtained by having equal volumes on each side of the recycle heat exchanger. Therefore, volumes V1 and V2 have been chosen to be equal. The final design parameters and variables are shown in Table 17.

These parameters and variables provide the exact (non-strictly proper) transfer functions in Table 18a and the strictly proper transfer functions in Table 18b. As in Chapter 2, these transfer functions were calculated using the program DTXFCN and the design parameters and variables. DTXFCN calculated both the exact and strictly proper transfer functions, the poles and zeros of the transfer functions, the lumped heat transfer parameters, temperatures TI and T2 and the slowest pole to most significant zero ratio, RPZ. Again, the strictly proper transfer functions were

Table 15. Individual transfer function gains as functions of the process parameters

$$\frac{\overline{TF}}{X} = \frac{-(TH - T2)\ F\ Z\ Y}{F^3\ X + F^2\ (X\ Y + Z) + F\ Z\ Y\ (1 + X)}$$

$$\frac{\overline{TF}}{TS} = \frac{F^2\ X\ Y + F\ Z\ Y}{F^3\ X + F^2\ (X\ Y + Z) + F\ Z\ Y\ (1 + X)}$$

$$\frac{\overline{TH}}{X} = \frac{(TH - T2)\ F^2\ Z}{F^3\ X + F^2\ (X\ Y + Z) + F\ Z\ Y\ (1 + X)}$$

$$\frac{\overline{TH}}{TS} = \frac{F^2\ X\ Y + F\ Z\ Y\ (1 + X)}{F^3\ X + F^2\ (X\ Y + Z) + F\ Z\ Y\ (1 + X)}$$

Table 16a. The 1,1 element of the Relative Gain Array as a function of the design temperatures

$$\lambda_{11} = \frac{2\ TH - T1 - TF}{TH + TS - T1 - TF}$$

Table 16b. The 1,1 element of the Relative Gain Array as a function of the process parameters

$$\lambda_{11} = \frac{1}{1 + \frac{F^2\ X\ \rho^2\ CP^2 + F\ \rho\ CP\ U1\ A1}{U3\ A3\ [F\ X\ \rho\ CP + U1\ A1\ (1 + X)]}}$$

Table 17. Final design process parameter values for the heat exchanger network

$V1 = V2 = 0.04\ m^3$	$TS = 200.0\ °C$
$V3 = 0.01\ m^3$	$T1 = 41.0\ °C$
$U1 = 1250\ W / m^2\ K$	$TH = 58.5\ °C$
$U3 = 2800\ W / m^2\ K$	$TF = 52.6\ °C$
$A1 = 1.5\ m^2$	$\rho = 1000\ Kg / m^3$
$A3 = 0.08\ m^2$	$Cp = 4186\ J / Kg\ K$

Table 18a. Non-strictly proper transfer functions for the heat exchanger network using the design process parameters

$$\frac{\overline{TF}}{X} = \frac{-0.1888E\text{-}3\ s^3 - 0.15449E\text{-}4\ s^2 - 0.32772E\text{-}6\ s - 0.12236E\text{-}9}{0.16E\text{-}4\ s^3 + 0.13958E\text{-}5\ s^2 + 0.33885E\text{-}7\ s + 0.14492E\text{-}9}$$

$$\frac{\overline{TF}}{TS} = \frac{0.42809E\text{-}7\ s^2 + 0.18848E\text{-}8\ s + 0.15379E\text{-}10}{0.16E\text{-}4\ s^3 + 0.13958E\text{-}5\ s^2 + 0.33885E\text{-}7\ s + 0.14492E\text{-}9}$$

$$\frac{\overline{TH}}{X} = \frac{0.9894E\text{-}9}{0.16E\text{-}4\ s^3 + 0.13958E\text{-}5\ s^2 + 0.33885E\text{-}7\ s + 0.14492E\text{-}9}$$

$$\frac{\overline{TH}}{TS} = \frac{0.85619E\text{-}7\ s^2 + 0.33065E\text{-}8\ s + 0.20564E\text{-}10}{0.16E\text{-}4\ s^3 + 0.13958E\text{-}5\ s^2 + 0.33885E\text{-}7\ s + 0.14492E\text{-}9}$$

Table 18b. Strictly proper transfer functions for the heat exchanger network using the design process parameters

$$\frac{\overline{TF}}{X} = \frac{-0.1888E\text{-}3\ s^3 - 0.15449E\text{-}4\ s^2 - 0.32772E\text{-}6\ s - 0.12236E\text{-}9}{0.16E\text{-}4\ s^4 + 0.17396E\text{-}4\ s^3 + 0.14297E\text{-}5\ s^2 + 0.3403E\text{-}7\ s + 0.14492E\text{-}9}$$

$$\frac{\overline{TF}}{TS} = \frac{0.42809E\text{-}7\ s^2 + 0.18848E\text{-}8\ s + 0.15379E\text{-}10}{0.16E\text{-}4\ s^4 + 0.17396E\text{-}4\ s^3 + 0.14297E\text{-}5\ s^2 + 0.3403E\text{-}7\ s + 0.14492E\text{-}9}$$

$$\frac{\overline{TH}}{X} = \frac{0.9894E\text{-}9}{0.16E\text{-}4\ s^4 + 0.17396E\text{-}4\ s^3 + 0.14297E\text{-}5\ s^2 + 0.3403E\text{-}7\ s + 0.14492E\text{-}9}$$

$$\frac{\overline{TH}}{TS} = \frac{0.85619E\text{-}7\ s^2 + 0.33065E\text{-}8\ s + 0.20564E\text{-}10}{0.16E\text{-}4\ s^4 + 0.17396E\text{-}4\ s^3 + 0.14297E\text{-}5\ s^2 + 0.3403E\text{-}7\ s + 0.14492E\text{-}9}$$

generated by adding a fast pole at S = -1.

The nonlinear open loop response, calculated using program DTHES2, and the linear open loop response of the strictly proper transfer function, simulated using the subroutine SMXPO of the CONSYD software package, are shown in Figures 8a and 8b.

REMARKS

1. The four design temperatures were calculated by using the equations in Table 16a to ensure a constant RGA, even though the individual transfer function gains may vary. Table 16b could be used to calculate the RGA for a given heat exchanger network without knowing any of the temperatures, that is, only process parameters and X need to be known.

2. Each heat exchanger design specified by DTXFCN must be checked to assure the design is physically realizable. It is possible that the design requires a heat exchanger with an area too large for the given volume or for the heat transfer area to be negative. In this thesis, a reasonable heat exchanger is considered to be one which consists of flow between flat plates spaced at least 5 cm apart. For some cases a bath type of heat exchanger may be necessary to maintain the 5 cm spacing between the plates (Figure 9). Using a bath

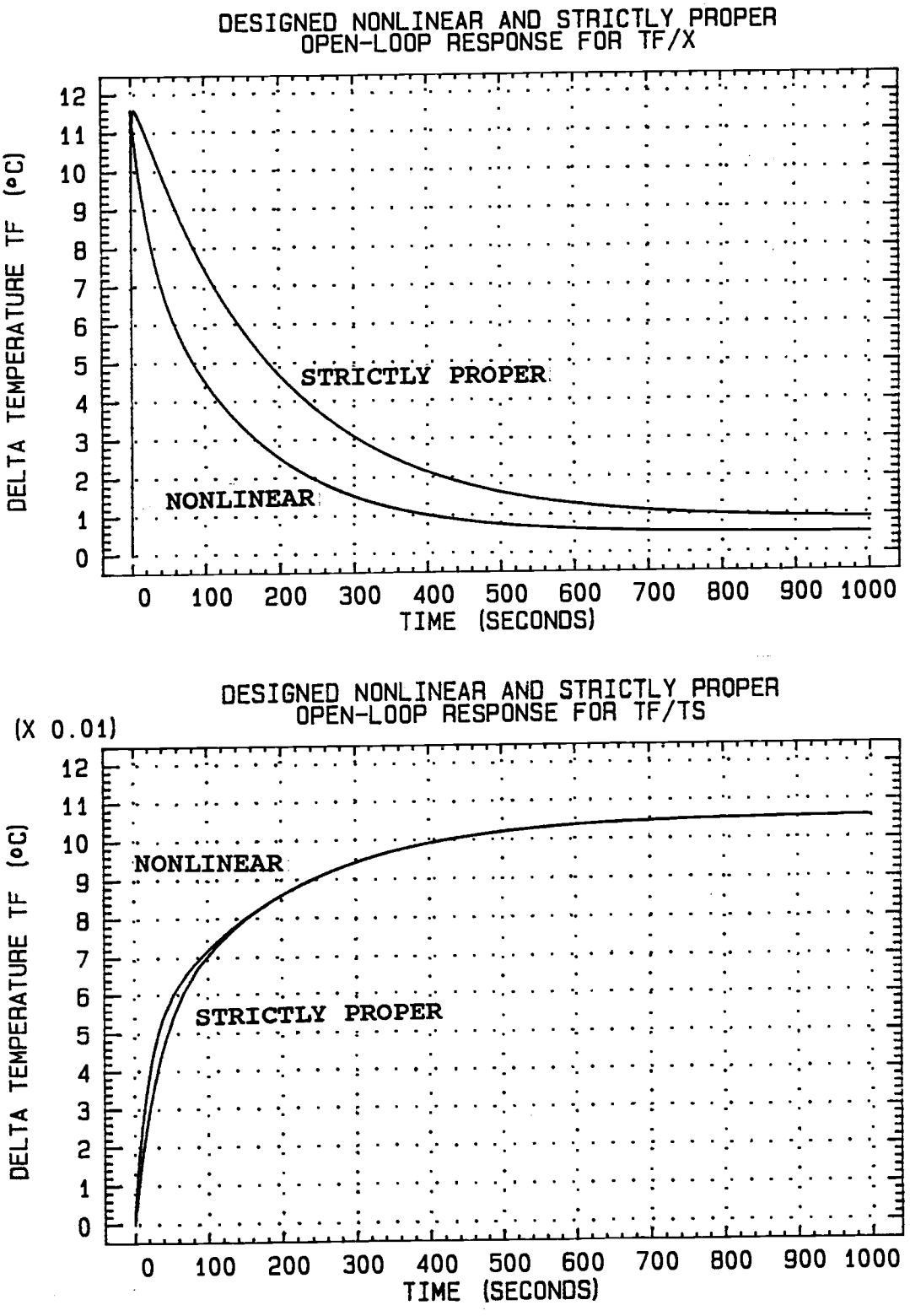

Fig. 8a. Designed nonlinear and strictly proper open-loop TF responses to unit step changes in the manipulated variables

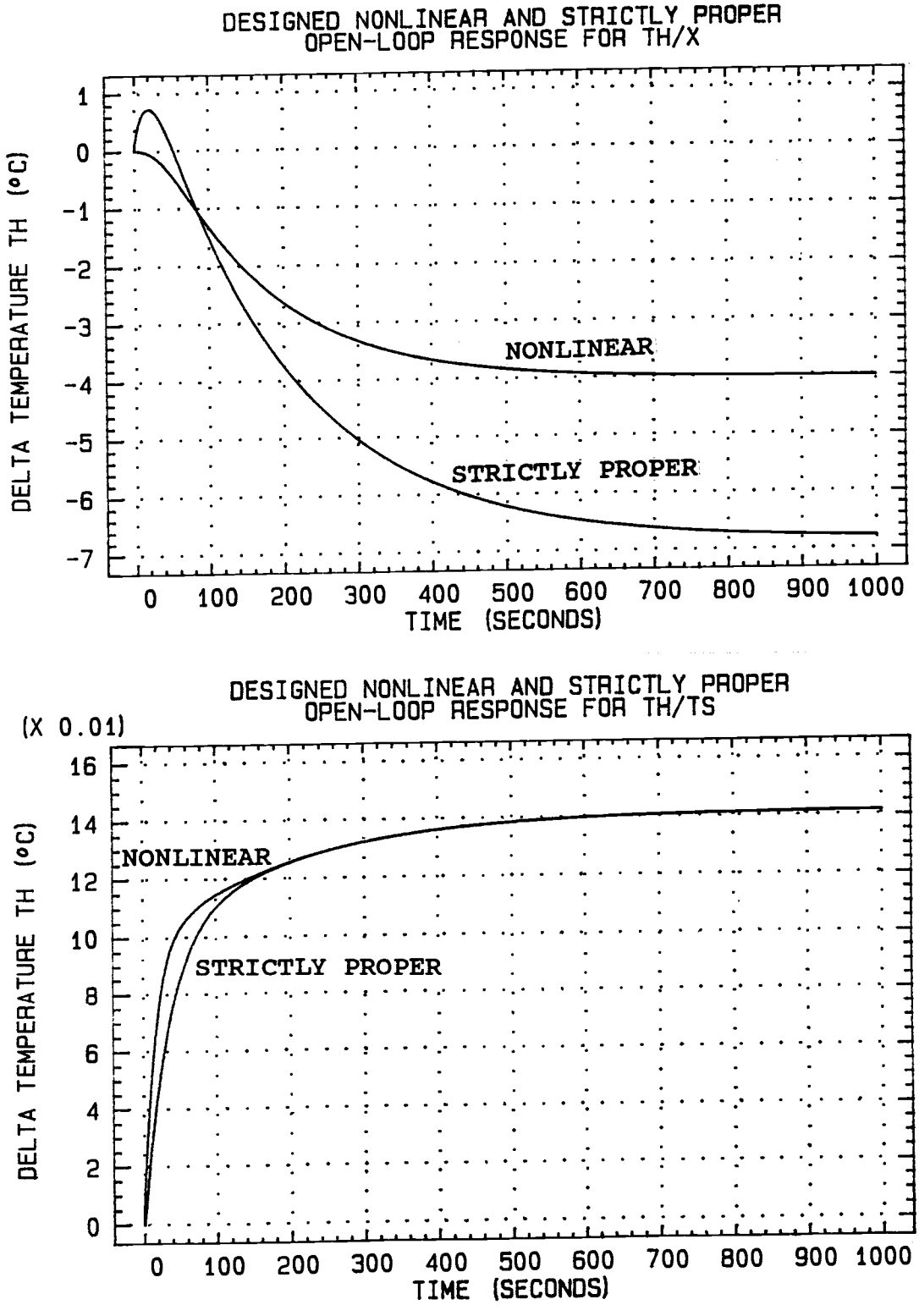

Fig. 8b. Designed nonlinear and strictly proper open-loop TH responses to unit step changes in the manipulated variables

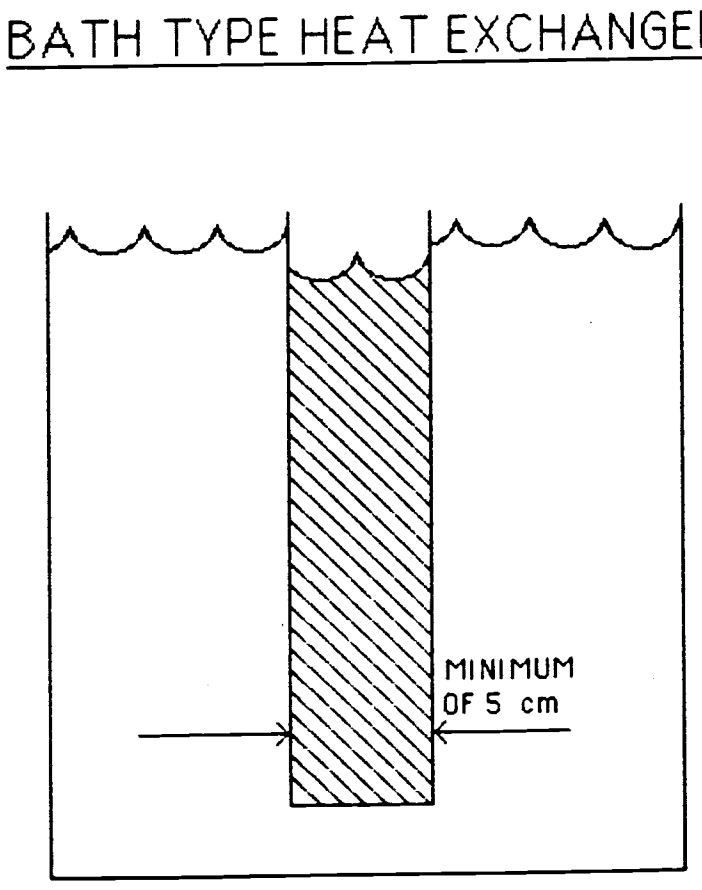

Fig. 9. Diagram of a "reasonable" heat exchanger

type of heat exchanger increases the heat transfer area over a single plate while maintaining the simplicity of the design. A description of the process involved in verifying the reasonable design of the heat exchanger is given in the Appendix D.

3. There are two conflicting objectives in the design of the steam heat exchanger: the areas of the steam and recycle heat exchangers. Because the steam is the only place for the addition of energy to the network, this area should be as large as possible to allow maximum heat transfer for a given volume and time. However, to maintain the target temperatures, the recycle heat transfer area must be increased 20 times that of the increase in steam heat transfer area. Therefore, even a slight increase in the area of the steam heat exchanger requires a very large increase in the area of the recycle heat exchanger.

CHAPTER 5 - COMPUTER SIMULATED CONTROL OF THE SIMPLE HEAT EXCHANGER NETWORK

The purpose of this chapter is to show that the nominal heat exchanger design is difficult to control using two Proportional-Integral (PI) controllers. If two multi-loop continuous PI controllers control the process adequately the process is considered simple to control. If PI control is not adequate, but a multivariable controller has acceptable control, the process is considered complex but controllable. The first algorithm uses two PI controllers, tuned using either Cohen-Coon or a slightly modified Ziegler-Nichols method (Stephanopolous, 1984). The second algorithm is for an Internal Model Controller (IMC) using parameter values suggested by Garcia and Morari (1982). The nominal heat exchanger network is shown to have significant output deviations for a change in the TH set point for the PI controllers using either Cohen-Coon or modified Ziegler-Nichols tuning parameters, while the IMC controller has very fast response with no significant deviation. The programs used for the closed-loop simulations are shown in Table 19.

This chapter is divided into two sections. The first discusses the PI controllers and contains the closed-loop responses for set point changes using either

Table 19. Programs used for closed-loop simulations using PI and IMC control algorithms

Control parameters found from:	Program used for simulation	
	Linear	Nonlinear
Cohen-Coon	SMXPO	MYSNTEG
Modified Ziegler-Nichols	SMXPO	MYSNTEG
Internal Model Control (Garcia and Morari)	EIMC (specific model mismatch)	EIMC (no model mismatch)

Cohen-Coon or modified Ziegler-Nichols tuning parameters. Closed-loop simulations are performed on the linear and nonlinear process models. The second section discusses the IMC controller performance with and without modeling errors. In the first case either the linear or nonlinear model is used as both the process model and the plant. Using the same model as both process model and plant represents an exact knowledge of the process, i.e., no plant-model mismatch. Because complete knowledge of a process is seldom available, the second case uses program STEPG (Levien, 1988) to simulate this lack of information by fitting an equation to the nonlinear open-loop step response to determine approximate transfer function models to use in the IMC control algorithm.

Proportional-Integral control method

This section uses two CONSYD (Morari and Ray, 1986) programs to simulate closed-loop responses for the linear and nonlinear process models to set point changes. The linear process is simulated by SMXPO, using the strictly proper transfer functions. The nonlinear process is simulated by SNTEG which must be linked to the set of differential equations in PLANT1, written for this thesis and listed in Appendix B, to

form program MYSNTEG.

The pairing of the manipulated variables and outputs was determined by the RGA recommendations and Figure 10. Figure 10 shows that the only energy input to the process is from the steam. Therefore, the only way for the output temperature TF to change significantly is to have it paired to the steam temperature, TS. This leaves temperature TH to be paired to the flow fraction, X. By using two PI controllers the interactions of the other two transfer functions, TF/X and TH/TS are ignored and TF/X is the transfer function with the drastic dynamic response. By using the multivariable controller algorithm in the next section these transfer functions are taken into account.

The controller parameters were determined from the open-loop step response for the nonlinear model. For comparison, both Cohen-Coon and modified Ziegler-Nichols techniques are used to determine the PI tuning parameters. The equations used to determine the PI tuning parameters from Cohen-Coon and Ziegler-Nichols techniques are shown in Tables 20 and 21, respectively (Stephanopolous, 1984). The Cohen-Coon parameters for the equations of Table 20 were determined from Figures 11 and 12. The modified Ziegler-Nichols tuning parameters were determined from the gain margin and the crossover frequency found by using the CONSYD program

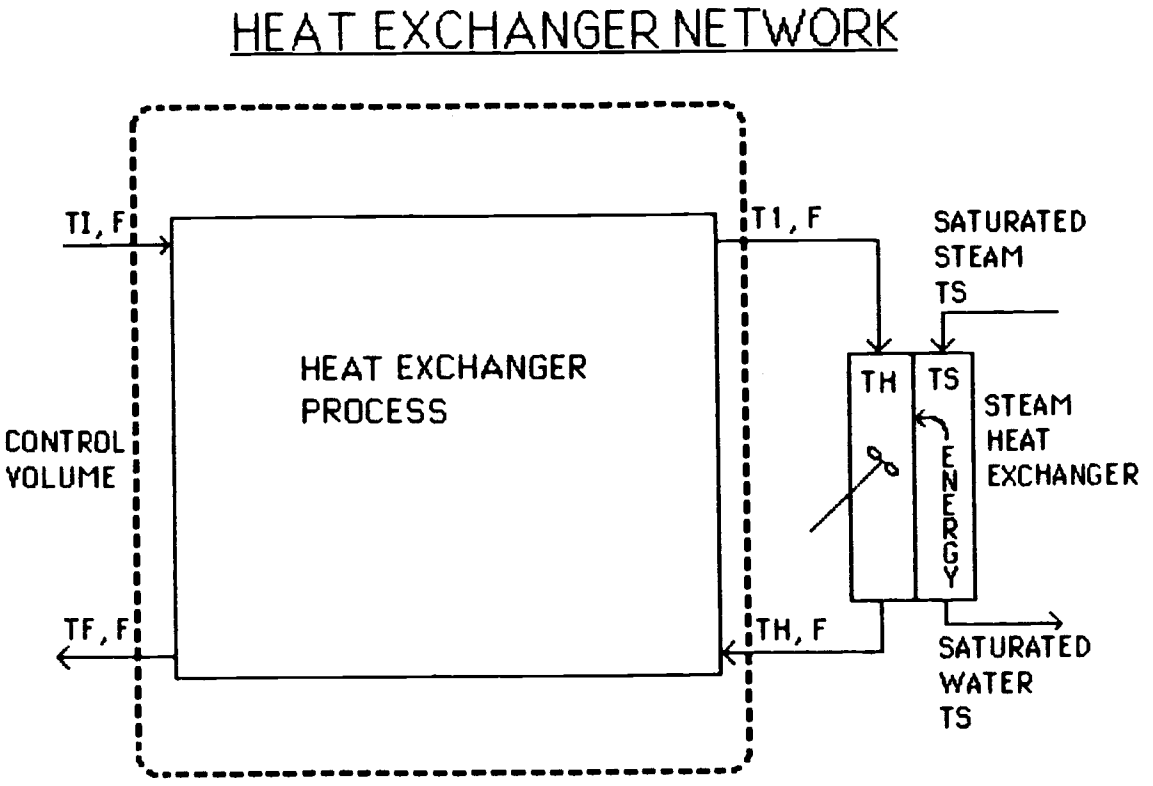

Fig. 10. Control volume showing necessity of pairing TF with TS and TH with X

Table 20. Equations for determining Cohen-Coon tuning parameters for PI controllers

$$K = \frac{\text{steady-state output}}{\text{steady-state input}}$$

$$\tau = \frac{\text{steady-state output}}{\text{slope at inflection point}}$$

t_d = elapsed time before system response

$$K_c = \frac{\tau * [0.9 + t_d / (12 * \tau)]}{K * t_d}$$

$$\tau_I = \frac{t_d * (30 + 3 * t_d / \tau)}{9 + 20 * t_d / \tau}$$

Table 21. Equations for determining Ziegler-Nichols tuning parameters for PI controllers

$$\text{Ultimate gain} = K_u = \frac{1}{\text{amplitude ratio of the system's response at the crossover frequency}}$$

$$\text{Ultimate period} = P_u = \frac{2 * \pi}{\text{crossover frequency}}$$

$$K_c = K_u / 2.2$$

$$\tau_I = P_u / 1.2$$

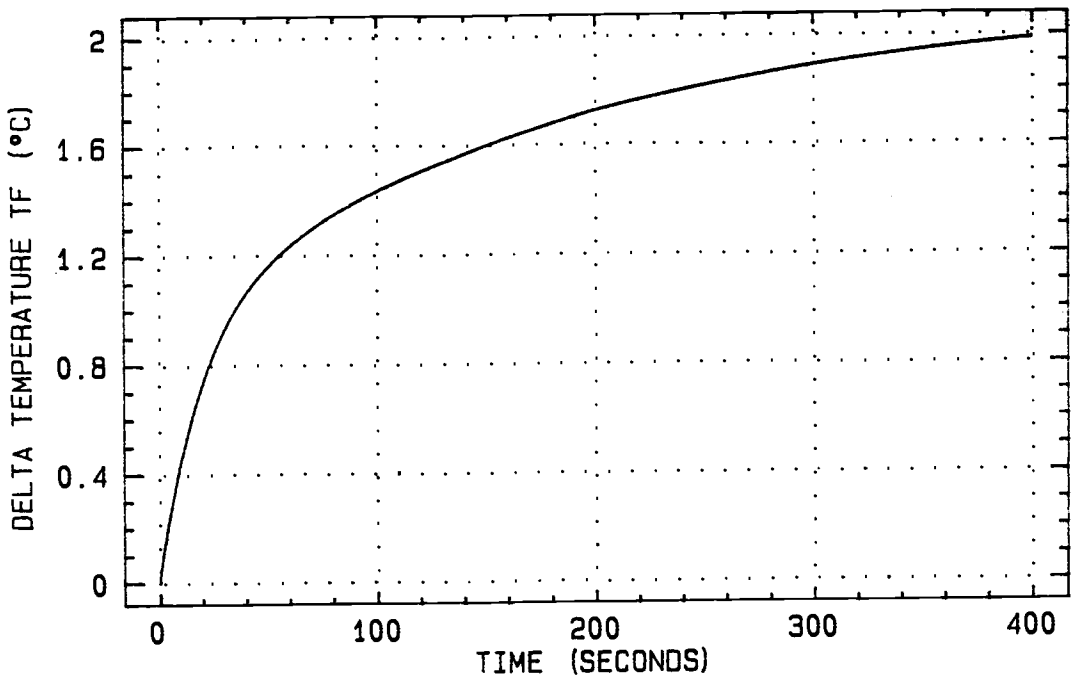

Fig. 11. Nominal open-loop TF response to a 20 °C change in TS for determining the Cohen-Coon PI tuning parameters

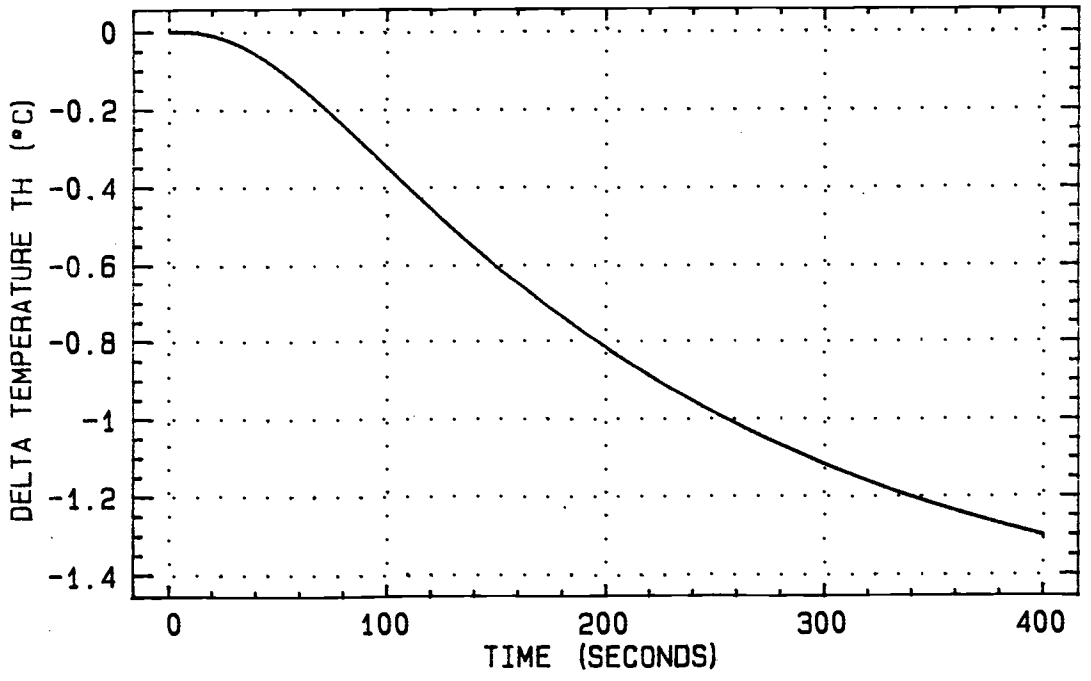

Fig. 12. Nominal open-loop TH response to a -0.2 change in X for determining the Cohen-Coon PI tuning parameters

BODE. It was necessary to modify the transfer functions used by BODE, by adding a 1 second dead time, in order to reach a crossover frequency to be able to determine the Ziegler-Nichols tuning parameters. The resulting tuning parameters are found in Table 22 which shows a drastic difference in the tuning parameters for the two techniques. For the TF/TS controller, the C-C gain is nearly a third of the modified Z-N gain while the C-C time constant is twice that of the modified Z-N time constant. The TH/X controller parameter differences are not that significant.

In order to find feasible set point changes, the gains for the linear and nonlinear transfer functions were determined and are shown in Table 23. The linear gains were determined from their respective transfer functions. The nonlinear gains were determined by running the DTHES2 simulation to 20,000 seconds for individual changes in the manipulated variables. The open-loop step response value at this time was considered the new steady-state value from which the gain could be determined.

Table 24 and Figure 13 show the region of feasible output temperature variations from the nominal steady state while allowing changes in both outputs. The maximum output temperature variations for the linear model are calculated using the gains found in Table 22.

Table 22. Summary of tuning parameters for PI controllers

Cohen-Coon tuning parameters

TH/X CONTROLLER		TF/TS CONTROLLER	
K_C	τ_I	K_C	τ_I
0.97953	92.87213	68.97468	13.18409

Ziegler-Nichols tuning parameters

TH/X CONTROLLER		TF/TS CONTROLLER	
K_C	τ_I	K_C	τ_I
1.1043636	122.79809	203.1091	5.8748152

Table 23. Comparison of individual gains for linear and nonlinear transfer functions

	LINEAR GAINS	
	Flow fraction (X)	Steam temperature (TS)
TF	-0.84433	0.10612
TH	6.82728	0.14192

	NONLINEAR GAINS (at t = 20,000 seconds)	
	Flow fraction (X)	Steam temperature (TS)
TF	-0.49677	0.10612
TH	4.01677	0.14190

Table 24. Comparison of maximum temperature changes possible for linear and nonlinear transfer functions allowing both outputs to change

LINEAR MODEL

	DELTA X = -0.5	
	DELTA TS = -100	DELTA TS = 200
DELTA TH	-17.60364	24.96636
DELTA TF	-10.56978	21.64617

	DELTA X = 0.5	
	DELTA TS = -100	DELTA TS = 200
DELTA TH	-10.77636	31.79364
DELTA TF	-11.03417	20.80183

NONLINEAR MODEL (at t = 20,000 seconds)

	DELTA X = -0.5	
	DELTA TS = -100	DELTA TS = 200
DELTA TH	-16.25667	16.76179
DELTA TF	-10.35530	22.66151

	DELTA X = 0.5	
	DELTA TS = -100	DELTA TS = 200
DELTA TH	-13.19491	33.97653
DELTA TF	-10.73546	20.53265

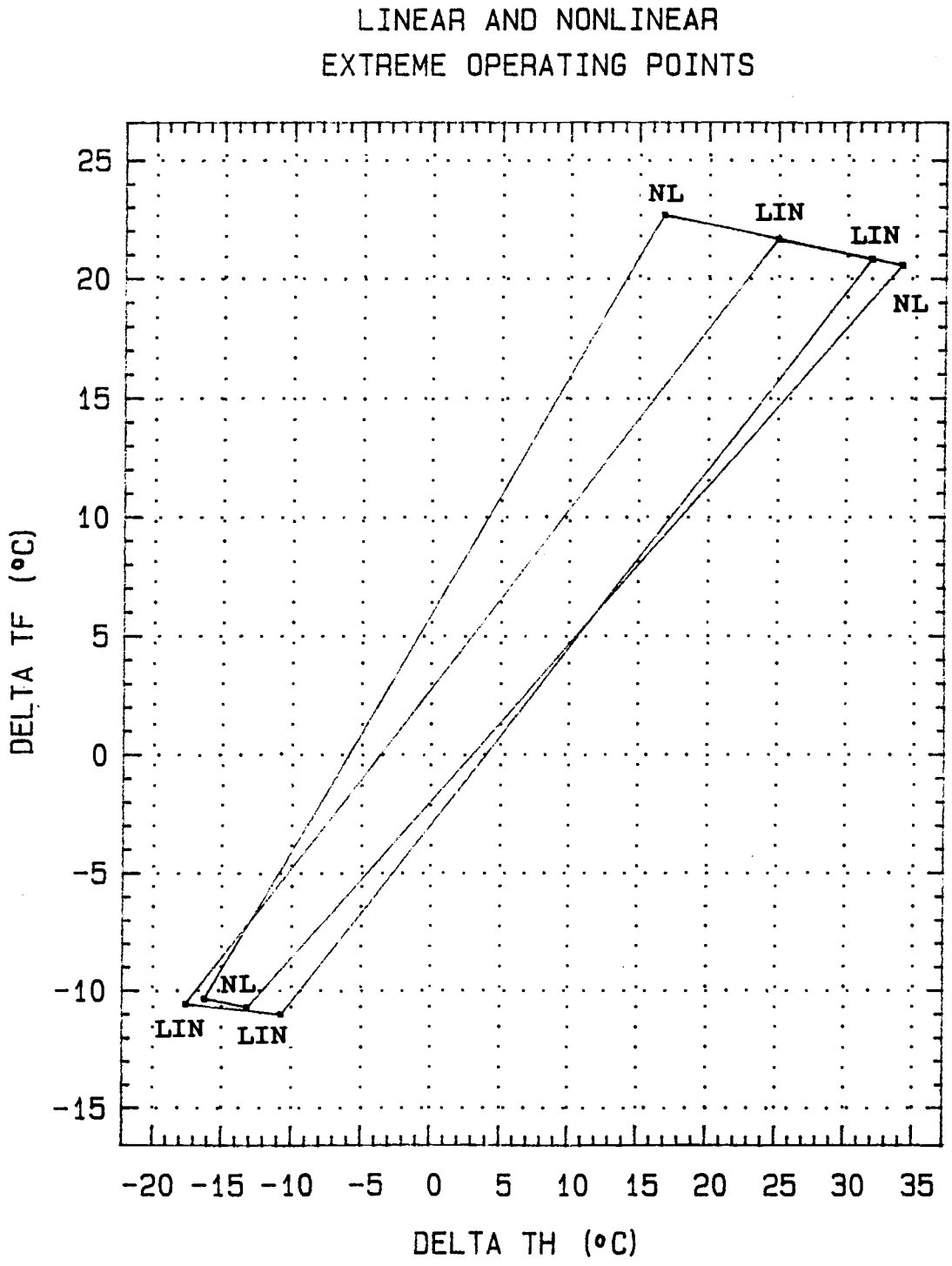

Fig. 13. Linear and nonlinear extreme operating envelope allowing changes in both outputs

The maximum output temperature variations for the nonlinear are determined by DTHES2 simulations to 20,000 seconds for the extreme allowable values of flow fraction ($-0.5 < \Delta X < 0.5$) and steam temperature ($-100 < \Delta TS < 200$). The nonlinear gains could not be used to calculate the region as the gains vary according to the step size taken in the manipulated varible. This can be seen by using the nonlinear gains of Table 23 to calculate the various temperature changes and comparing them to the simulated changes of Table 24.

In order to choose set point changes which are feasible at steady state for both linear and nonlinear closed-loop simulations, the linear and nonlinear transfer function gains are used in the matrix equations of Table 25 to determine the approximate maximum set point changes allowable in one output while maintaining the other output at its original steady-state value. These approximate maximum values are shown in Table 26.

Figures 14 through 17 show plots of the closed-loop response of the linear model to set point changes of 1 °C in either output while under PI control. These plots show that neither set of PI tuning parameters are able to control the process for the linear model as the closed-loop responses continuously oscillate. The manipulated variable responses shown in Figure 14 are representative of the four cases and show that the

Table 25. Equations for estimating the maximum allowable single setpoint change without affecting the second output

The general form:

$$\underline{y} = \underline{\underline{G}}\,\underline{u}$$

Linear matrix equation:

$$\begin{bmatrix} \Delta TF \\ \Delta TH \end{bmatrix} = \begin{bmatrix} -0.84433 & 0.10612 \\ 6.82728 & 0.14192 \end{bmatrix} \begin{bmatrix} \Delta X \\ \Delta TS \end{bmatrix}$$

Nonlinear matrix equation:

$$\begin{bmatrix} \Delta TF \\ \Delta TH \end{bmatrix} = \begin{bmatrix} -0.49677001 & 0.10612369 \\ 4.0167681 & 0.14190212 \end{bmatrix} \begin{bmatrix} \Delta X \\ \Delta TS \end{bmatrix}$$

Table 26. Approximate maximum single setpoint changes allowable with no change in the second steady-state output value

Linear:

$$-2.97 < \Delta TF < 2.92$$

$$-2.79 < \Delta TH < 2.85$$

Nonlinear:

$$-1.75 < \Delta TF < 1.75$$

$$-2.34 < \Delta TH < 2.34$$

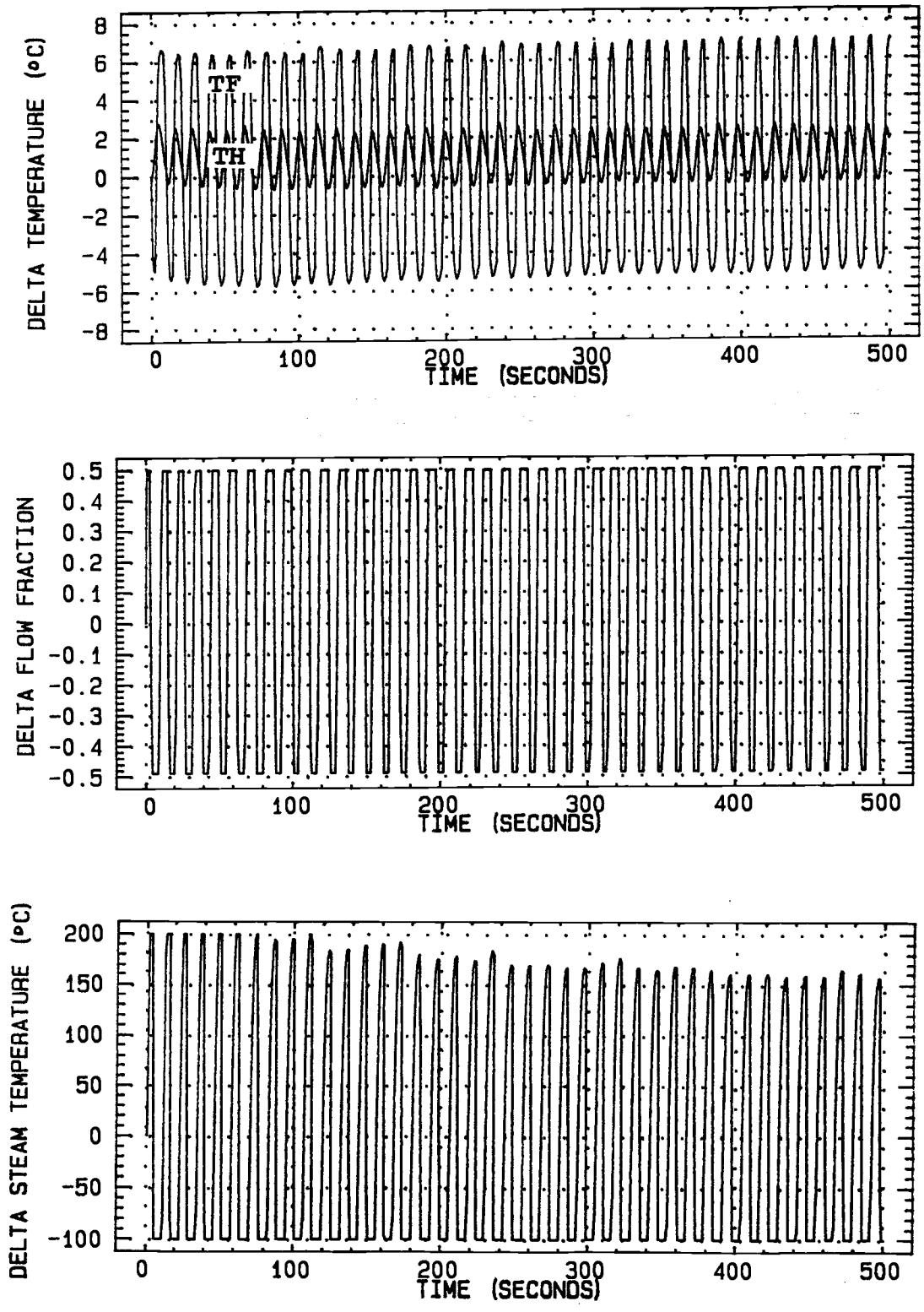

Fig. 14. Closed-loop output and manipulated variable responses to a 1 °C set point change in TF using Cohen-Coon PI tuning parameters

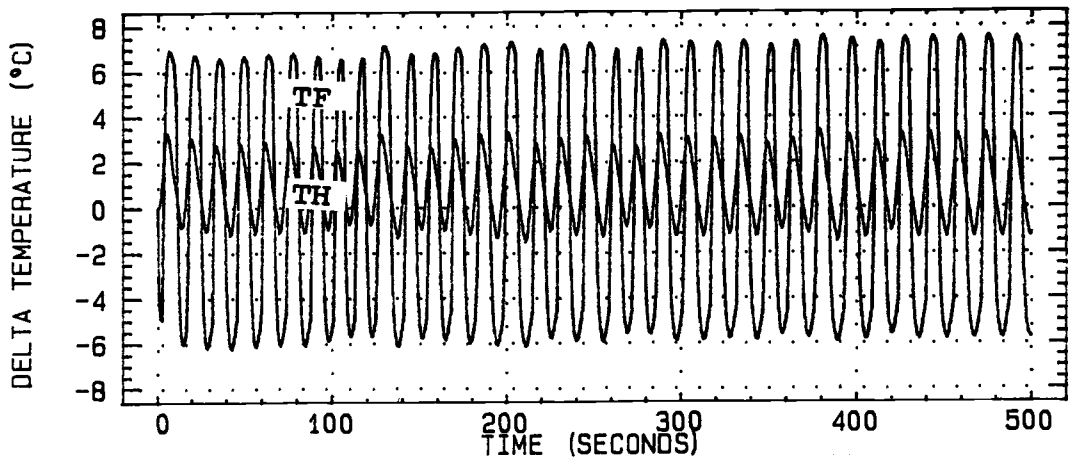

Fig. 15. Closed-loop output responses to a 1 °C set point change in TF using the modified Ziegler-Nichols PI tuning parameters

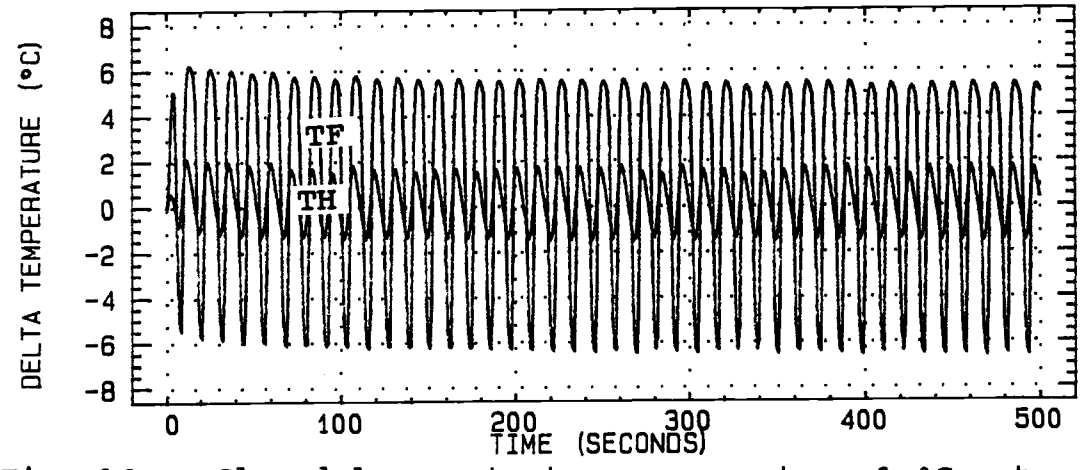

Fig. 16. Closed-loop output responses to a 1 °C set point change in TH using Cohen-Coon PI tuning parameters

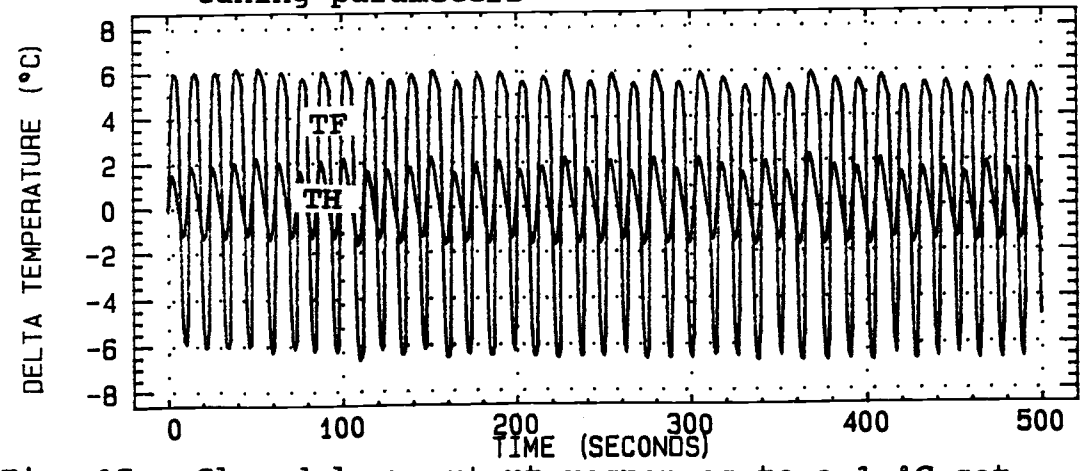

Fig. 17. Closed-loop output responses to a 1 °C set point change in TH using the modified Ziegler-Nichols PI tuning parameters

manipulated variables continuously slam back and forth between their maximum and minimum constraints.

Figures 14 and 15 show the linear closed-loop responses to a set point change of 1.0 °C in TH using C-C and modified Z-N PI tuning parameters, respectively. Figure 14 also shows the manipulated variable response to the set point change.

Figures 16 and 17 show the linear closed-loop responses to a set point change of 1.0 °C in TF using C-C and modified Z-N PI tuning parameters, respectively.

Figures 18 and 19 show closed-loop responses using detuned PI controllers to set point changes of 1 °C for TH and TF, respectively, for the linear model. Detuning was accomplished by decreasing the controller gains to 37 % of their original values for the TH/X controller and 18 % of the original C-C which is 13 % of the original modified Z-N values for the TF/TS controller, while leaving the controller time constants at their original values. Such detuning yields stable yet highly oscillatory, unacceptable closed-loop responses.

Figures 20 through 23 show closed-loop responses using PI controllers to set point changes of 1 °C for the nonlinear model.

Figures 20 and 21 show the nonlinear closed-loop output and manipulated variable responses to a set point change of 1.0 °C in TH using C-C and modified Z-N PI

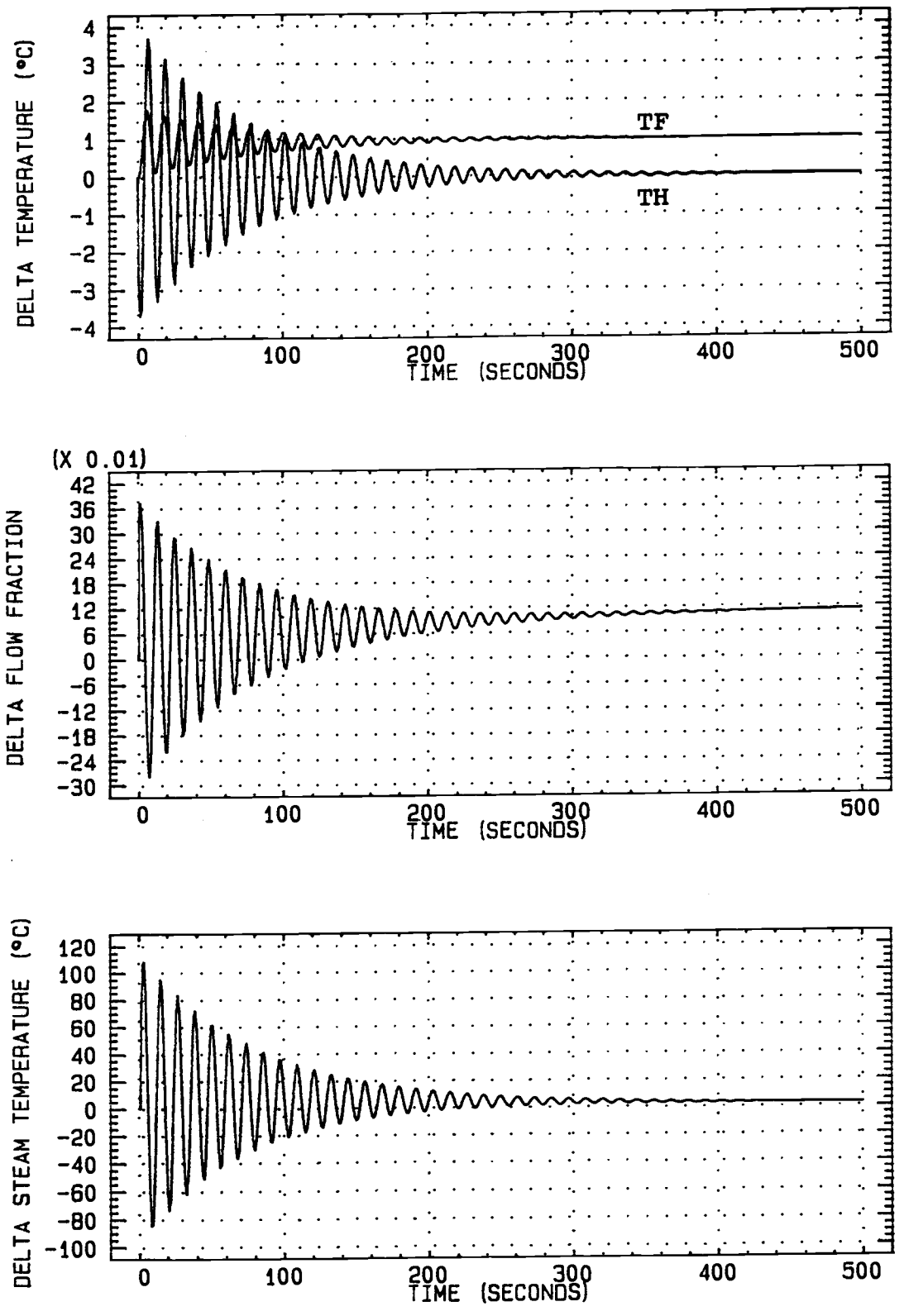

Fig. 18. Closed-loop output and manipulated variable responses to a 1 °C set point change in TF using detuned tuning parameters

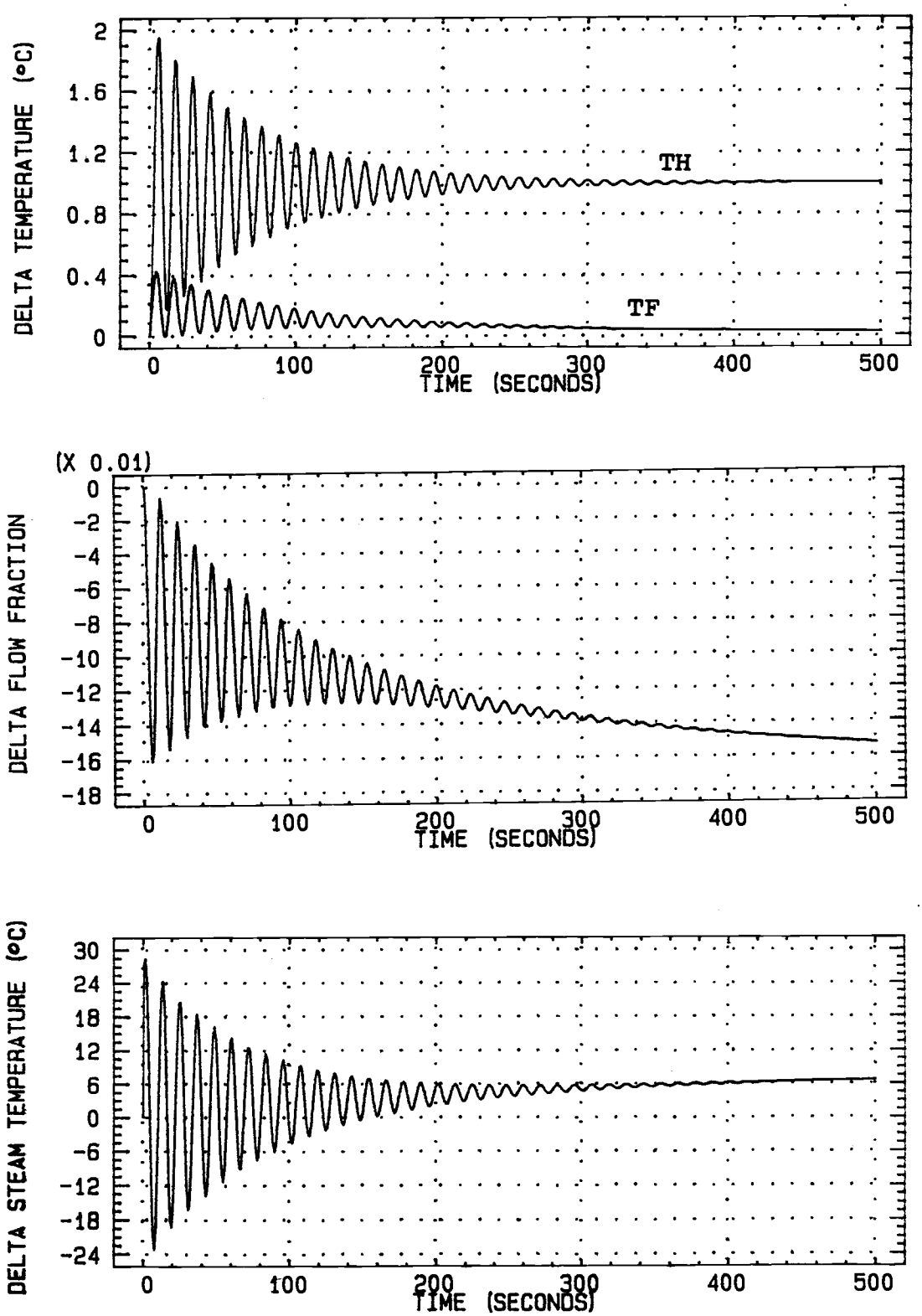

Fig. 19. Closed-loop output and manipulated variable responses to a 1 °C set point change in TH using detuned tuning parameters

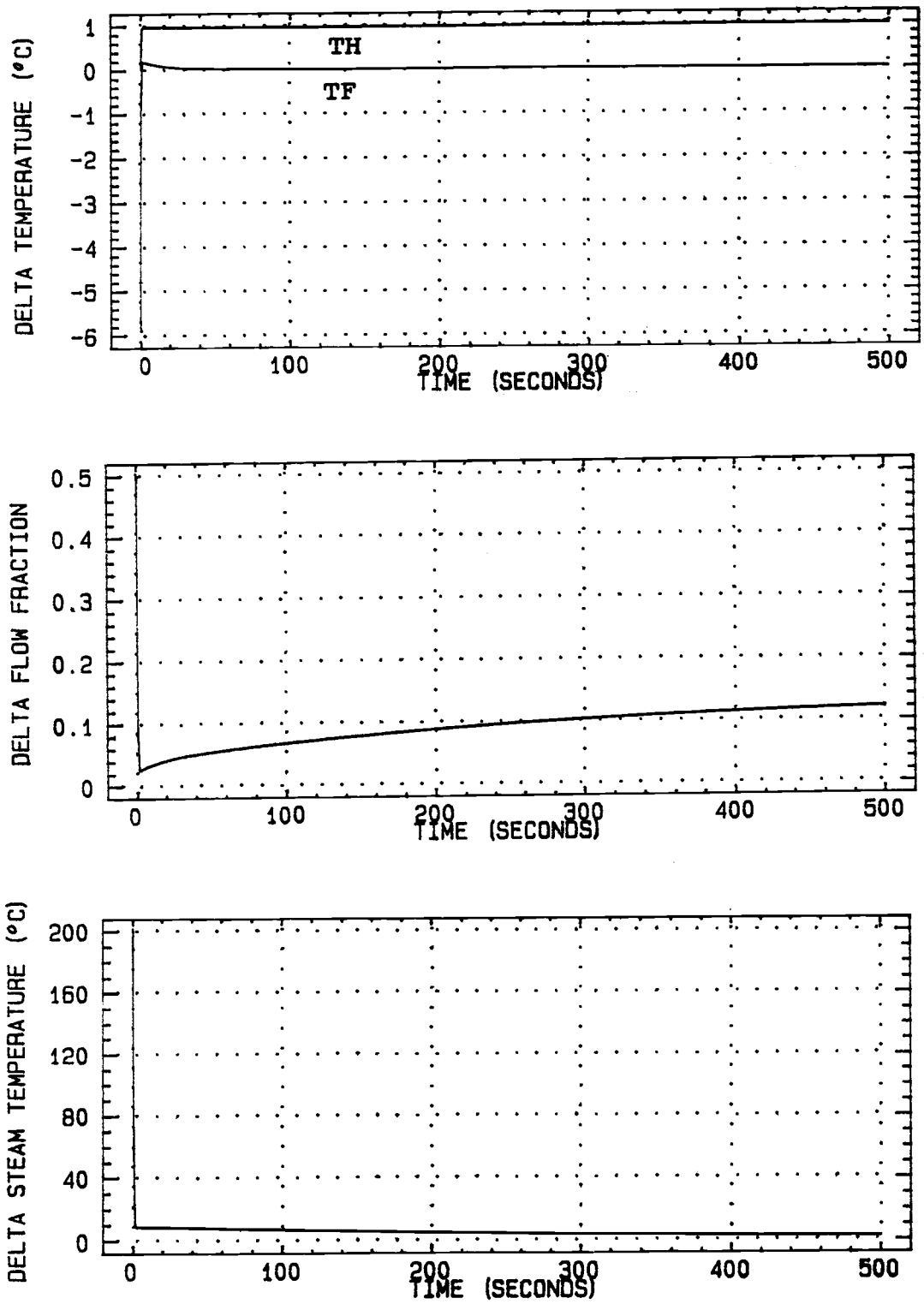

Fig. 20. Closed-loop output and manipulated variable responses to a 1 °C set point change in TH using the nonlinear model and Cohen-Coon PI tuning parameters

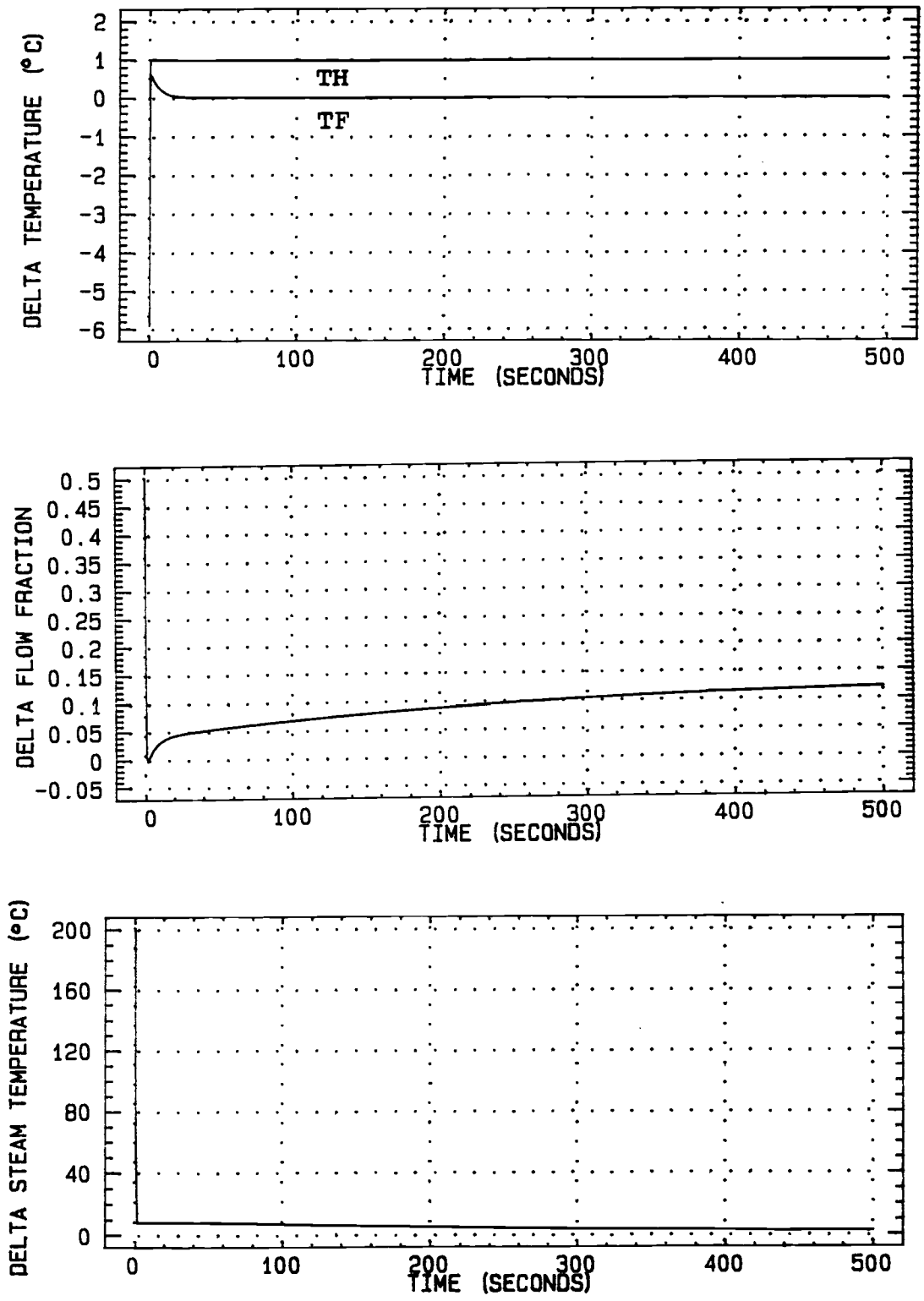

Fig. 21. Closed-loop output and manipulated variable responses to a 1 °C set point change in TH using the nonlinear model and the modified Ziegler-Nichols PI tuning parameters

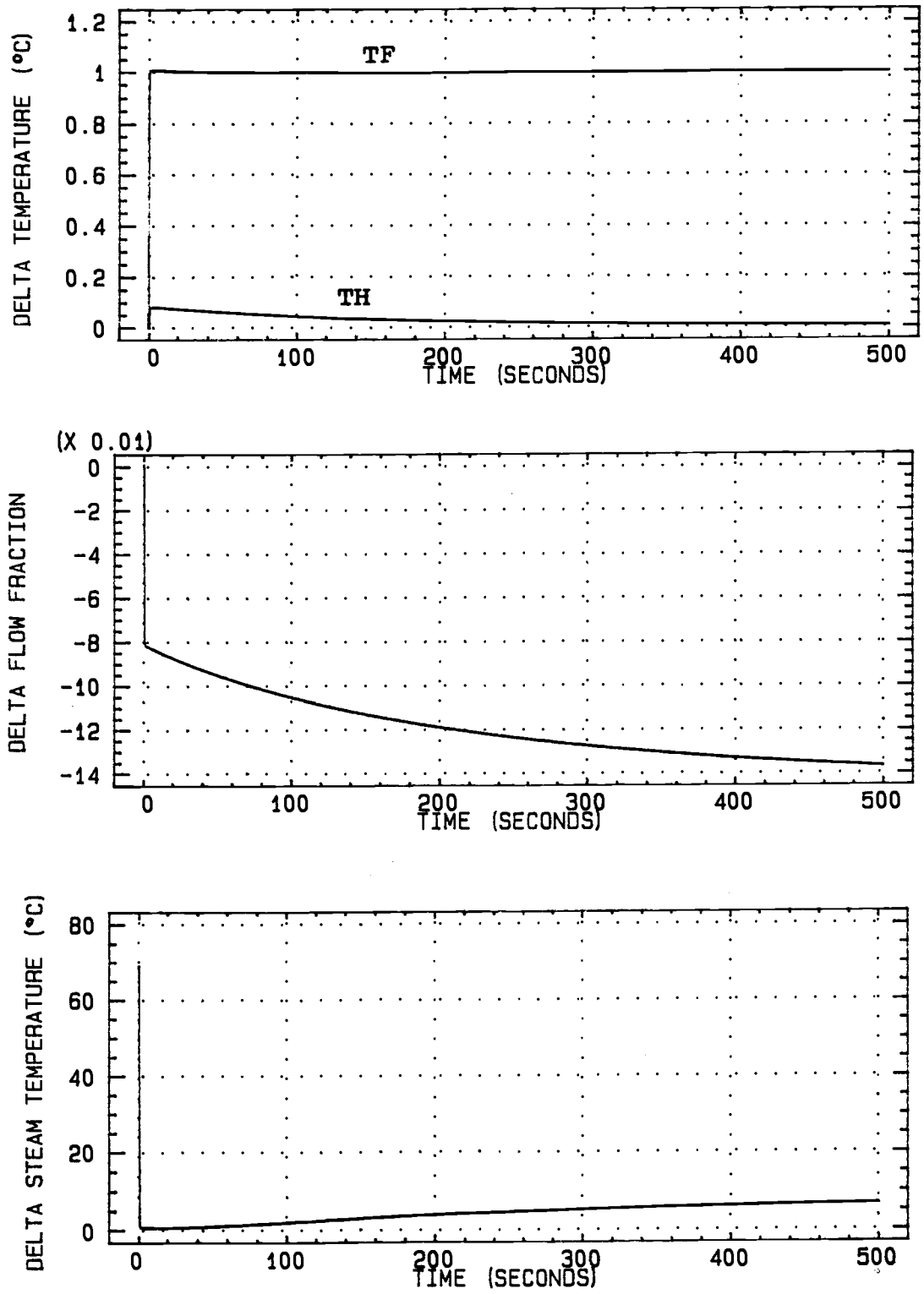

Fig. 22. Closed-loop output and manipulated variable responses to a 1 °C set point change in TF using the nonlinear model and Cohen-Coon PI tuning parameters

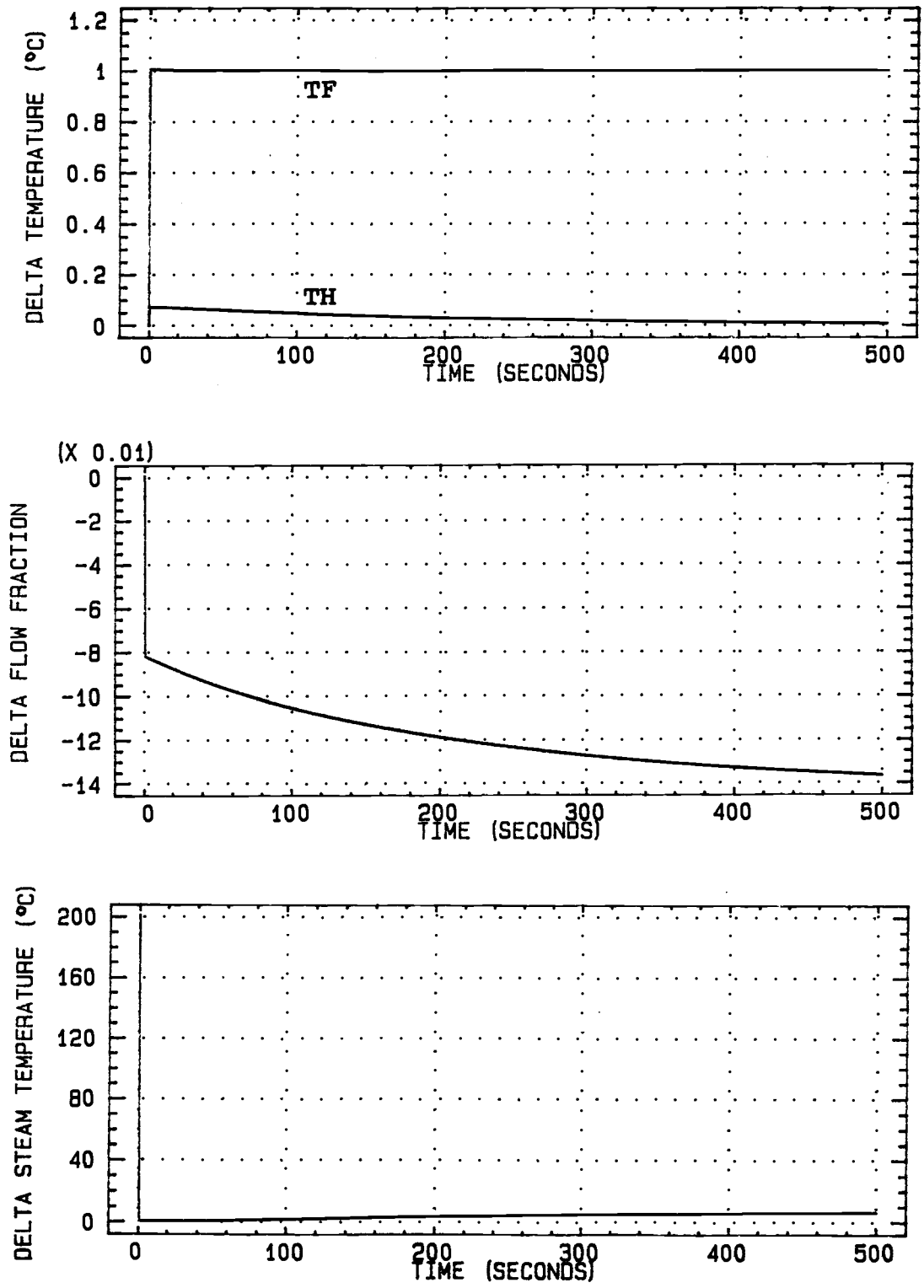

Fig. 23. Closed-loop output and manipulated variable responses to a 1 °C set point change in TF using the nonlinear model and the modified Ziegler-Nichols PI tuning parameters

tuning parameters, respectively. From the plots of the response, TF is shown to drop immediately 6 °C which is considered marginally acceptable. From the manipulated variable responses, it can be seen that the initial response is to close the bypass valve and allow the steam temperature to go to its maximum constraint value. Even with the large differences between the C-C and Z-N tuning parameters, the closed-loop responses are nearly identical for the set point changes investigated due to the manipulated variable constraints. The constraints are shown to be the reason for the similarity by Figures 22 and 23, where the initial actions taken by the controller are not confined to the maximum constraint value.

Figures 22 and 23 show the nonlinear closed-loop output and manipulated variable responses to a set point change of 1.0 °C in TF using C-C and modified Z-N PI tuning parameters, respectively. These plots show that although the closed-loop responses are nearly identical, the modified Z-N tuning parameters initially force the steam temperature to the maximum constraint value while the C-C parameters call for much smaller initial deviations. The difference in the controller gains from the two tuning methods is now evident. The large Z-N gain forces TS to the constraint value, while the C-C gain requires much less initial deviation in TS and

yields nearly the same response.

Figures 24 and 25 show the closed-loop output and manipulated variable responses using detuned PI controllers to set point changes of 1 °C for TH and TF, respectively, for the nonlinear model. The detuned PI parameters are the same as above. These responses are much slower than those of Figures 20 through 23, which is to be expected by the much smaller controller gains.

Internal Model Control method

The Internal Model Control (IMC) algorithm differs from the PI control algorithm as it is a multivariable rather than multiloop control scheme. IMC compensates for the interactions by incorporating a process model. Control actions are taken based upon the difference between the actual process output and the output predicted by the internal process model. By basing the control response on a model, IMC allows for interactions between manipulated variables and the off diagonal outputs. The differences between the ordinary feedback control and the IMC control diagrams can be seen in the block diagrams of Figure 26. Figure 26a shows the block diagram for an ordinary feedback control structure. Figure 26b shows the block diagram for a feedback controller with a process model added to the controller

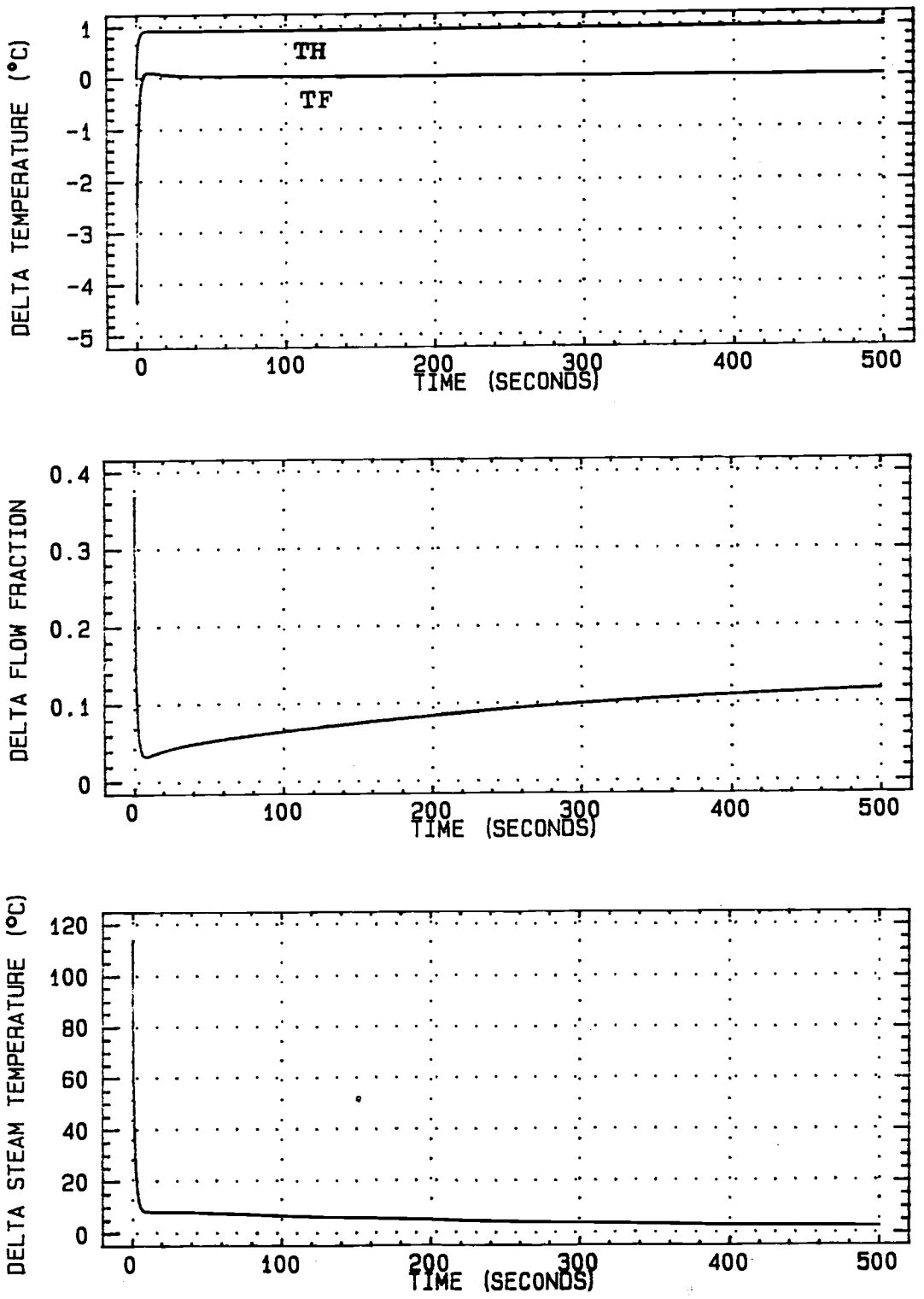

Fig. 24. Closed-loop output and manipulated variable responses to a 1 °C set point change in TH using the nonlinear model and detuned tuning parameters

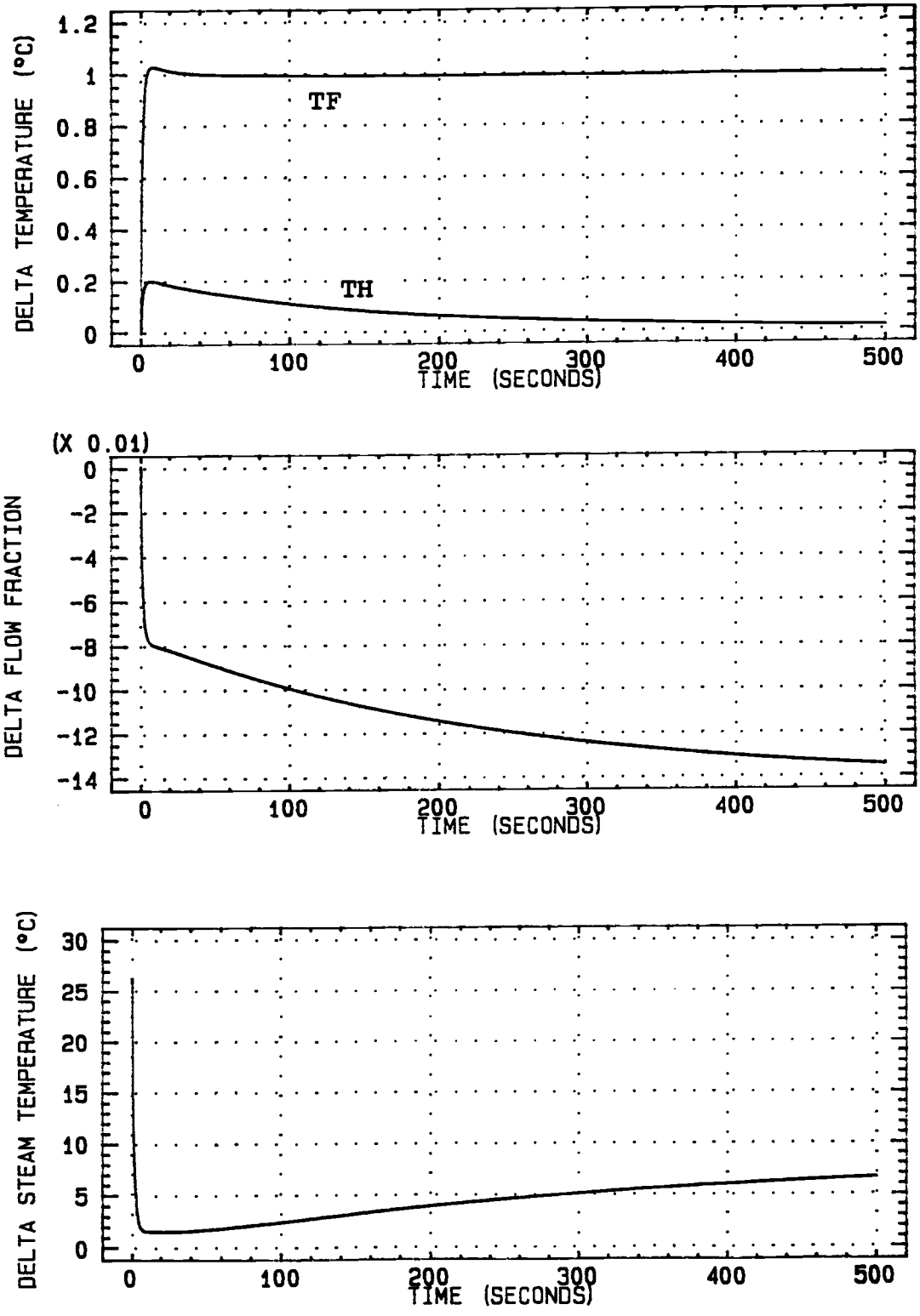

Fig. 25. Closed-loop output and manipulated variable responses to a 1 °C set point change in TF using the nonlinear model and detuned tuning parameters

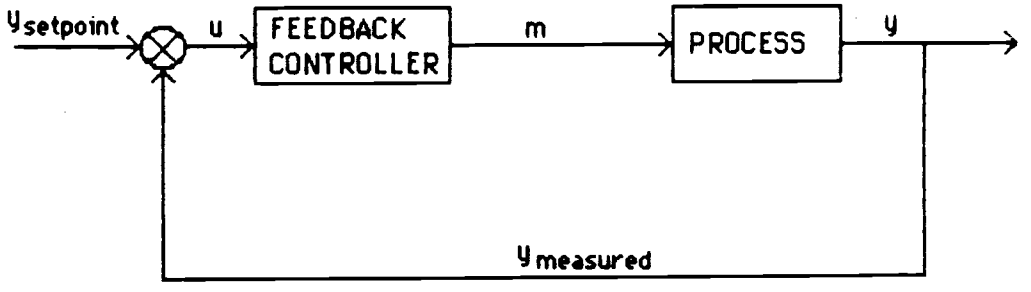

Fig. 26a. Standard feedback control block diagram

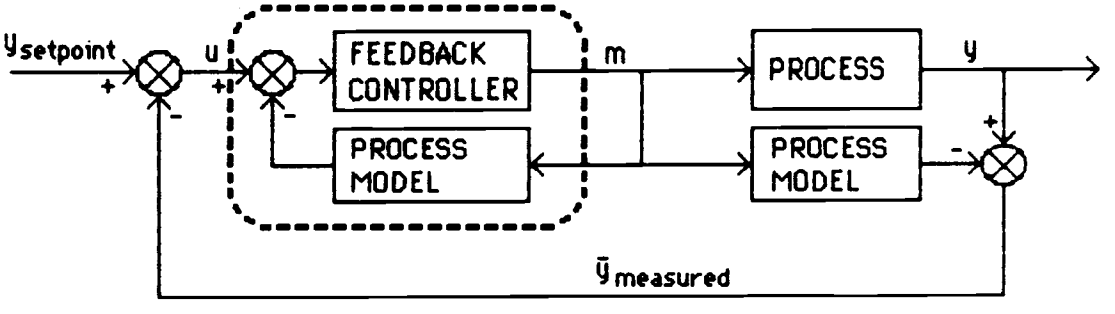

Fig. 26b. Combined feedback control with process model in parallel to create IMC control block diagram

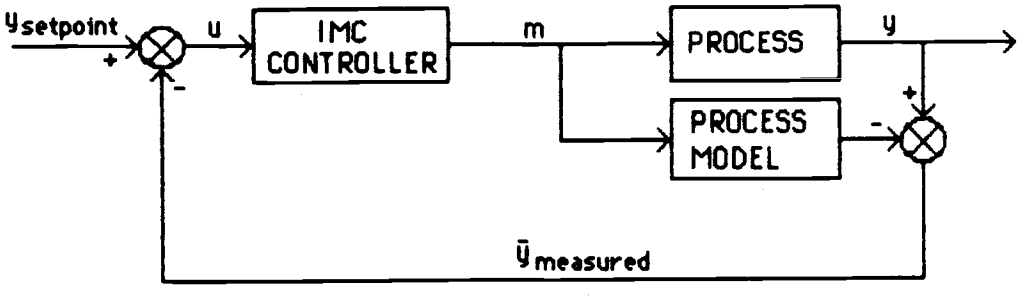

Fig. 26c. IMC control block diagram

and in parallel with the process. The dashed lines show how the controller and process model are combined into the IMC control structure of figure 26c.

The five IMC algorithm tuning parameters have been described in Garcia and Morari (1982) along with advice on how to choose the tuning parameters for different models of the plant. Each of the parameters, their description and suggestions on how to choose the values are shown in Table 27. The parameter values used in the IMC simulations are shown in Table 28.

In this section linear simulations based upon both linear and nonlinear step responses are simulated. An approximate process model created by STEPG in order to test the robustness of IMC in the more normal event of plant-model mismatch is also simulated. The IMC simulation program EIMC (Levien, 1988) uses the impulse response coefficients (IRC) of the open-loop step response of each output to a step change in each manipulated variable to determine the closed-loop response to a set point change. The IRCs for the linear open-loop step response are calculated by the program LAPLCTX written for this thesis. The IRCs for the nonlinear open-loop response are calculated by program IMPULSE using the output from the simulation program DTHES2. The IRCs for the approximate process models are calculated by program STEPG. As the best TF/X STEPG

Table 27. Description of the IMC tuning parameters and suggestions for their values

N - Number of IRCs being used

T - Sampling Time - any integer value, increase T for stability

M - Input Suppression Parameter - for perfect control M = P = N, decrease M for stability

β_i - Input Penalty Parameter Matrix - increase β_i for stability, $\beta_i \neq 0$ leads to offset

γ_i - Output Penalty Parameter - use $\gamma_i = 1$ unless γ_i is time varying

P - Optimization Horizon - increase P for stability

TAU - Time Delay

Table 28. IMC tuning parameter values used in the EIMC simulations

N = 20	$\gamma(1,1) = 1$
	$\gamma(1,2) = 0$
T = 45	$\gamma(2,1) = 0$
	$\gamma(2,2) = 1$
M(1) = 20	
M(2) = 20	P = 20 (perfect control)
$\beta(1,1) = 0$	TAU(1,1) = 1
$\beta(1,2) = 0$	TAU(1,2) = 1
$\beta(2,1) = 0$	TAU(2,1) = 1
$\beta(2,2) = 0$	TAU(2,2) = 1

fits are those that use the maximum deviation as the old steady state, IRCs from STEPG have to be modified to reflect the large initial deviation in the open-loop step response of TF/X by adding the initial negative response value to the first IRC value. As the maximum model truncation order (N) for program EIMC is 20, the IRCs are determined using a sampling time (T) of 45 seconds to a final time of 900 seconds.

Tables 29 and 30 show the linearized exact and strictly proper inverse Laplace transfer function equations, respectively, used to determine the IRCs in program LAPLCTX.

All simulations using program EIMC use IRCs from the nonlinear model as the plant since this is the exact response derived from the differential equations. Although the IRCs are from the nonlinear model, the actual simulation is a linear simulation based upon the nonlinear model.

Figures 27 and 28 show EIMC simulated closed-loop responses to set point changes using the linear model IRCs in the IMC controller algorithm and the nonlinear model IRCs for the plant and should be compared to Figures 14 through 17. This indicates that multivariable IMC controllers may be more robust than multiple PI feedback controllers.

Figure 27 shows the EIMC simulated closed-loop

Table 29. Inverse Laplace linearized exact (non-strictly proper) equations for determining impulse response coefficients for EIMC

$$\overline{\frac{TF}{X}} = -0.84433 - 11.244 * \exp(-0.54061E\text{-}2 * t) + 2 * \exp(-0.040916 * t) * [0.14415 * \cos(0.1153E\text{-}2 * t) + 6.4395 * \sin(0.1153E\text{-}2 * t)]$$

$$\overline{\frac{TF}{TS}} = 0.10612 - 0.05899 * \exp(-0.54061E\text{-}2 * t) + 2 * \exp(-0.040916 * t) * [-0.023565 * \cos(0.1153E\text{-}2 * t) + 0.18572 * \sin(0.1153E\text{-}2 * t)]$$

$$\overline{\frac{TH}{X}} = 6.8272 - 9.0619 * \exp(-0.54061E\text{-}2 * t) + 2 * \exp(-0.040916 * t) * [1.1173 * \cos(0.1153E\text{-}2 * t) + 18.405 * \sin(0.1153E\text{-}2 * t)]$$

$$\overline{\frac{TH}{TS}} = 0.1419 - 0.047545 * \exp(-0.54061E\text{-}2 * t) + 2 * \exp(-0.040916 * t) * [-0.047177 * \cos(0.1153E\text{-}2 * t) + 0.53493 * \sin(0.1153E\text{-}2 * t)]$$

Table 30. Inverse Laplace linearized strictly proper equations for determining impulse response coefficients for EIMC

$$\overline{\frac{TF}{X}} = -0.84433 - 11.305 * \exp(-0.54061E\text{-}2 * t) + 11.865 * \exp(-t) + 2 * \exp(-0.040916 * t) * [0.14232 * \cos(0.11465E\text{-}2 * t) + 6.7547 * \sin(0.11465E\text{-}2 * t)]$$

$$\overline{\frac{TF}{TS}} = 0.10612 - 0.059311 * \exp(-0.54061E\text{-}2 * t) + 0.27967E\text{-}2 * \exp(-t) + 2 * \exp(-0.040916 * t) * [-0.024803 * \cos(0.11465E\text{-}2 * t) + 0.1947 * \sin(0.11465E\text{-}2 * t)]$$

$$\overline{\frac{TH}{X}} = 6.8272 - 9.1112 * \exp(-0.54061E\text{-}2 * t) + 0.67588E\text{-}4 * \exp(-t) + 2 * \exp(-0.040916 * t) * [1.1419 * \cos(0.11465E\text{-}2 * t) + 19.301 * \sin(0.11465E\text{-}2 * t)]$$

$$\overline{\frac{TH}{TS}} = 0.1419 - 0.047803 * \exp(-0.54061E\text{-}2 * t) + 0.56245E\text{-}2 * \exp(-t) + 2 * \exp(-0.040916 * t) * [-0.04986 * \cos(0.11465E\text{-}2 * t) + 0.56083 * \sin(0.11465E\text{-}2 * t)]$$

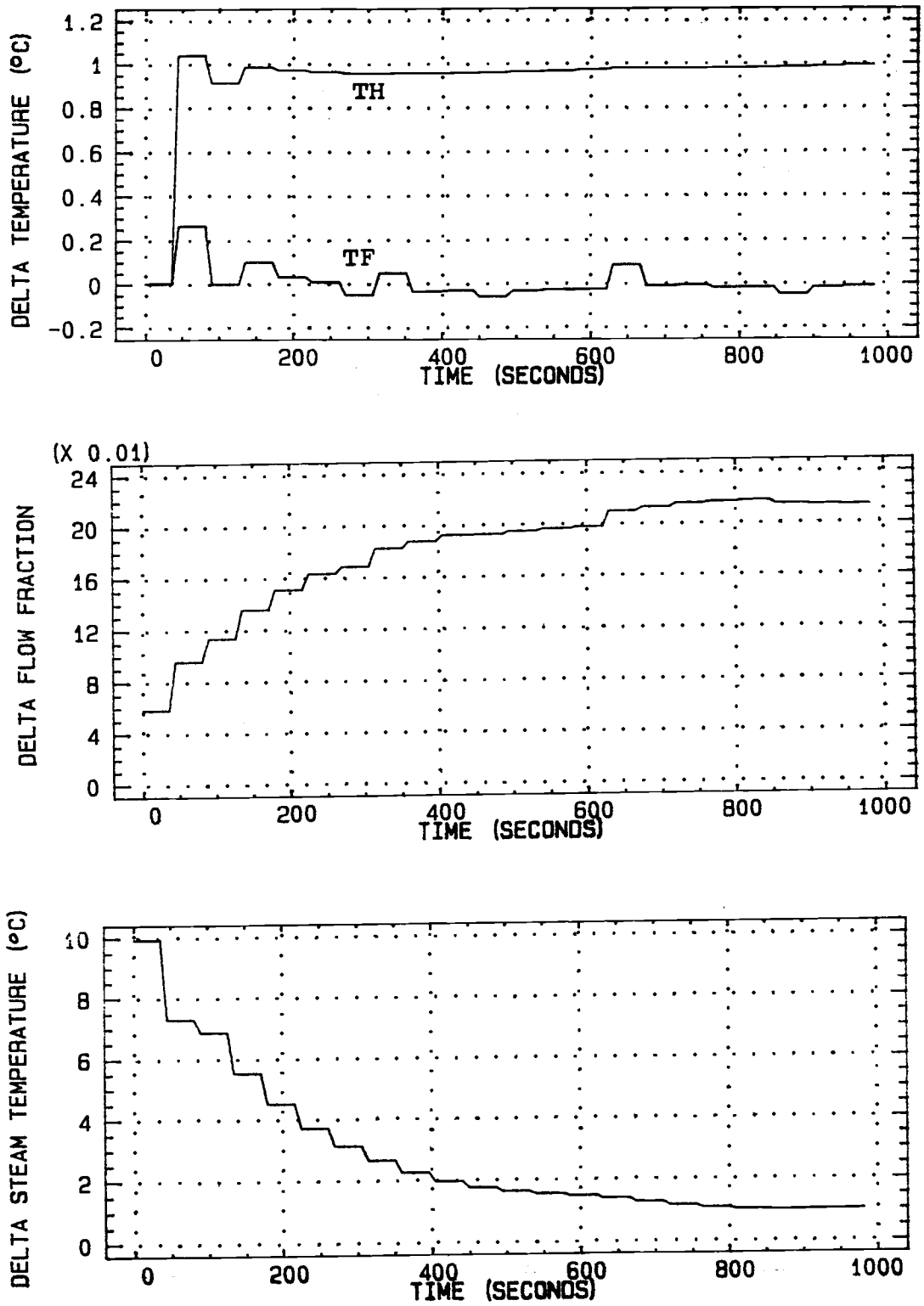

Fig. 27. IMC closed-loop output and manipulated variable responses to a 1 °C set point change in TH using the linear model and nonlinear plant

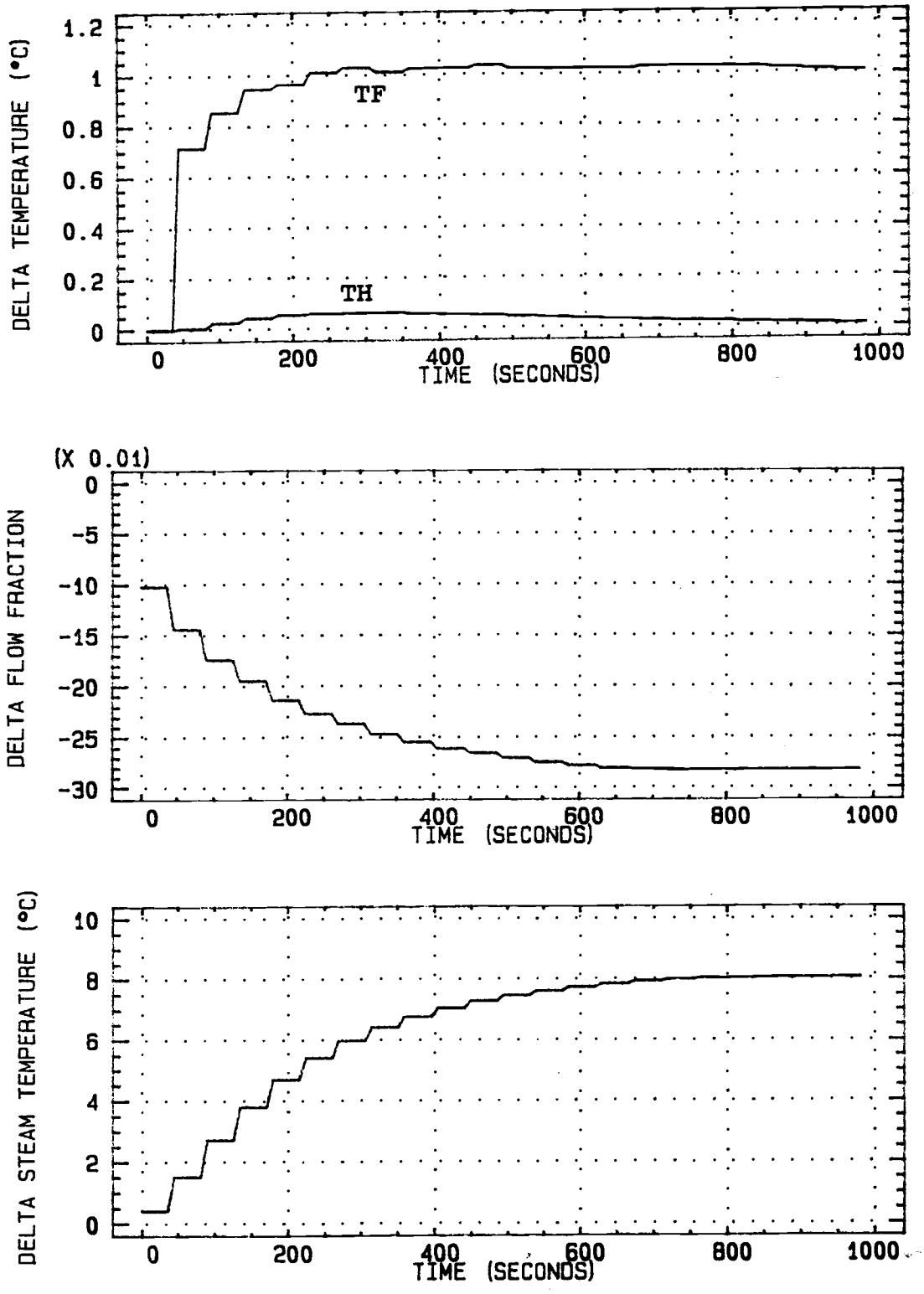

Fig. 28. IMC closed-loop output and manipulated variable responses to a 1 °C set point change in TF using the linear model and nonlinear plant

response to a set point change of 1.0 °C in TH and should be compared with the continuously oscillating closed-loop response of Figures 14 and 15.

Figure 28 shows the EIMC simulated closed-loop response to a set point change of 1.0 °C in TF and should be compared with the continuously oscillating response of Figures 16 and 17.

Figures 29 and 30 show the EIMC simulated closed-loop responses to set point changes of the linear model IRCs in both the IMC controller algorithm and the plant and should be compared to Figures 14 through 19. Figures 31 and 32 show the EIMC simulated closed-loop responses to set point changes of the nonlinear model IRCs in both the IMC controller algorithm and the plant and should be compared to Figures 20 through 25. These four sets of closed-loop responses assume complete knowledge of the system, that is, no plant-model mismatch. This is the same assumption made in Figures 14 through 25.

Figures 29 and 30 show the EIMC simulated closed-loop responses to set point changes of 1.0 °C in TH and TF, respectively. These plots show no deviation from the set point after the initial step is taken in either output. This compares with the continuously oscillatory response of Figures 14 through 17 and the stable, but highly oscillatory response of Figures 18 and 19.

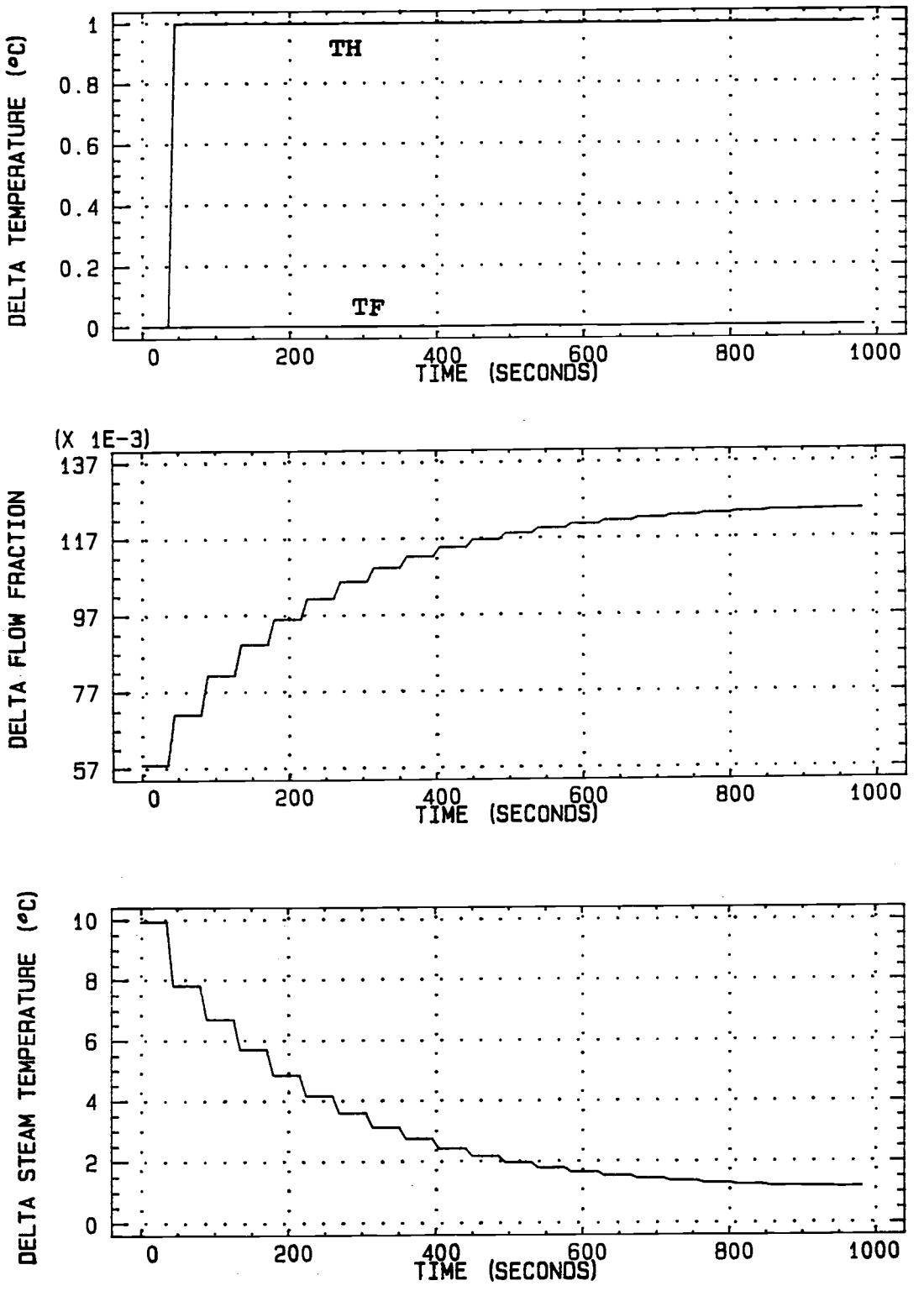

Fig. 29. IMC closed-loop output and manipulated variable responses to a 1 °C set point change in TH using the linear model and linear plant

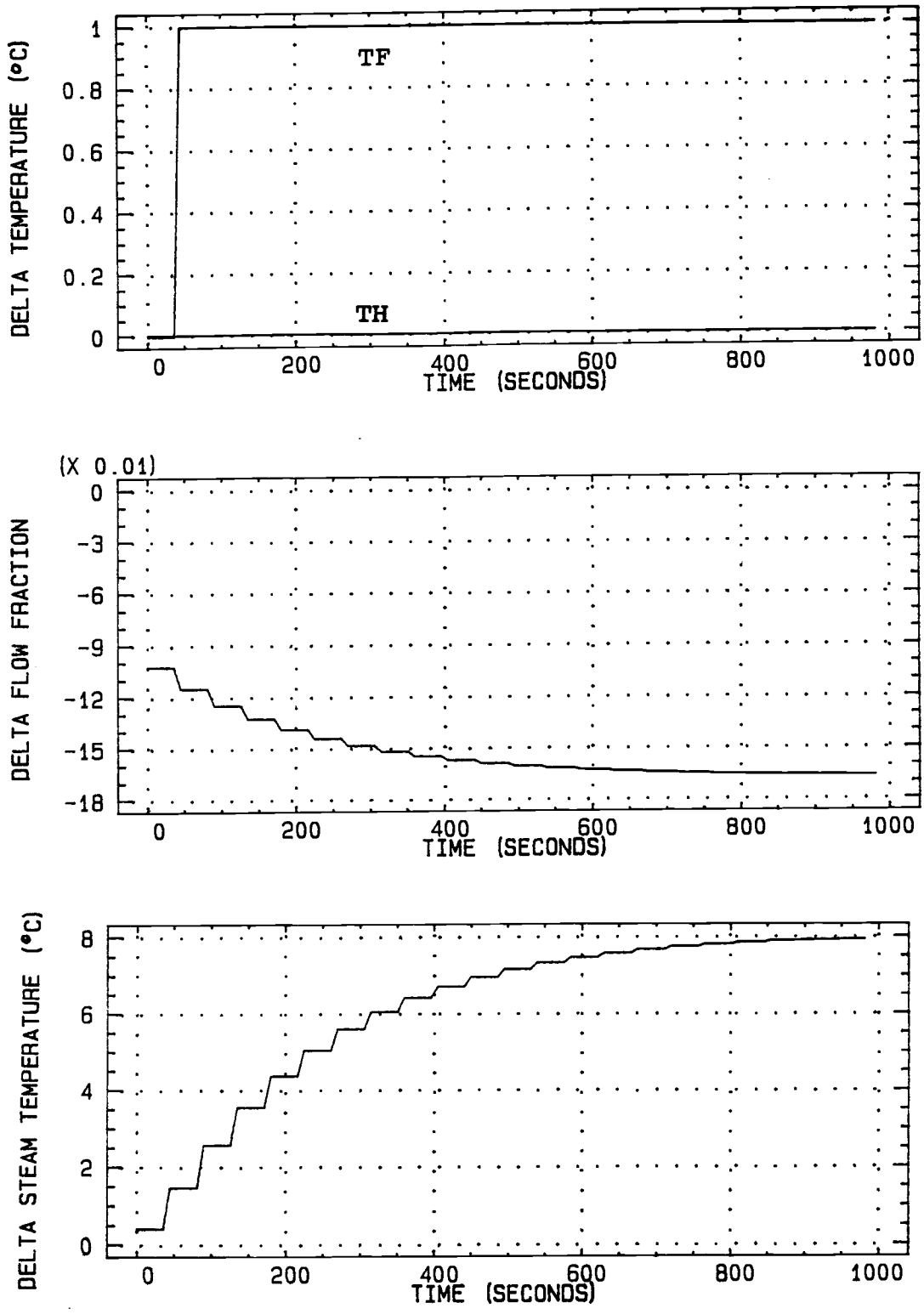

Fig. 30. IMC closed-loop output and manipulated variable responses to a 1 °C set point change in TF using the linear model and linear plant

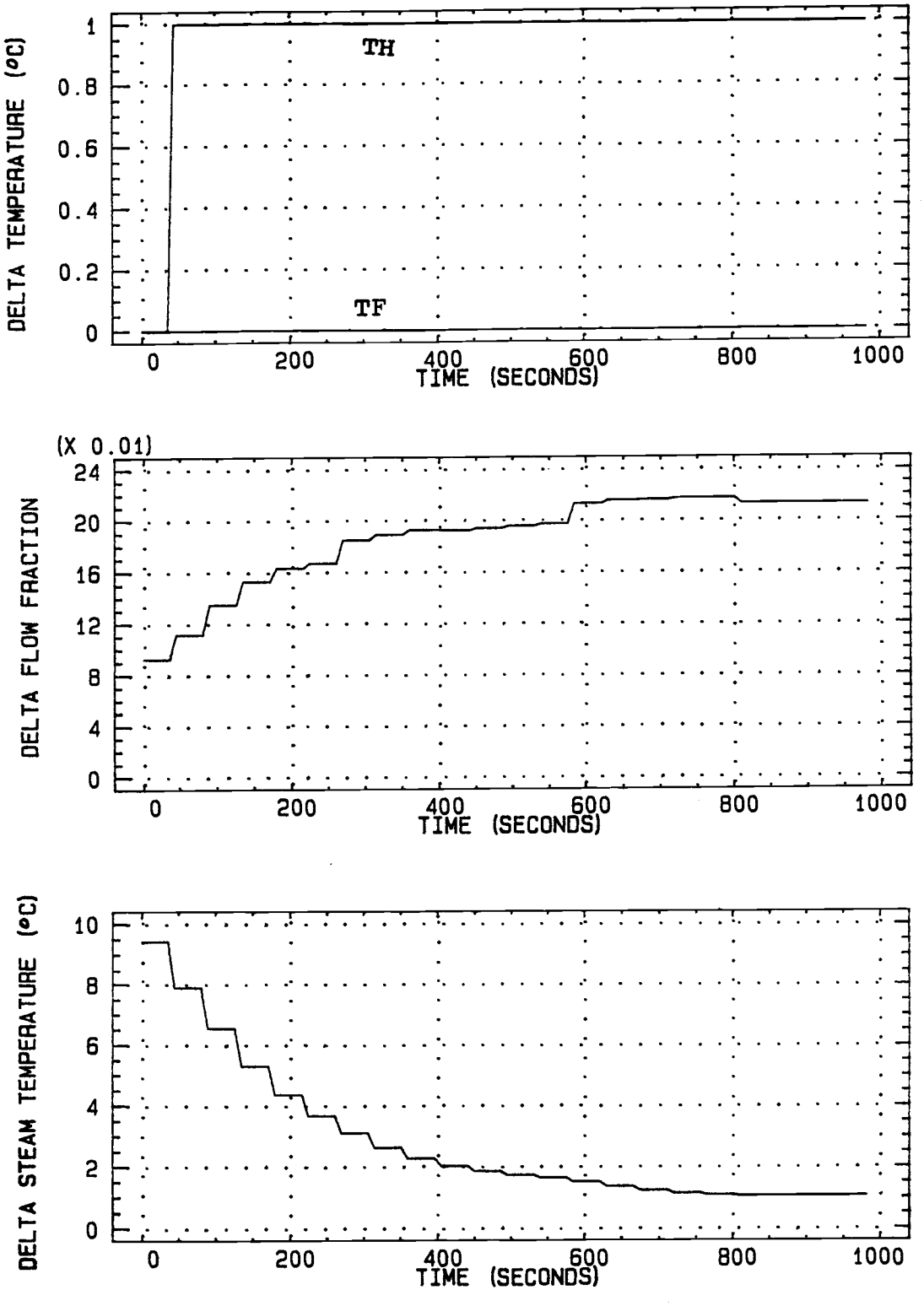

Fig. 31. IMC closed-loop output and manipulated variable responses to a 1 °C set point change in TH using the nonlinear model and nonlinear plant

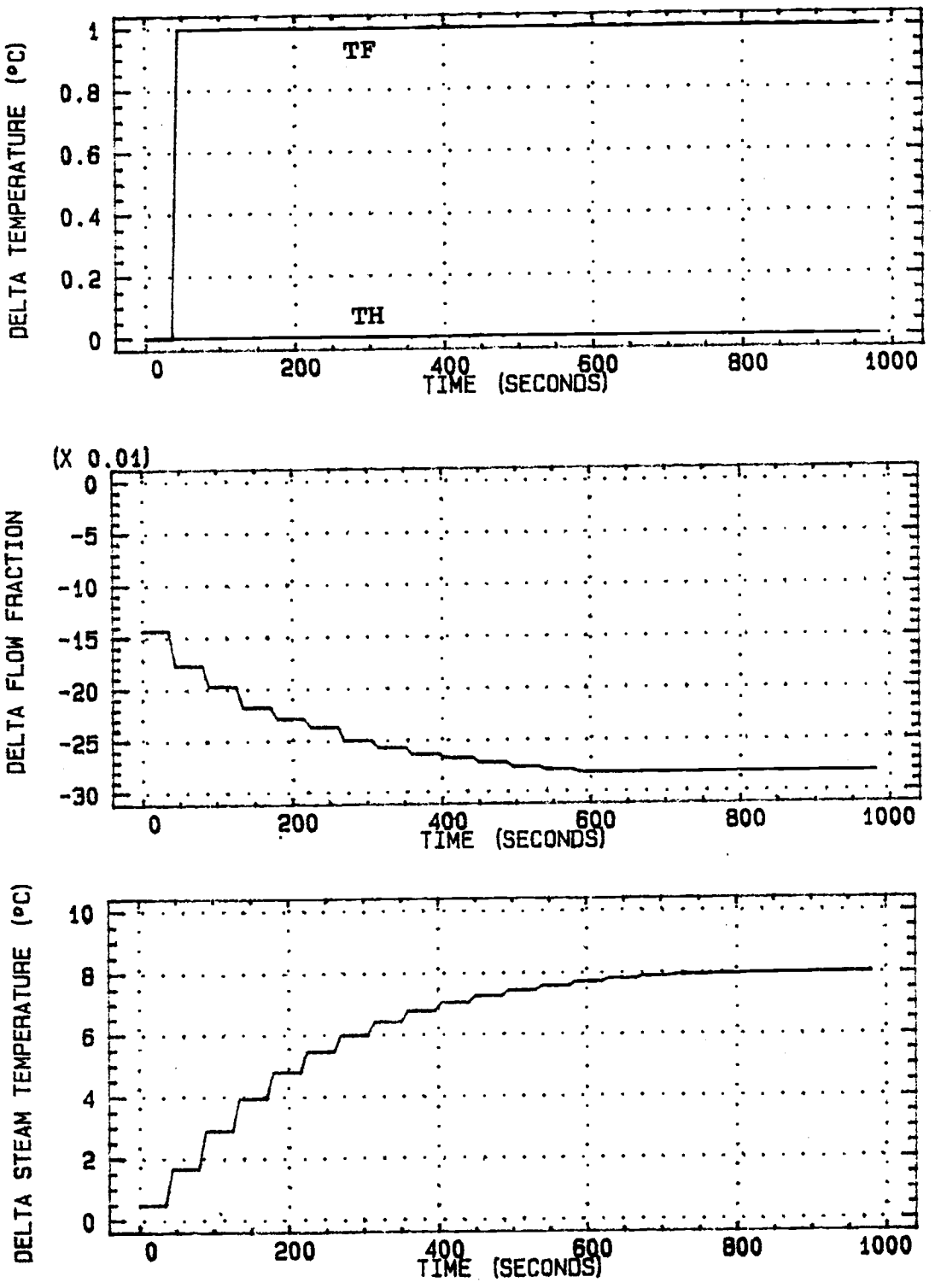

Fig. 32. IMC closed-loop output and manipulated variable responses to a 1 °C set point change in TF using the nonlinear model and nonlinear plant

Figures 31 and 32 show the EIMC simulated closed-loop responses to a set point change of 1.0 °C in TH and TF, respectively. These plots show no deviation from the setpoint after the initial step is taken in either output. Figure 31 compares with Figures 20 and 21 which have initial offset and then settle to the set point for TH and show a large initial negative deviation then overshoot the set point before finally reaching the set point for TF. Figure 32 compares with Figures 22 and 23 which overshoot the TF set point then settle quickly at the set point and have an initial deviation from the TH set point with a very slow settling to the set point. An advantage of the IMC controller is that the manipulated variables do not slam against the constraints as they do when two PI controllers are used.

Since it is very rare to have no plant-model mismatch, it is reasonable to use an approximate process model to see how plant-model mismatch affects the IMC closed-loop response to set point changes. A process model was created using program STEPG to fit the nonlinear open-loop step response. The model types for each of the transfer functions are shown in Table 31. Table 32 shows the model parameters used by program STEPG to calculate the model responses for each transfer function.

Figures 33 through 36 show comparisons of the open

Table 31. Approximate models for the nonlinear response determined by STEPG for creating impulse response coefficient files for EIMC

$\overline{TF}_X$ models:	1st order critically damped 2nd order
$\overline{TF}_{TS}$ models:	1st order overdamped 2nd order
$\overline{TH}_X$ models:	1st order critically damped 2nd order
$\overline{TH}_{TS}$ models:	1st order overdamped 2nd order

Table 32. Model parameters used in STEPG

Model Name	Model Type*	Initial Steady-State output Value	Steady-State Gain	System Time Constant
TFX	6	-9.780171	9.20604	124.9969
TFTS	7	1.3307E-2	9.29E-2	61.18570
THX	6	3.3480E-4	3.99598	107.4922
THTS6	7	2.5512E-3	0.01395	57.00140

* Model Type refers to model used in STEPG.
Type 6 - 1st over 2nd order critically damped
Type 7 - 1st over 2nd order overdamped

Model Name	Time Delay	Damping Factor	PHI
TFX	-4.5329	1.0	125.235
TFTS	-5.4E-2	1.69369	85.4714
THX	28.7798	1.0	60.1825
THTS6	1.09062	1.85141	137.204

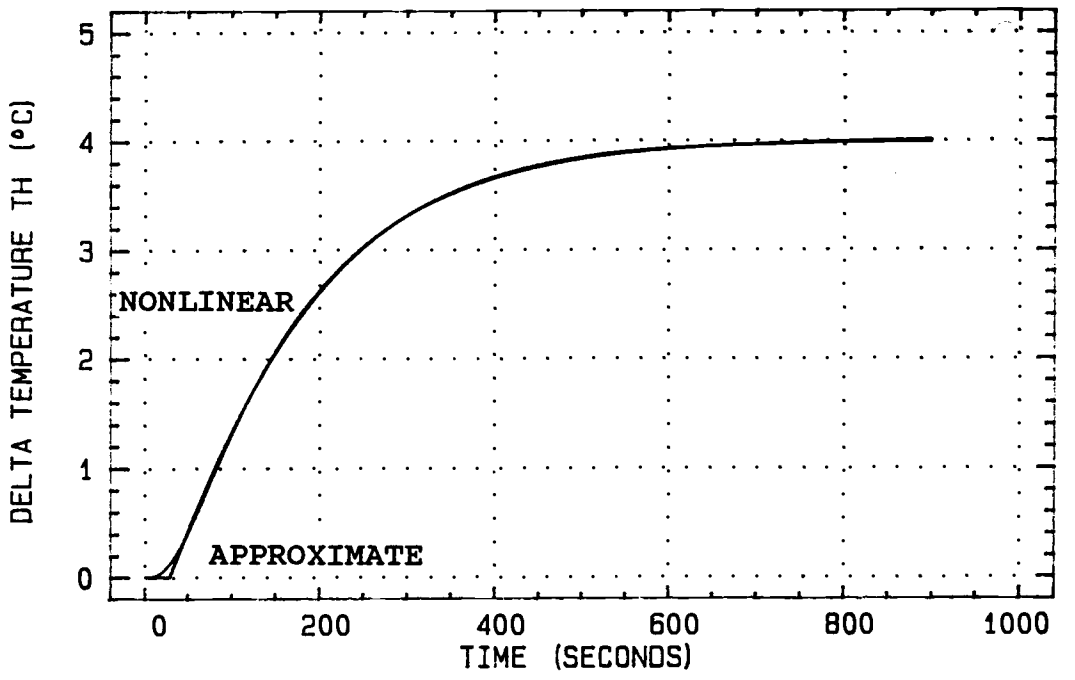

Fig. 33. Open-loop responses to a unit step change in X for the approximate and nonlinear models for TH

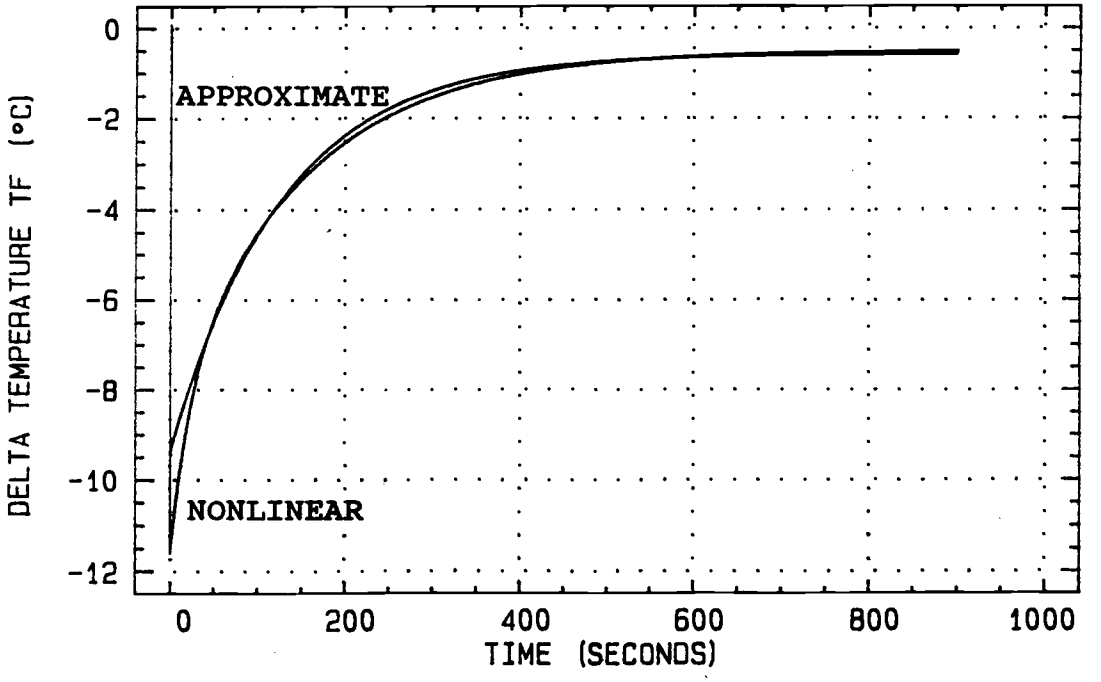

Fig. 34. Open-loop responses to a unit step change in X for the approximate and nonlinear models for TF

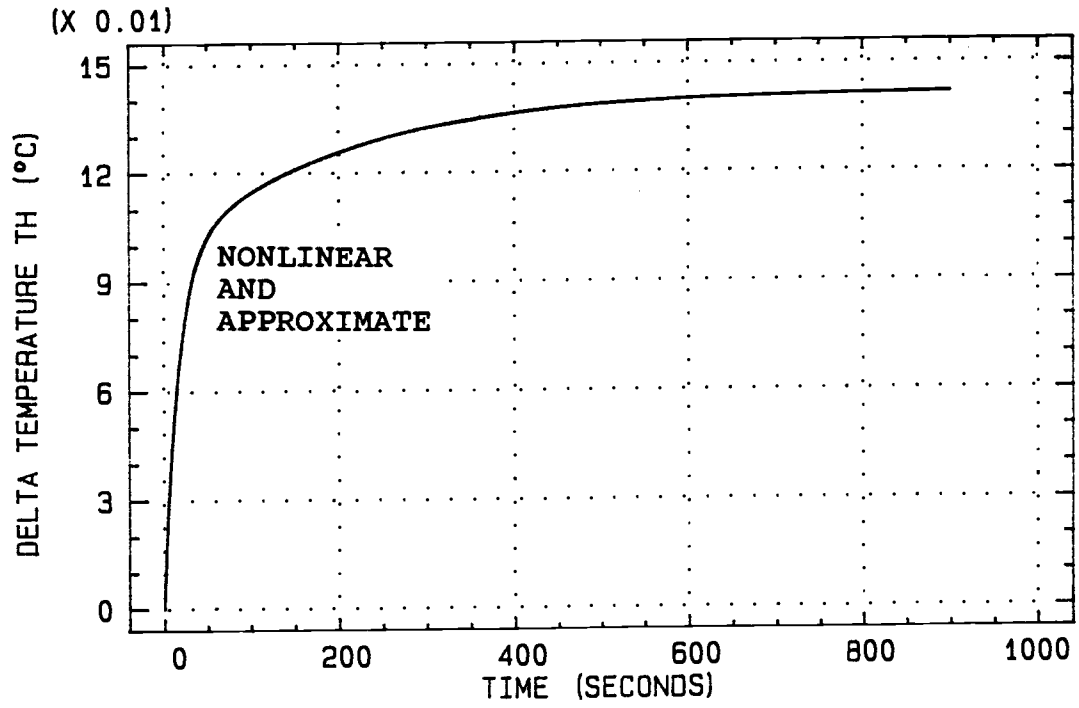

Fig. 35. Open-loop responses to a unit step change in TS for the approximate and nonlinear models for TH

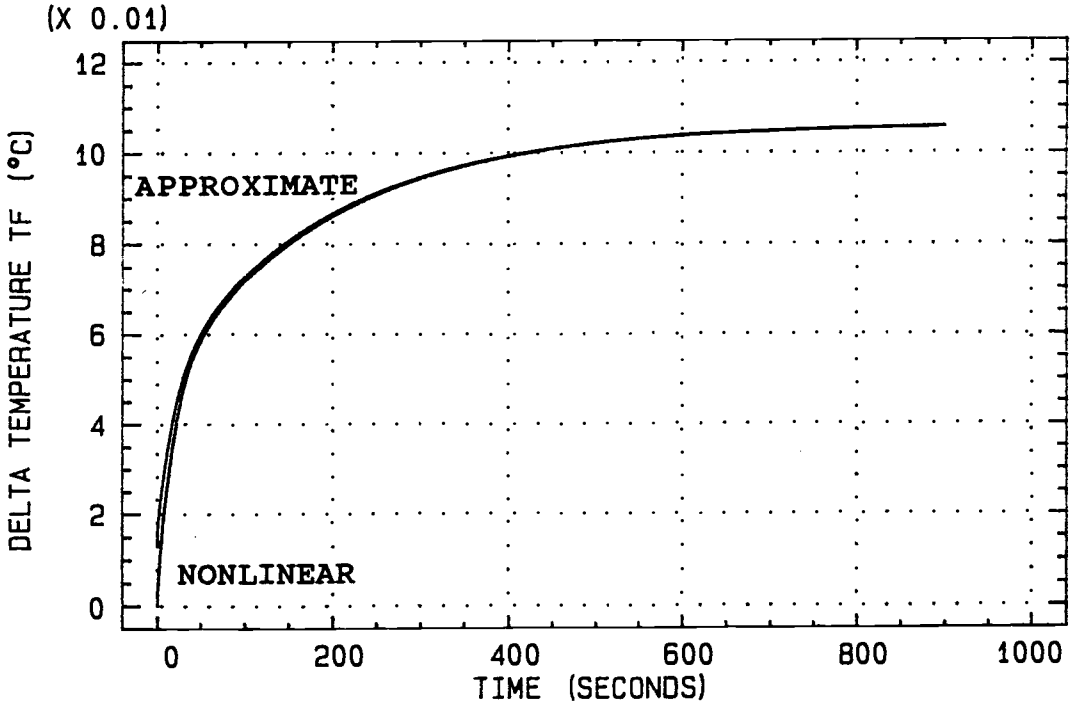

Fig. 36. Open-loop responses to a unit step change in TS for the approximate and nonlinear models for TF

loop step response of approximate process models with the nonlinear process model using program STEPG for each transfer function.

Figure 33 shows the open-loop comparison for the TH/X transfer function using a 1st over 2nd order critically damped model and the nonlinear process model. With the exception of the dead time in the model the response is very close to the nonlinear response and is a very good process approximation.

Figure 34 shows the open-loop comparison for the TF/X transfer function using a 1st over 2nd order critically damped model and the nonlinear process model. Although the initial approximately 120 seconds of the model's response deviates slightly from the nonlinear response, the use of this process model is reasonable.

Figure 35 shows the open-loop comparison for the TH/TS transfer function using a 1st over 2nd order overdamped model and the nonlinear process model. This is a very good approximate process model with very little deviation from the nonlinear open-loop step response.

Figure 36 shows the open-loop comparison for the TF/TS transfer function using a 1st over 2nd order overdamped model and the nonlinear process model. This is a very good approximate process model with very little deviation from the nonlinear open-loop response.

Using the IRCs from the approximate models above and the nonlinear model IRCs as the plant in the IMC control algorithm yields the closed-loop responses shown in Figures 37 and 38 to a set point change of 1 °C in TH and TF, respectively. In comparison to the responses using the linear model as the internal model, these responses are similar for a change in TH and are better for a change in TF.

REMARKS

1. Even with the drastic difference between the Cohen-Coon and Ziegler-Nichols PI tuning parameters the closed-loop responses are very similar for both linear and nonlinear models. Although the similarity may be partly caused by the constraints on the manipulated variables, this is not the only cause as the responses are similar even when the constraints are not reached as in Figure 22. Therefore, there is not one set of correct tuning parameters but there may be many sets of parameters that yield similar closed-loop response to set point changes. Although the responses are similar, they are not identical and output specifications may favor one set of tuning parameters over another. Although the responses to set point changes are similar, the closed-loop response to input disturbances may be

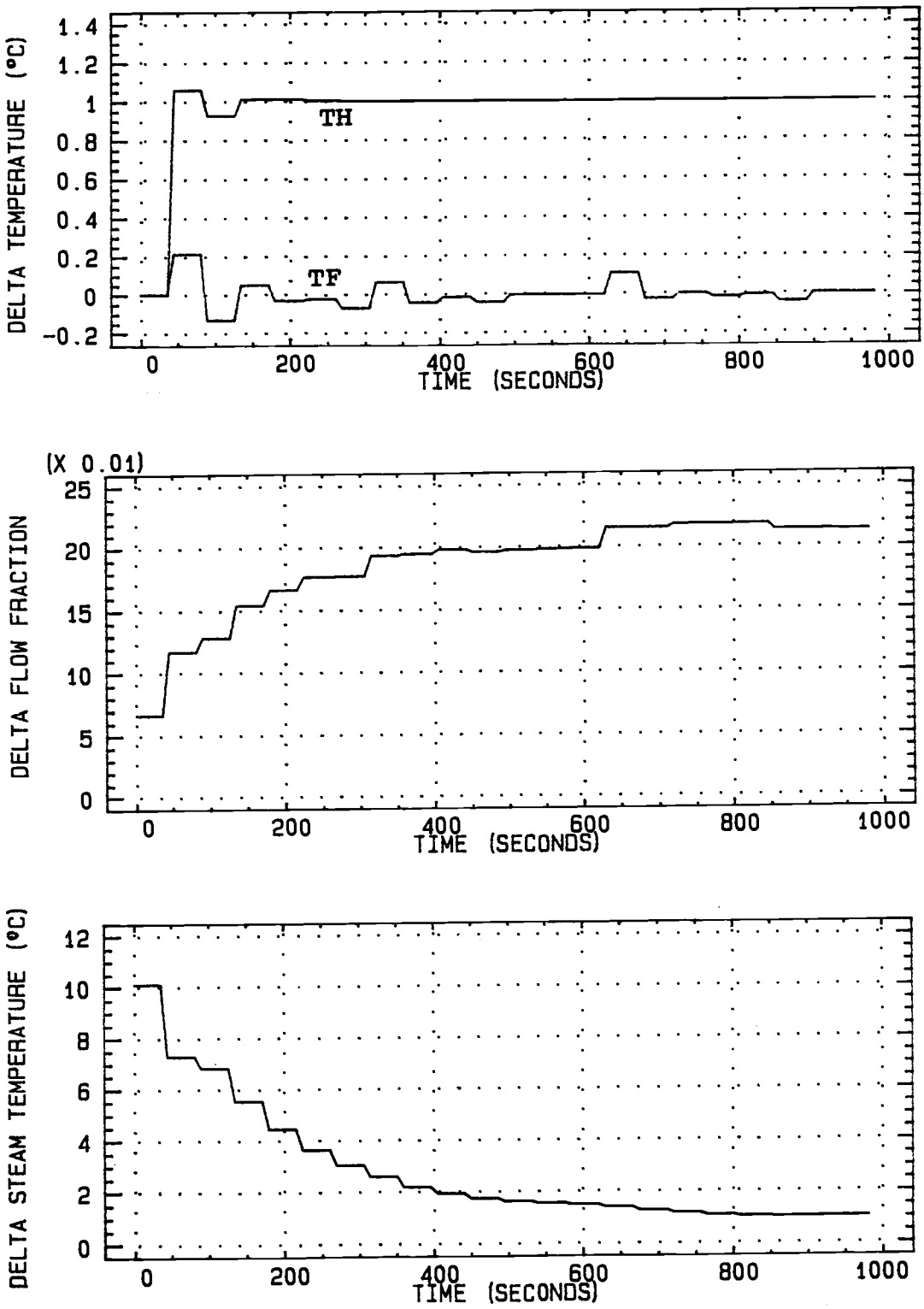

Fig. 37. IMC closed-loop output and manipulated variable responses to a 1 °C set point change in TH using the approximate model and the nonlinear plant

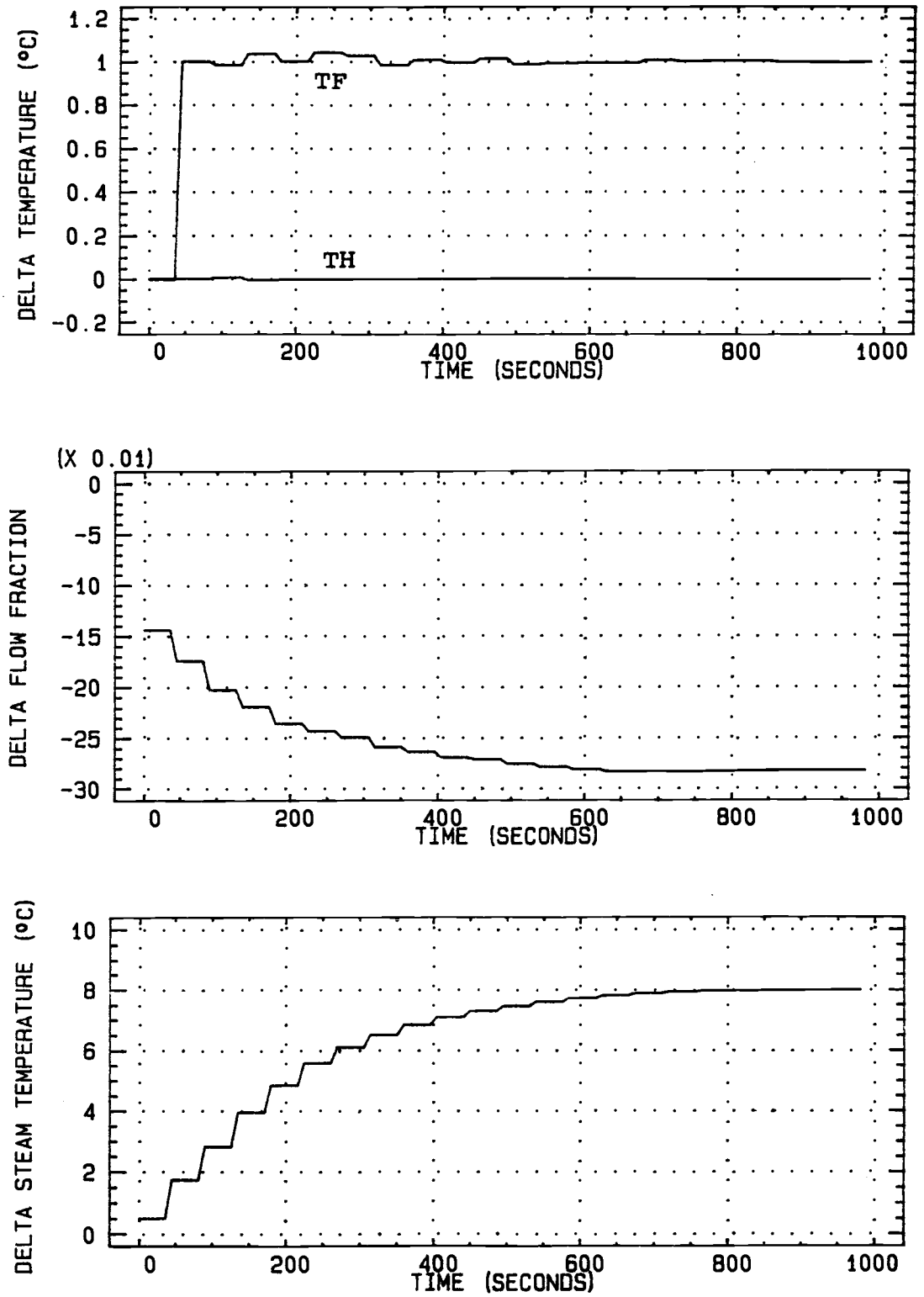

Fig. 38. IMC closed-loop output and manipulated variable responses to a 1 °C set point change in TF using the approximate model and the nonlinear plant

different and could be an area of further study.

2. Neither Cohen-Coon nor Ziegler-Nichols PI tuning parameters work for set point changes of the linear model. In both cases the closed-loop responses continuously oscillate and manipulated variables continuously oscillate between their minimum and maximum constraint values. Detuning the controllers resulted in stable yet highly oscillatory, unacceptably slow responses.

3. Both Cohen-Coon and Ziegler-Nichols PI tuning parameters work well for set point changes of the nonlinear model. In both cases the closed-loop responses are nearly identical because of the constraints on the manipulated variables.

4. Whereas the PI control algorithm can only react to what has already happened, the IMC algorithm has the advantage of being able to predict the process response by using the internal process model. This advantage gives IMC controllers based on a stable model inverse the ability to reach the set point in only one sampling time, for no plant-model mismatch. Another advantage of the IMC control algorithm over ordinary feedback control algorithms is that there are fewer, if any, times that the manipulated variables will slam against their constraints.

5. A maximum model truncation order larger than

20 in program EIMC would have created a faster closed-loop response to set point changes due to a smaller sampling time allowing more changes in the manipulated variables in a given time.

6. Comparisons of Figures 14, 15, and 16, 17 with Figures 27 and 28, respectively, show that the IMC algorithm is more robust than the PI control algorithm for the linear model.

7. A comparison of Figures 20, 21 and 22, 23 with Figures 31 and 32 show that the IMC controller has a faster closed-loop response to a set point change for all cases shown except for output TF. This exception may not hold with a larger allowable maximum model truncation order (smaller sampling time) in program EIMC.

8. Figures 27, 28, 37 and 38 show that for reasonable process models, a linear and an approximate fitted model, the closed-loop response of the IMC controller is very good, thus showing its robustness in comparison with the two PI controllers.

CHAPTER 6 - SUMMARY AND CONCLUSIONS

This thesis has addressed a simple heat exchanger network as a dynamically interactive process with two inputs and two outputs and small steady-state interactions. The process is composed of two simple heat exchangers, a flow control valve and a steam pressure valve. The simplicity of this process is demonstrated by having only to measure temperatures and to manipulate flow rates.

Using control volumes to determine ordinary differential equations, both linear and nonlinear process models were developed and examined. The final process design in Chapter 3 shows significant dynamic interactions while having small steady-state interactions as measured by the Relative Gain Array.

Equations have been presented to allow design of a physical process having desired steady-state interactions or system parameters. Using this procedure allows the design of physical networks to test actual controllers or to run simulations for a desired system design with physical significance to test prospective controllers or control algorithms.

Two control methods were employed to test the controllability of the network with significant interactions. The first control method employed

continuous multiloop PI feedback controllers using either Cohen-Coon or Ziegler-Nichols tuning parameters and provided unsatisfactory control to set point changes in the linear model. The nonlinear model with PI control using the radically different Cohen-Coon or Ziegler-Nichols tuning parameters yielded similar and marginally satisfactory closed-loop performance. Even though the controller gains call for different manipulated variable values, these values are constrained and the actual value used is initially the same for each controller and thus causing similar responses. The closed-loop response to set point changes in TH yield significant initial deviation in TF.

The second control method employed the use of the multivariable Internal Model Control algorithm. Even with significant dynamic interactions, the closed-loop response to the set point changes for both linear and nonlinear models reached their new set points after only one sample time, with no plant-model mismatch. To examine the robustness of the IMC algorithm, an approximate model was created using program STEPG and the closed-loop responses were again examined. The closed-loop responses using the approximate model as the internal model and the nonlinear model as the plant provided satisfactory response.

It is concluded that it is possible to create a

dynamically interactive process, consisting of simple heat exchangers, that is difficult to control adequately using traditional control algorithms. It is also possible to design this simple heat exchanger network to have large dynamic interactions with small steady-state interactions.

Areas of future research include the incorporation of dead time to the process model, using more complicated heat exchangers, using PID control algorithms, the use of self tuning PIs to account for the manipulated variable constraints, the use of steady-state and/or dynamic decouplers, using more Impulse Response Coefficients with the IMC control algorithm and testing the closed-loop responses of the controllers to input disturbances.

The incorporation of dead time to the process model would make a more exact model for a physical system. The dead time could be varied physically by adding lengths of insulated pipe between heat exchangers and temperature measurement points.

Using more complicated heat exchangers may increase the heat transfer rate and may reduce the heat transfer area of the heat exchanger needed. Complicating the heat exchanger may also complicate the ODE for the control volume involved.

The use of PID and self tuning controllers should

decrease the response time to set point changes and input disturbances to the process. The self tuning controllers could also take the manipulated variable constraints into account by finding tuning parameters that give an adequate response even with the constraints.

The use of steady-state and/or dynamic decouplers was beyond the scope of this study and could be an area of further research.

Using more IRCs with the IMC control algorithm would decrease the response time by decreasing the sample time.

The study of input disturbances was beyond the scope of this thesis and could be an area of further research.

BIBLIOGRAPHY

Byrne, G. D. and A. C. Hindmarsh, "A Polyalgorithm for the Numerical Solution of Ordinary Differential Equations," UCRL-75652, Lawrence Livermore Laboratory, PO Box 808, Livermore, CA 94550, April 1974, also in ACM Transactions on Mathematical Software, 1, p. 71-96 (1975).

Callaghan, P. J., P. L. Lee and R. B. Newell, "A Pilot-Scale Heat Recovery System for Computer Process Control Teaching and Research," Chemical Engineering Education, 22(2), p. 168-71 (1988).

Coughanowr, D. R. and L. B. Koppel, Process Systems Analysis and Control, McGraw-Hill Book Co., New York, p. 153 (1965).

Economou, C. G. and M. Morari, "Internal Model Control. 6: Multiloop Design," Ind. Eng. Chem. Process Des. Dev., 25(2), p. 411 (1986).

Garcia, C. E. and M. Morari, "Internal Model Control. 1. A Unifying Review and Some New Results," Ind. Eng. Chem. Process Des. Dev., 21(2), p. 317-18 (1982).

Grosdidier, P. and M. Morari, "Interaction Measures for Systems Under Decentralized Control," Automatica, 22(3), p. 309 (1986).

Jensen, N., D. G. Fisher and S. L. Shah, "Interaction Analysis in Multivariable Control Systems," AIChE J., 32(6), p. 959 (1986).

Lee, P. L. and K. L. Levien, "Performance Comparisons of Internal Model Control and Predictive Controllers," AIChE Annual Meeting (November 1986).

Levien, K. L., programs EIMC and STEPG, Oregon State University, Summer 1988 versions.

Mijares, G., J. D. Cole, N. W. Naugle, H. A. Preisig and C. D. Holland, "A New Criterion for the Pairing of Control and Manipulated Variables," AIChE J., 32(9), p. 1439 (1986).

Morari, M. and W. H. Ray, "CONSYD - CONtrol SYstem Design Software," Version 3.0 (September 1986).

Stephanopolous, G., Chemical Process Control: An Introduction to Theory and Practice, Prentice-Hall, Inc., New Jersey, pp. 170, 217, 311-12, 353 (1984).

Welty, J. R., C. E. Wicks and R. E. Wilson, Fundamentals of Momentum, Heat and Mass Transfer, Second Edition, John Wiley & Sons, Inc., New York, pp. 426, 750 (1976).

A P P E N D I C E S

APPENDIX A - SENSITIVITY OF THE FUNDAMENTAL TRANSFER FUNCTION TO DESIGN PARAMETERS

This Appendix shows the sensitivity of various system parameters to process parameters. This information is important for the design of an operable heat exchange network for laboratory use. It is also necessary in designing a network to test the feasibility of a specific set of parameters. This Appendix shows how to design a process with a desired set of system parameters and is divided into three sections:

a) Sensitivity of the placement of the network poles and the TF/X transfer function zeros to process parameters

b) Sensitivity of the system parameters to the value of the (1,1) element of the Relative Gain Array

c) Sensitivity of the system parameters to the gain ratios while maintaining the (1,1) element of the RGA constant.

In the first section, the sensitivity of system parameters is shown through the use of plots of the system parameters for the TF/X transfer function (g_{11}) and the heat transfer area of the recycle heat exchanger (A1) as functions of the process parameters. The system parameters plots show the relative speed of the process

to changes in set point and/or disturbances for each of the process designs studied. It should be recalled that the denominators of the four transfer functions and, therefore, the poles of each of the four transfer functions are identical. The numerators of the four transfer functions are different which leads to different zeros for each of the four transfer functions. This study is concerned with the zeros of the TF/X transfer function as this is the transfer function which has the interesting behavior, i.e., large dynamic yet small steady-state interaction.

The second section shows the effect various values of the (1,1) element of the RGA have on the system parameters and the four design temperatures (T1, TH, TF and TS) through the use of composite plots. The (1,1) element of the RGA is a measure of the steady-state interactions of the process. The final part of this section contains the open-loop responses to changes in the manipulated variables.

The third section of this chapter shows, through plots, the effect various steam temperature ratios, RTS, and flow fraction ratios, RX, have on the system parameters and heat transfer area while maintaining the RGA at the nominal value of 0.1419. The RTS and RX ratios are used in the equation for the RGA and are important in determining the individual gains and the

dynamic interactions. This section also contains the open-loop responses to changes in the manipulated variables for various RTS and RX values.

Sensitivity of system parameters to process parameters

This section contains plots which can be used to design a heat exchange network by choosing a set of poles, zeros, the RPZ ratio or the recycle heat exchanger heat transfer area from the plots shown. The pole and zero plots in this section are set to the same scale to show the relative effect of changes to each parameter. In each of the figures in this section, only the single parameter being studied is varied, all other specified parameters are maintained at their nominal values. In order to vary the parameter, the process flow rate, F, and the lumped recycle parameter, Z, are also varied.

Intuition tells us that increasing the overall heat transfer coefficient (U3), the steam temperature (TS), the steam heat exchanger heat transfer area (A3) or decreasing the volume of the heat exchangers (V1 and V3) leads to faster responses as is shown to be true from the pole movement shown in Figures 39 through 43, respectively. The slower response for an increase of

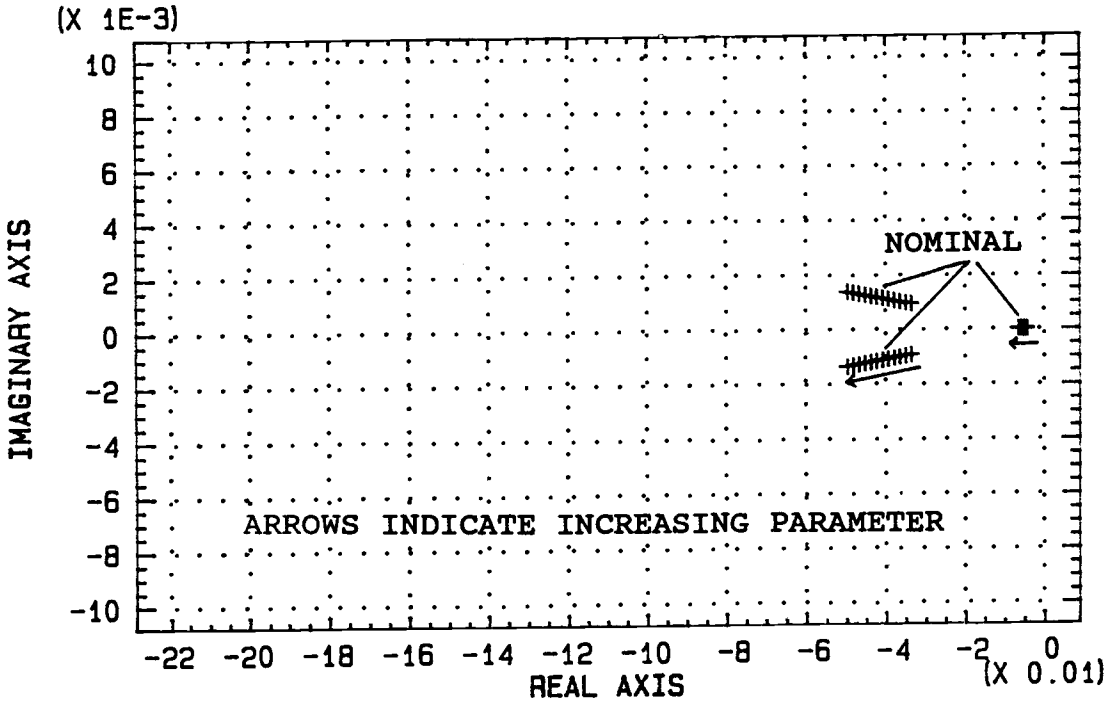

Fig. 39. Pole placement as a function of the steam heat transfer coefficient

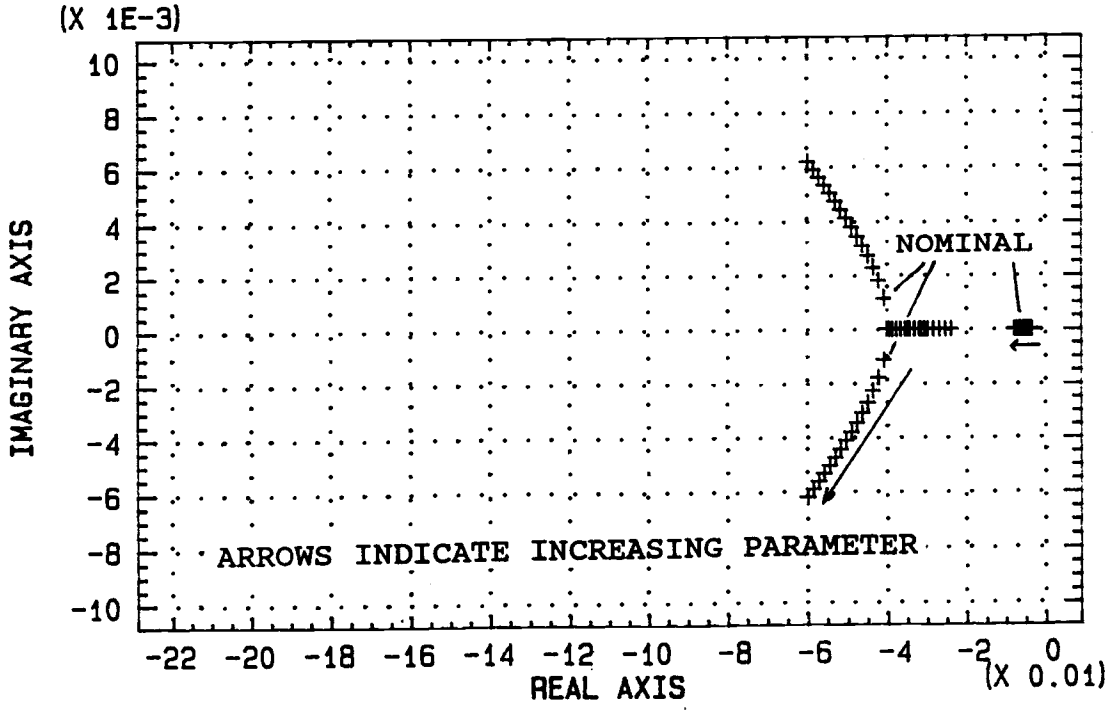

Fig. 40. Pole placement as a function of the steam temperature

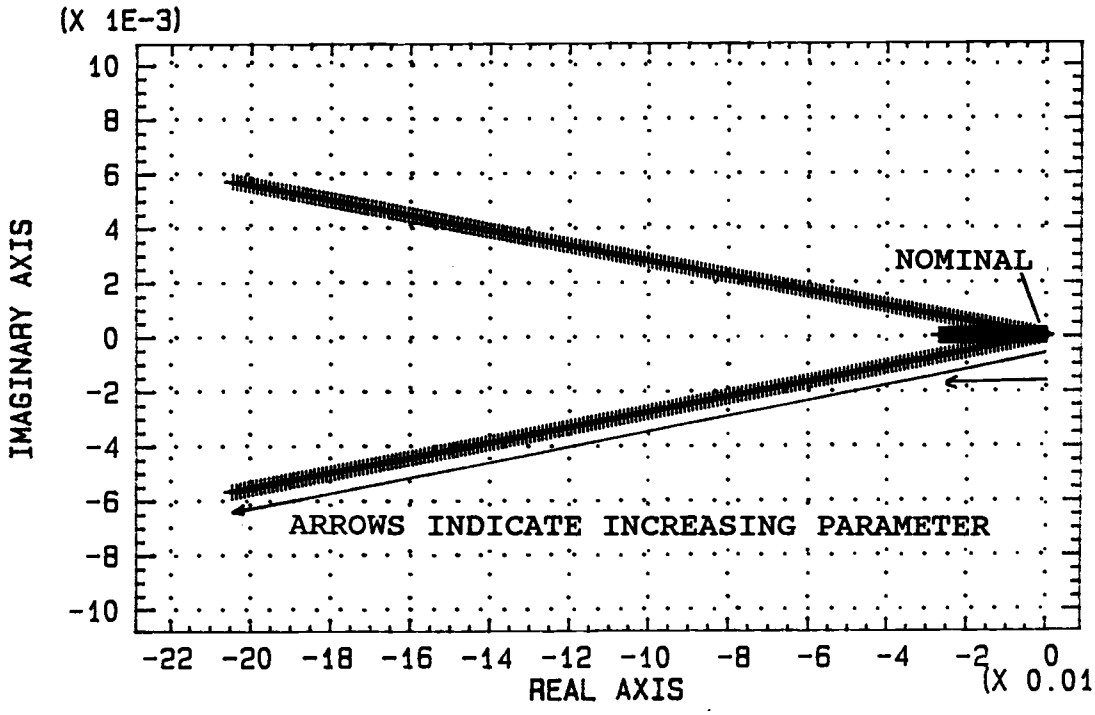

Fig. 41. Pole placement as a function of the recycle heat exchanger area

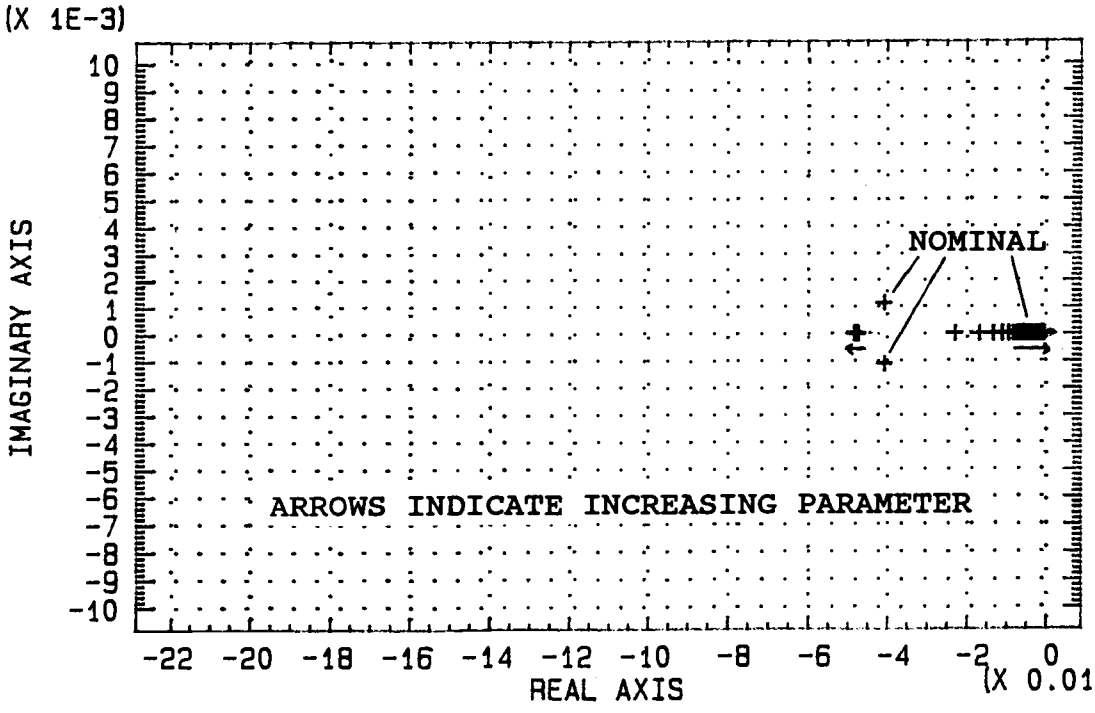

Fig. 42. Pole placement as a function of the recycle heat exchanger volume

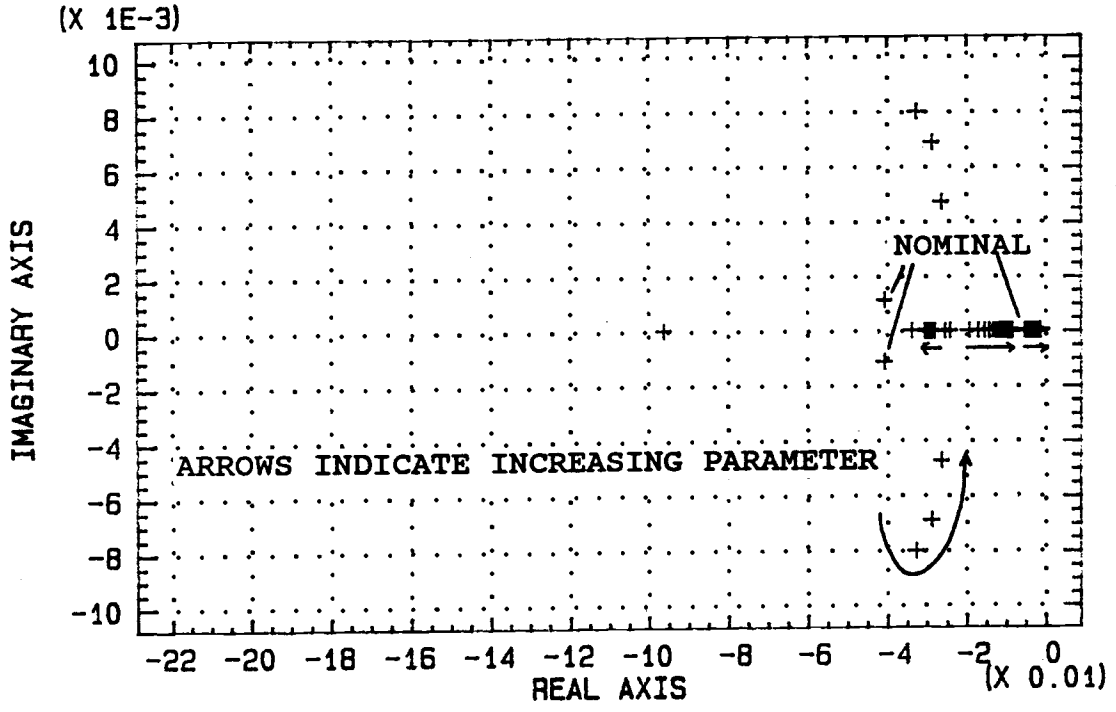

Fig. 43. Pole placement as a function of the steam heat exchanger volume

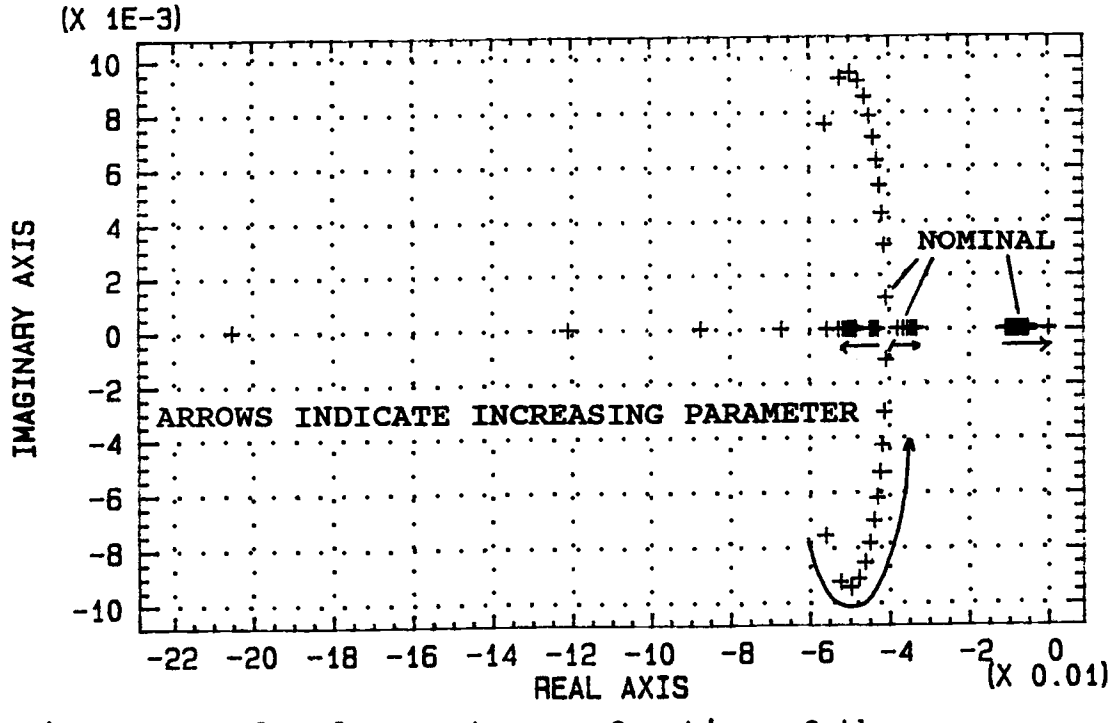

Fig. 44. Pole placement as a function of the flow fraction

the flow fraction (X) is more difficult to determine by intuition and is shown in Figure 44. Over the range of parameters studied (Table 33), the greatest pole movement occurs while changing the steam heat transfer area, A3.

Figure 44 shows the placement of the network system poles as a function of the flow fraction to the recycle heat exchanger (X). This plot is interesting because it is the only plot with poles in the right-half of the complex S-plane (RHP). Such systems are unstable as (Stephanopolous, 1984 and Coughanowr and Koppel, 1965) the RHP poles represent exponential terms which increase to infinity with time. In this particular case, the flow fraction values which yield RHP poles also physically result in negative heat transfer areas. To prevent division by zero, the range of flow fractions is from 0.00001 to 1.00001 of the total flow or from approximately 0.0 to 1.0. Flow fraction values less than 0.34 yield poles in the RHP and the discontinuities shown later in Figures 54 and 58a. Flow fractions greater than 0.33 yield stable poles in the left-half complex S-plane. Increasing the flow fraction to the recycle heat exchanger, above the minimum 0.34 value, moves the poles closer to the origin, resulting in slower poles. The slowest pole only moves slightly nearer the origin, indicating that only a slightly

Table 33. Summary of system parameter changes as a function of the process parameters

Process Parameter Changed	Range	Effect on response time to increased parameter	Range of slowest pole with increased parameter
U3	2300 — 3400 W/m^2 K	faster	-4.4E-3 — -6.6E-3
A3	2E-3 — 0.4 m^2	faster	-1.4E-4 — -2.7E-2
TS	150 — 270 °C	faster	-3.6E-3 — -8.0E-3
V1	0.04 — 0.32 m^3	slower	-5.4E-3 — -7.5E-4
V3	5E-3 — 0.2 m^3	slower	-5.5E-3 — -1.7E-3
X	0. — 1.	slower	-5.3E-3 — -6.7E-3

Process Parameter Changed	Range	Range of most significant zero with increased parameter	Range of RPZ ratio with increased parameter
U3	2300 — 3400 W/m^2 K	-3.1E-4 — -4.6E-4	14.2
A3	2E-3 — 0.4 m^2	-9.5E-6 — -1.9E-3	14.2
TS	150 — 270 °C	-3.6E-4 — -3.9E-4	9.9 — 20.3
V1	0.04 — 0.32 m^3	-3.8E-4 — -5.0E-5	14.2 — 14.0
V3	5E-3 — 0.2 m^3	-3.9E-4 — -1.6E-4	14.4 — 10.1
X	0. — 1.	-5.6E-4 — -2.9E-4	10.1 — 23.3

slower response would accompany an increase in the steady-state flow to the recycle heat exchanger. The slightly slower response may be caused by the increased temperature of the fluid entering the steam heat exchanger as this would decrease the temperature differential between the fluid and the steam, thereby decreasing the rate of heat transferred.

Figures 45 through 50 show the placement of zeros for the TF/X transfer function (g_{11}) as functions of U3, TS, A3, V1, V3 and X, respectively, over the same ranges used in the pole placement figures above. Table 33 shows the range for the most significant zero over the range of process parameters studied.

Figures 51 through 54 show plots of the ratio of the slowest pole position to most significant zero position, RPZ, for the TF/X transfer function (g_{11}) as functions of TS, V1, V3 and X, respectively, over the same ranges used in the figures above. These plots are included as this ratio is one of the "targets" to reach for creating open-loop responses of similar shape to those of the experimental data. Plots of the RPZ ratio as functions of the overall heat transfer coefficient and the heat transfer area of the steam heat exchanger are not shown as they have no effect on the RPZ ratio. Table 33 shows range over which the RPZ changes for the range of process parameters. The flow fraction (X), and

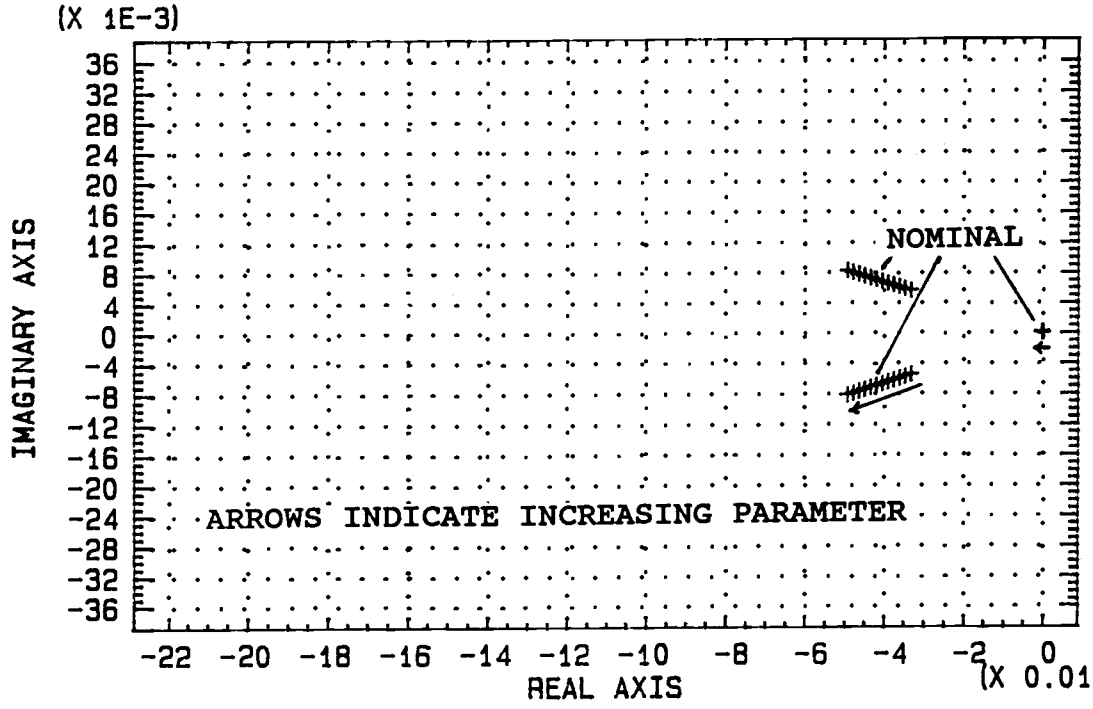

Fig. 45. Zero placement as a function of the steam heat transfer coefficient

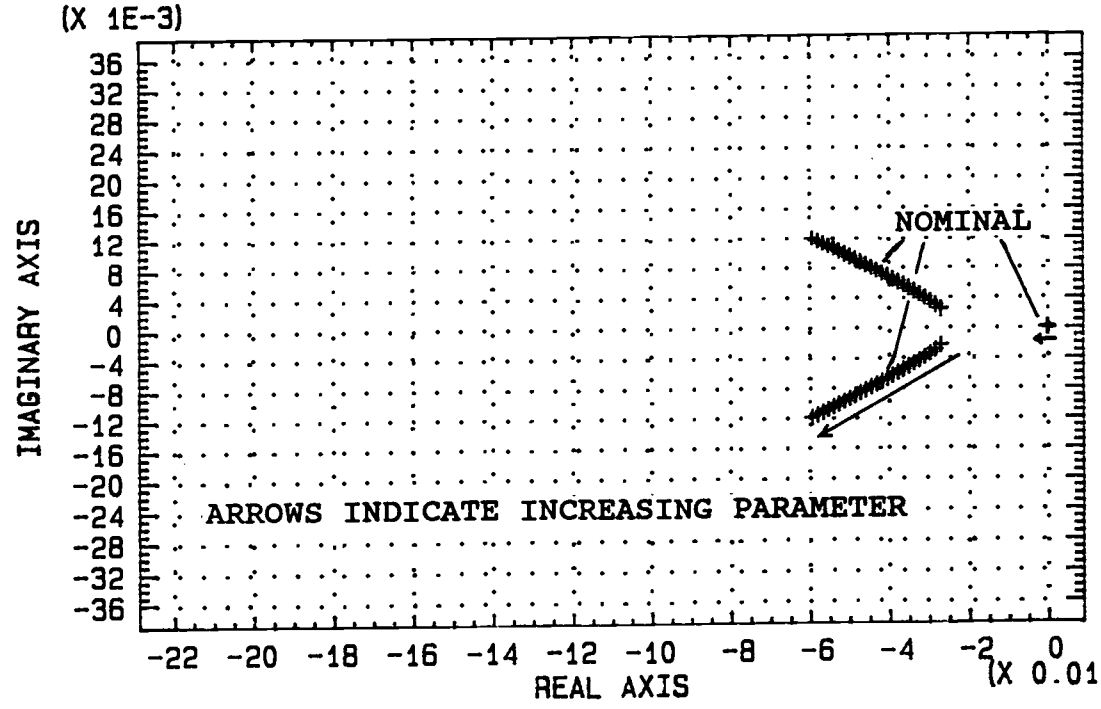

Fig. 46. Zero placement as a function of the steam temperature

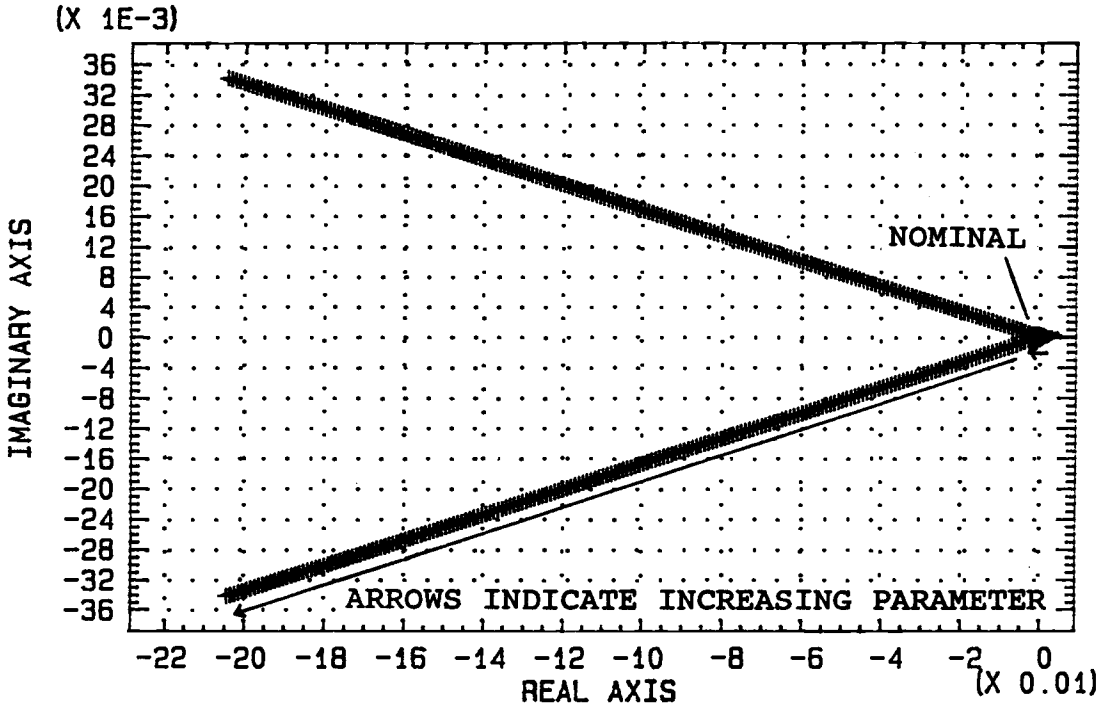

Fig. 47. Zero placement as a function of the steam heat transfer area

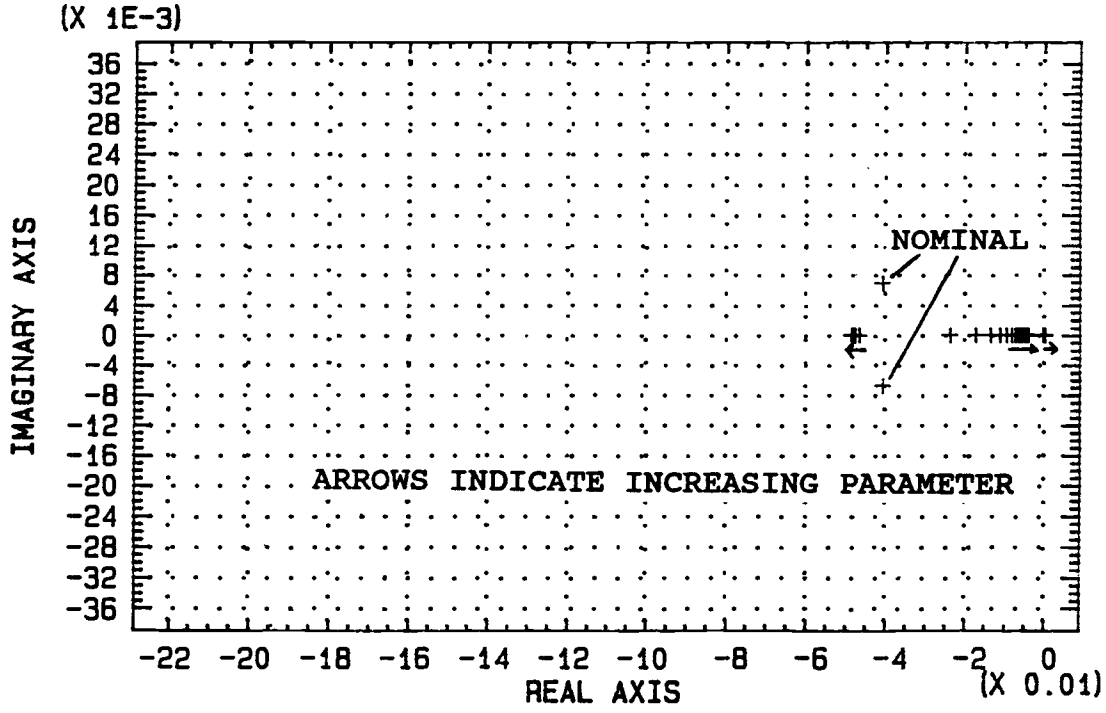

Fig. 48. Zero placement as a function of the recycle heat exchanger volume

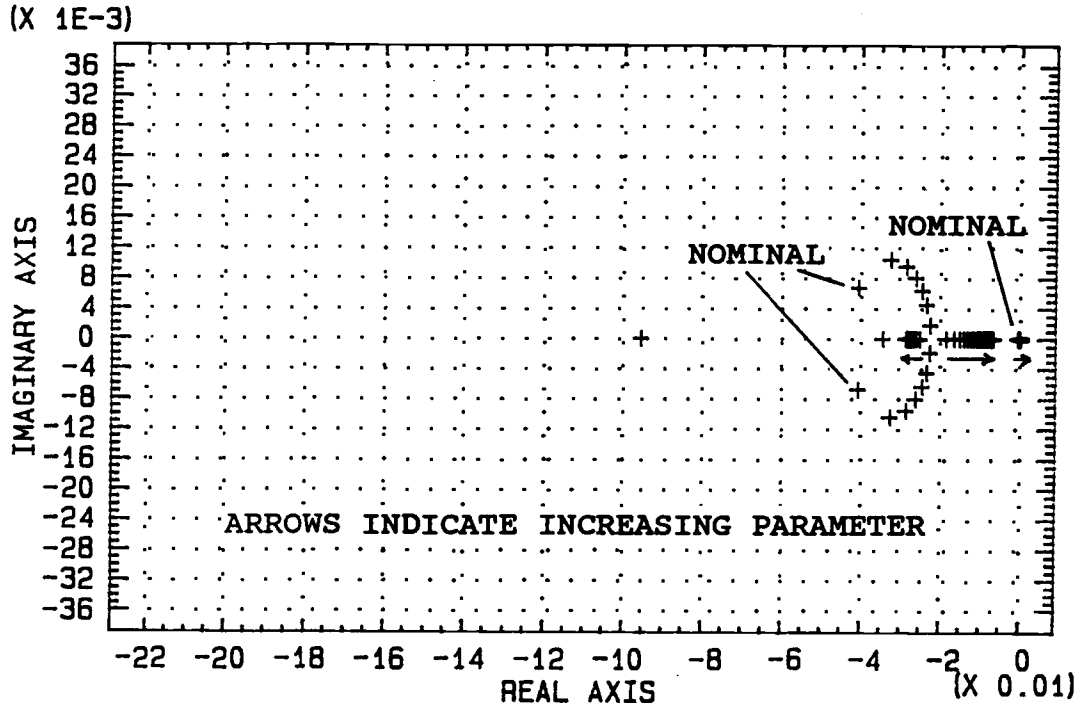

Fig. 49. Zero placement as a function of the steam heat exchanger volume

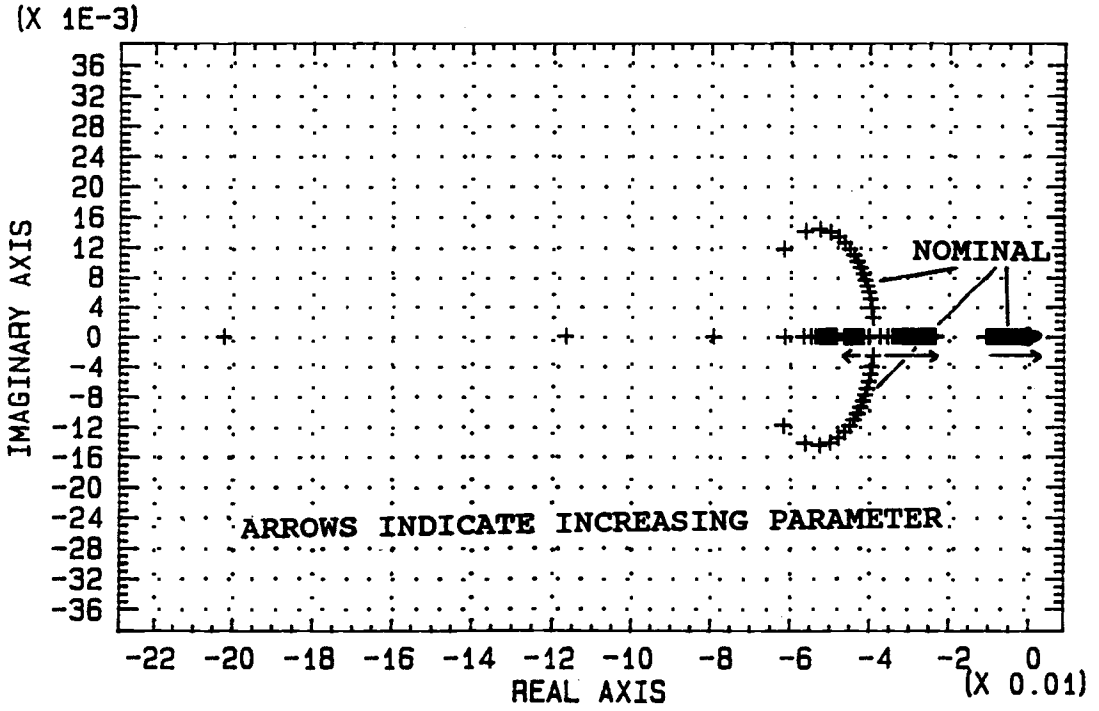

Fig. 50. Zero placement as a function of the flow fraction

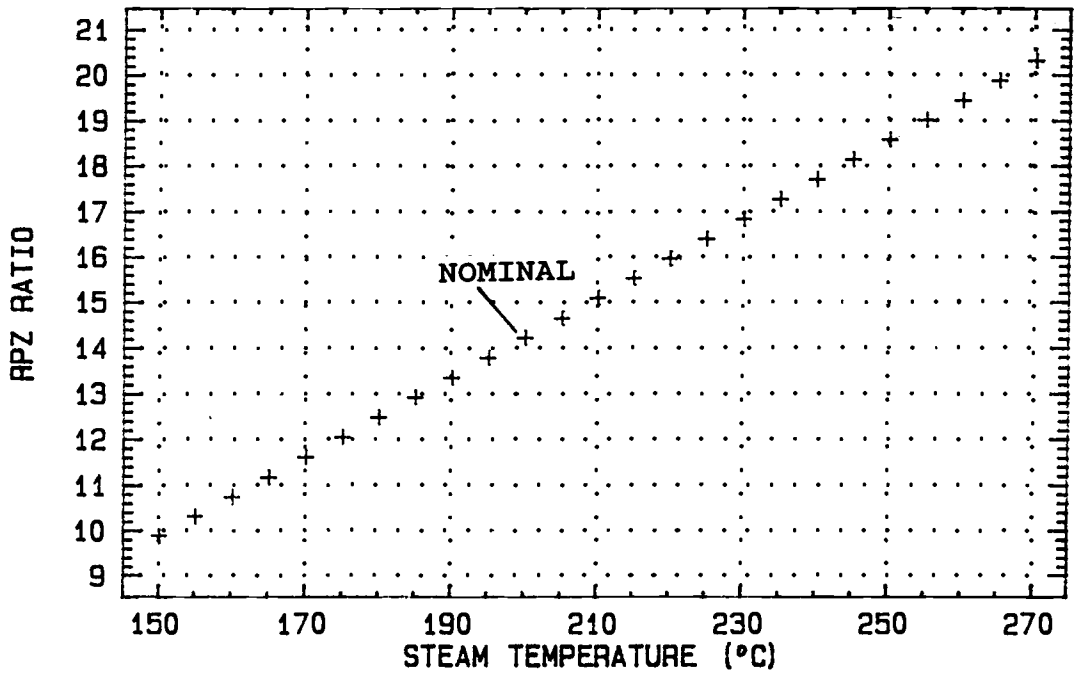

Fig. 51. RPZ ratio as a function of the steam temperature

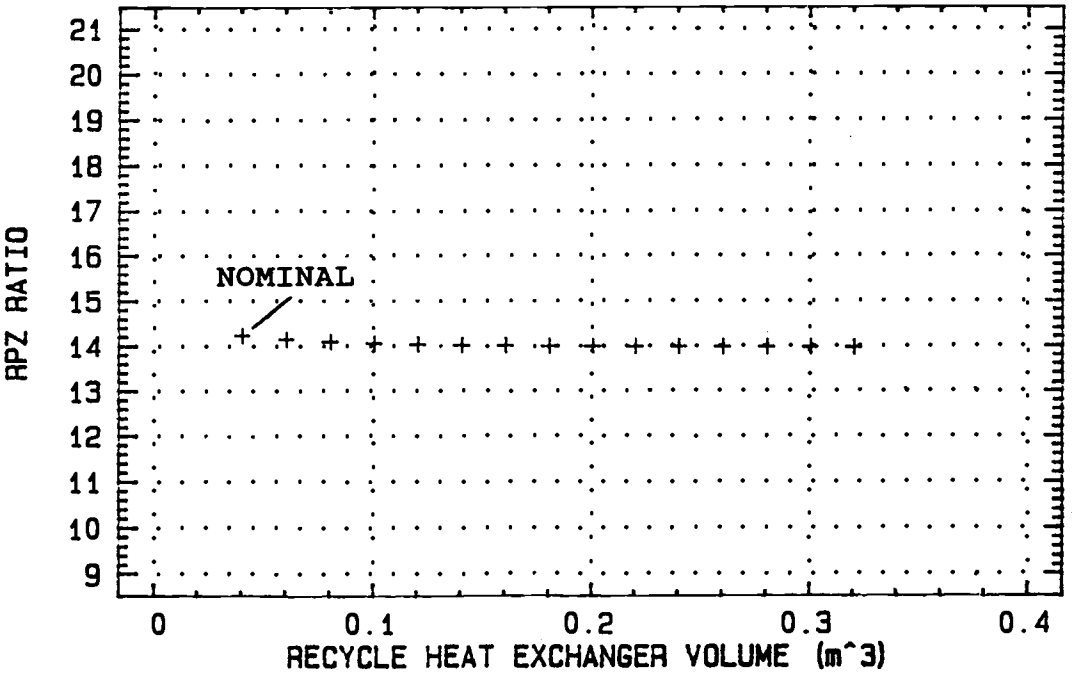

Fig. 52. RPZ ratio as a function of the recycle heat exchanger volume

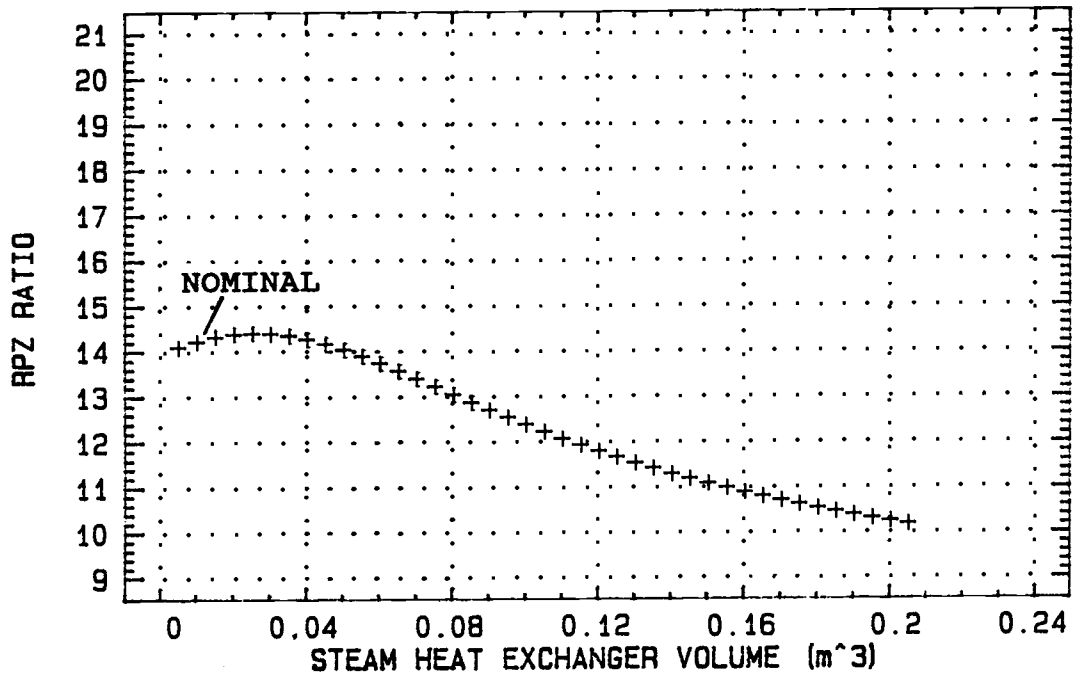

Fig. 53. RPZ ratio as a function of the steam heat exchanger volume

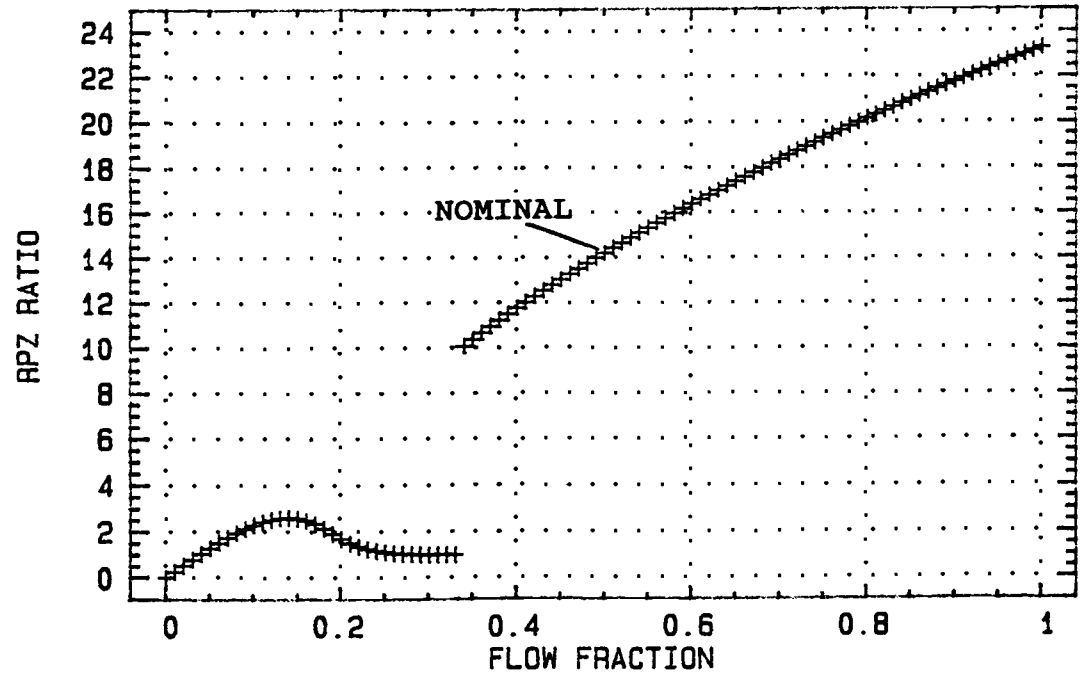

Fig. 54. RPZ ratio as a function of the flow fraction

TS have the greatest range of the RPZ ratio and would be good choices for changing the ratio.

Figures 55 through 58 show the effect U3, TS, A3, and X values have on the recycle heat exchanger heat transfer area required to achieve the design temperatures. Parameters V1 and V3 have no effect on the recycle heat transfer area. Before building a heat exchanger with the required area shown in these plots, a check against the volume of the recycle heat exchanger must be performed, as shown in Appendix D, as the area required may not be feasible for the given volume. As previously noted, the steam heat transfer area (A3) has the greatest effect on the recycle heat transfer area and would be a good choice for changing the recycle heat transfer area.

Figure 58a shows the recycle heat transfer area for the total range of flow fractions to the recycle heat exchanger. As in the previous plots with the independent variable of flow fraction, there is a jump discontinuity separating the feasible from the infeasible sections. From this plot it is obvious that for flow fraction values less than 0.34 the heat exchange network design is infeasible in that the required recycle heat transfer areas are less than zero. Figure 58b is a detailed plot for the feasible flow fraction values of 0.38 to 1.0. From this plot it is

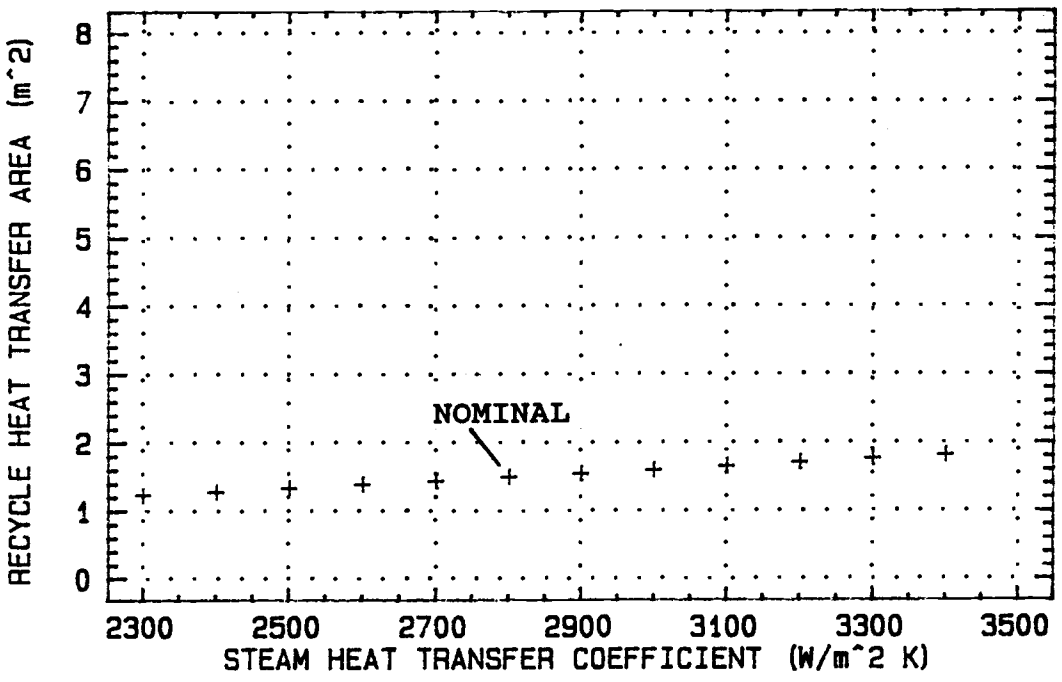

Fig. 55. Recycle heat transfer area as a function of the steam heat transfer coefficient

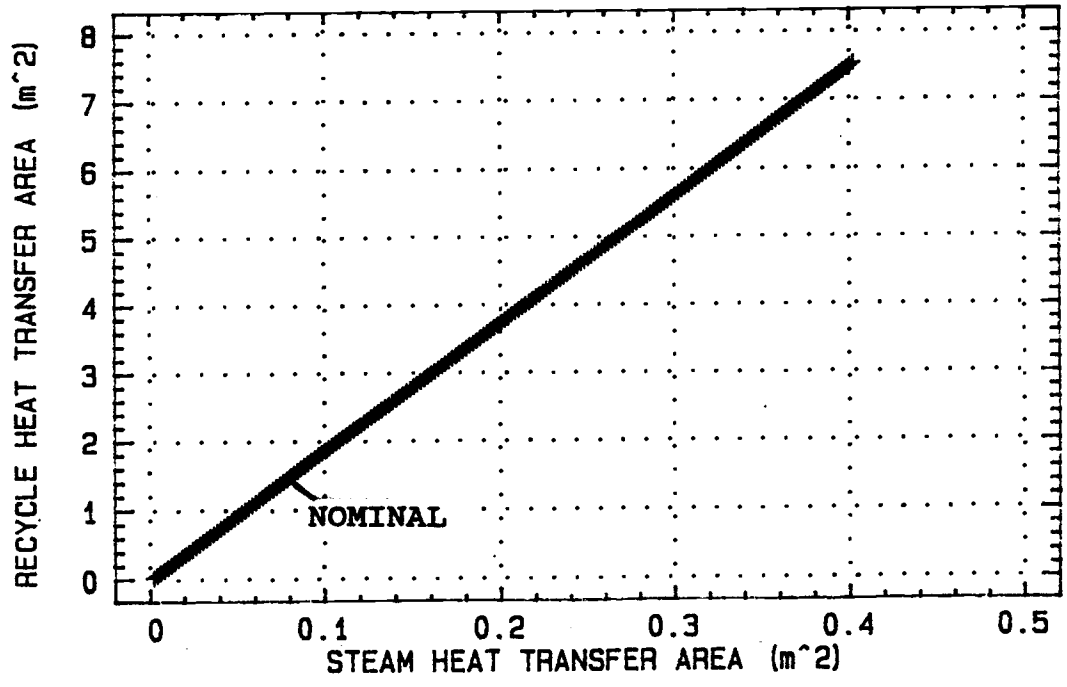

Fig. 56. Recycle heat transfer area as a function of the steam heat transfer area

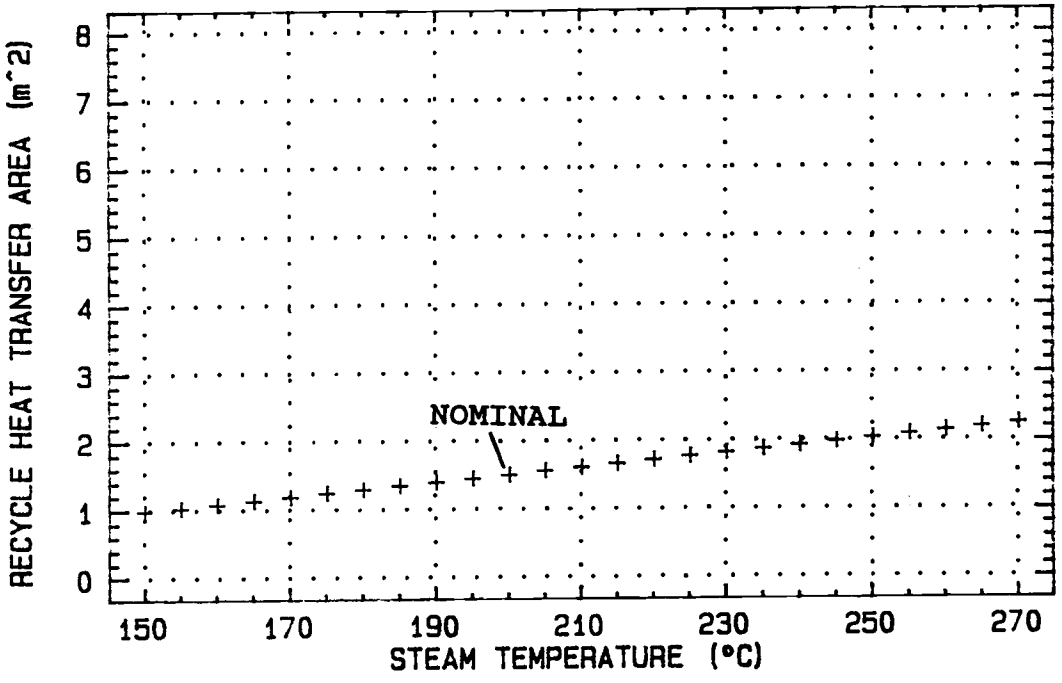

Fig. 57. Recycle heat transfer area as a function of the steam temperature

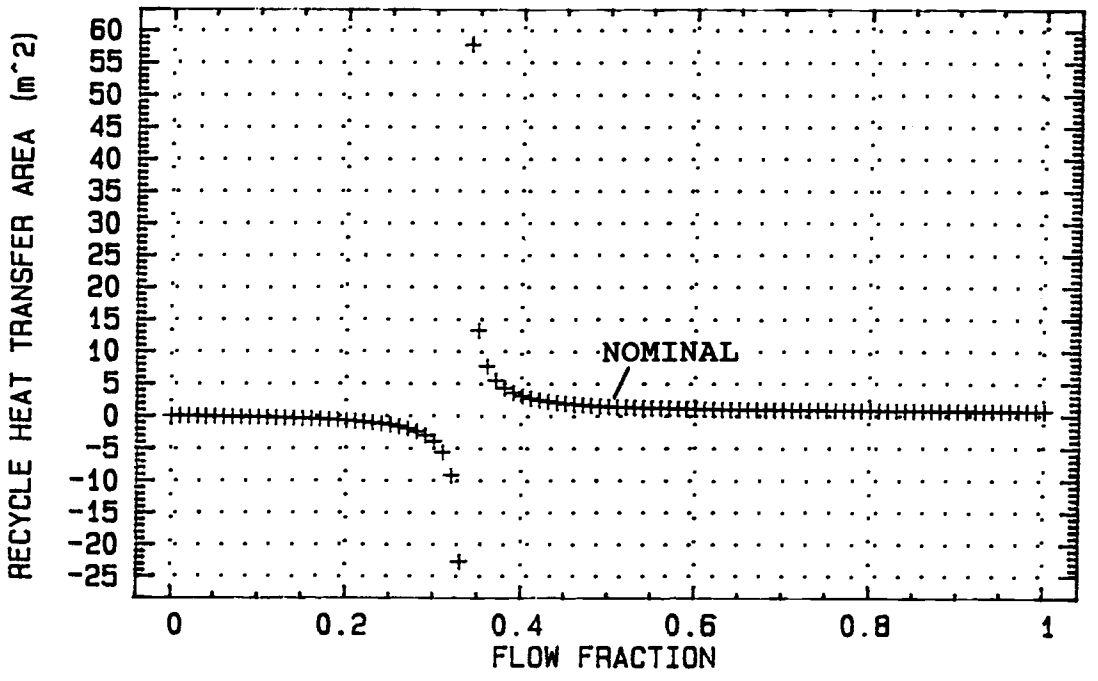

Fig. 58a. Recycle heat transfer area as a function of the flow fraction

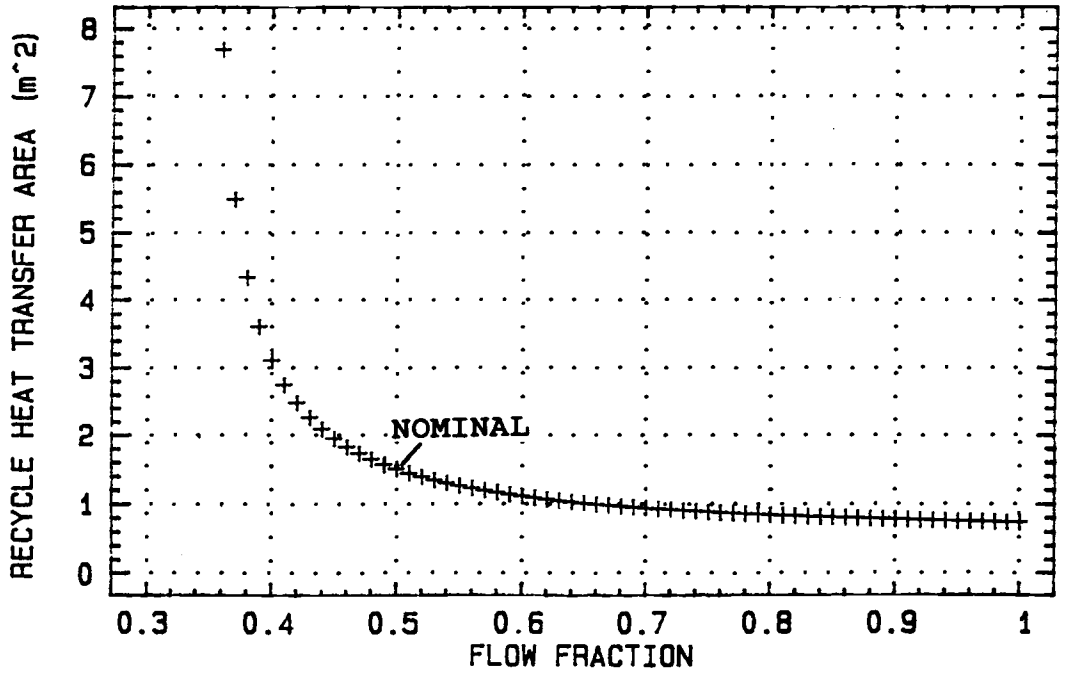

Fig. 58b. Valid recycle heat transfer area values as a function of the flow fraction

possible to see that for flow fractions less than the 0.45 to 0.5 range the recycle heat transfer area required to achieve the target temperatures decreases exponentially.

Sensitivity of system parameters to the (1,1) element of the RGA

The equations used to determine the temperatures in the following figures are found in Table 34a. Figures 59 through 62 show how each of the four target temperatures must change as a function of the (1,1) element of the RGA, if the other three target temperatures are to remain at their nominal values. The range of RGA values is from a very non-interactive 0.05 to an extremely interactive 0.5.

Figure 59 shows the required T1 temperature as a function of the (1,1) element of the RGA. From this plot it is seen that, for a (1,1) element value greater than about 0.17, the temperature drops below temperature TI and is, therefore, an infeasible range of (1,1) element values for this set of parameters.

Figure 60 shows the required TH temperature as a function of the (1,1) element of the RGA is valid for the values of 0.05 through 0.5.

Figure 61 shows the required steam temperature as a

Table 34a. Equations for determining the fourth design temperature when given the other three temperatures and the 1,1 element of the RGA.

$$TH = \frac{\lambda * TS + T1 * (1 - \lambda) + TF * (1 - \lambda)}{(2 - \lambda)}$$

$$TS = \frac{TH * (2 - \lambda) + T1 * (\lambda - 1) + TF * (\lambda - 1)}{\lambda}$$

$$T1 = \frac{TH * (2 - \lambda) - TS * \lambda + TF * (\lambda - 1)}{(1 - \lambda)}$$

$$TF = \frac{TH * (2 - \lambda) - TS * \lambda + T1 * (\lambda - 1)}{(1 - \lambda)}$$

Table 34b. Equations for determining the RTS and RX ratios.

$$RTS = \frac{2 * TH - T1 - TF}{(TH - T1)}$$

$$RX = \frac{-(TS - TH)}{(TH - T1)}$$

$$\lambda = \frac{1}{(1 - RX / RTS)}$$

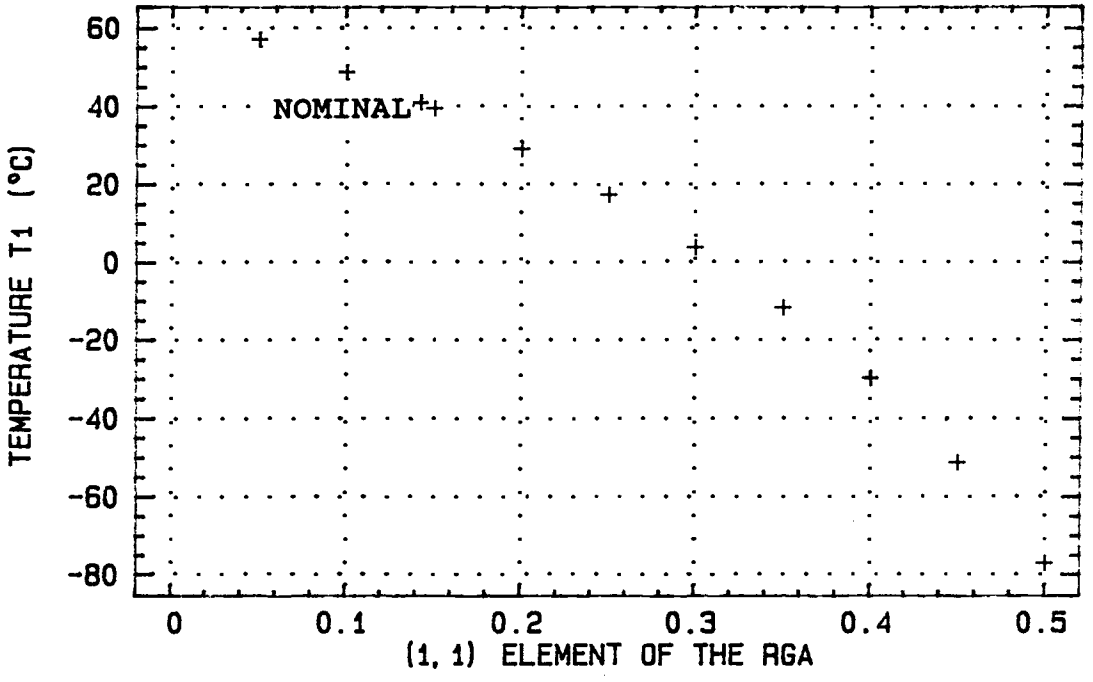

Fig. 59. Temperature T1 as a function of the (1,1) element of the RGA

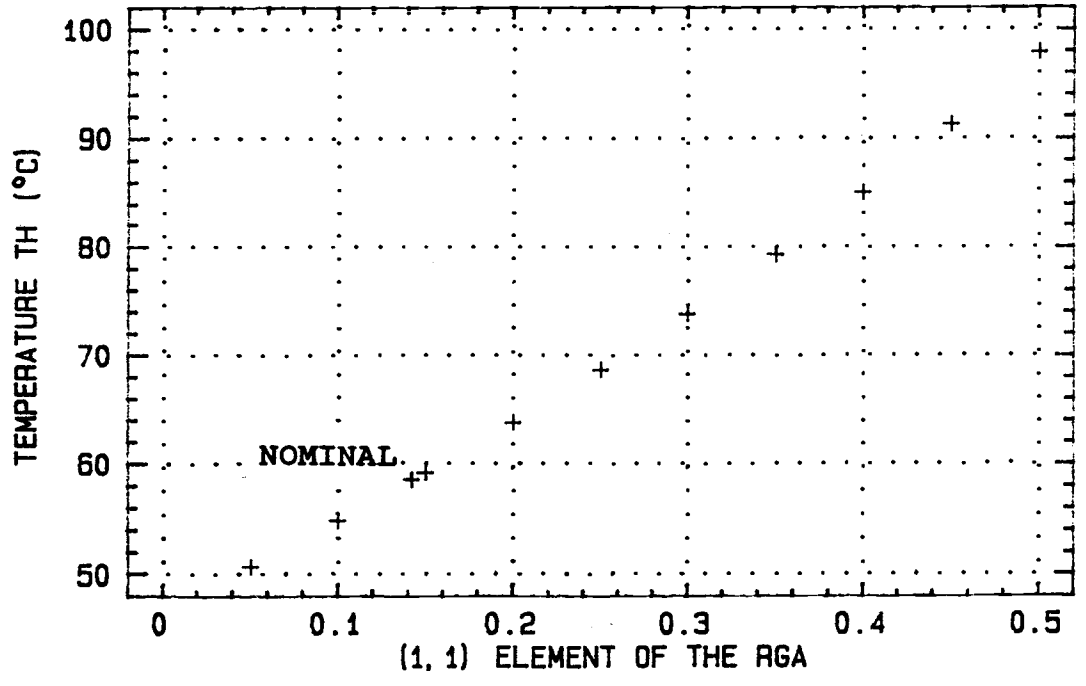

Fig. 60. Temperature TH as a function of the (1,1) element of the RGA

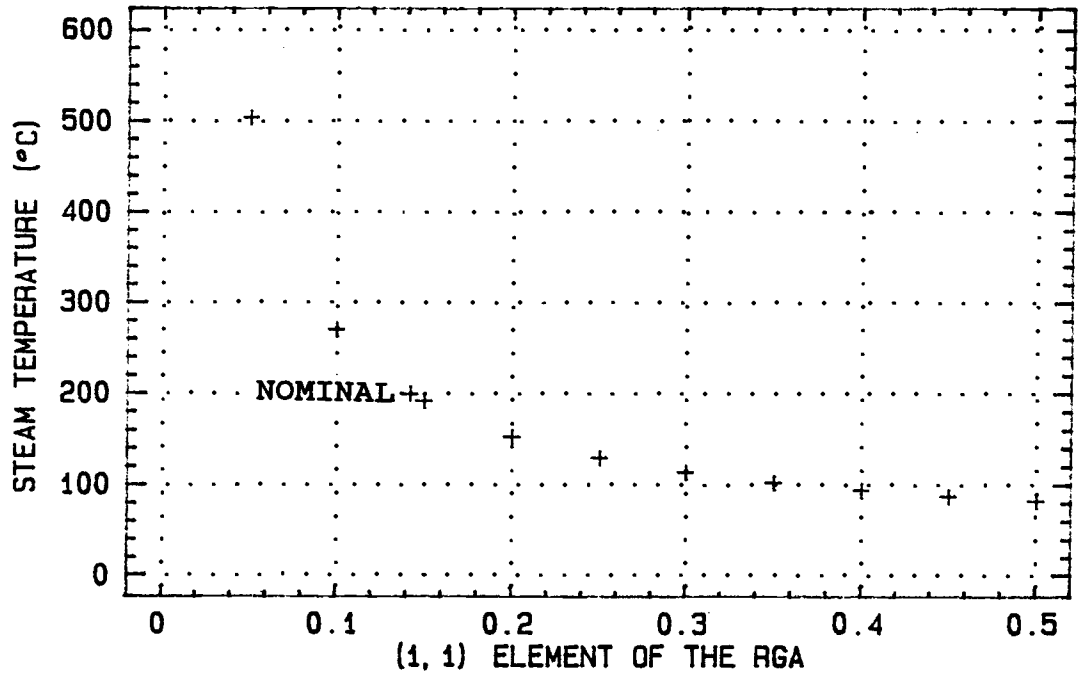

Fig. 61. Steam temperature as a function of the (1,1) element of the RGA

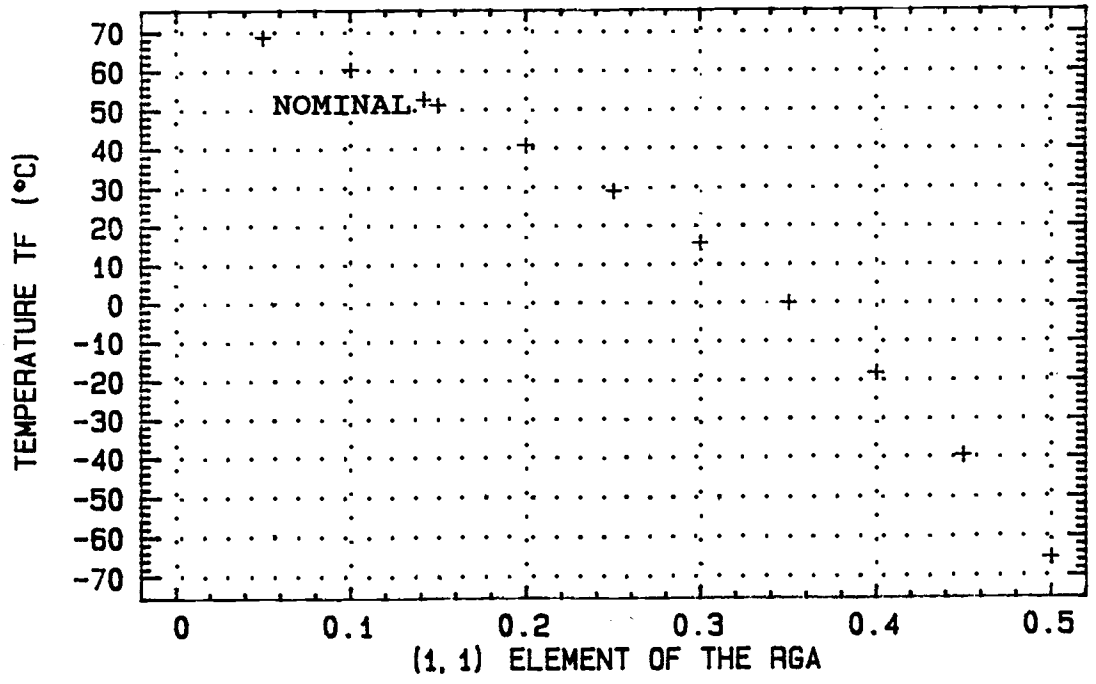

Fig. 62. Temperature TF as a function of the (1,1) element of the RGA

function of the (1,1) element of the RGA is valid for the values of 0.05 through 0.5. However, the higher steam pressures associated with higher steam temperatures would require a much heavier duty steam heat exchanger design and are considered undesirable.

Figure 62 shows the required TF temperature as a function of the (1,1) element of the RGA. This plot shows that values of the (1,1) element of the RGA greater than about 0.34 will yield temperatures less than zero. Another constraint on the final outlet temperature is that it cannot be less than the inlet temperature to the network. Since the nominal inlet temperature for this thesis is 35.1 °C the actual high value for the (1,1) element of the RGA is about 0.22. Therefore, these plots can be used as consistency checks for valid results.

The equations in Table 34b are used to determine the RX and RTS ratios when given the four target temperatures or the 1,1 RGA element and one of the ratios to determine the other. Where the ratios RX and RTS are the flow fraction and steam temperature ratios, respectively. That is, the ratios of the (2,1) to (1,1) and (2,2) to (1,2) elements of the RGA, respectively.

Figure 63 is a plot of the most significant zero as a function of the slowest pole over the range 0.05 to 0.5 for the (1,1) element of the RGA. Different RX and

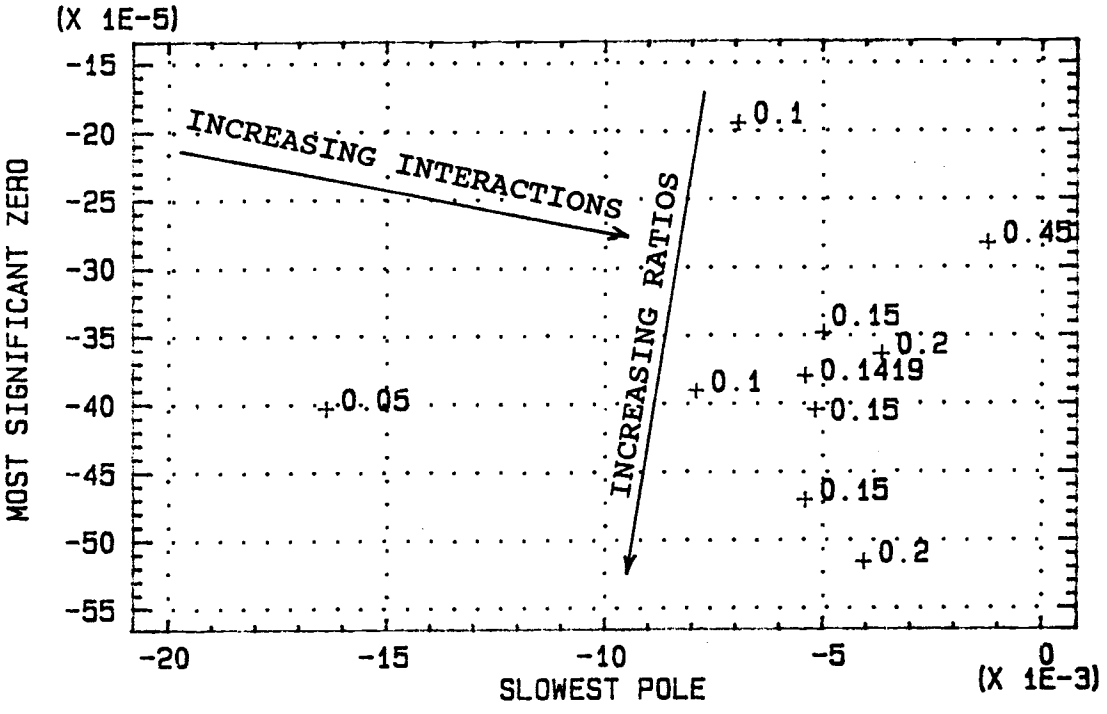

Fig. 63. Most significant zero as a function of the slowest pole and the (1,1) element of the RGA

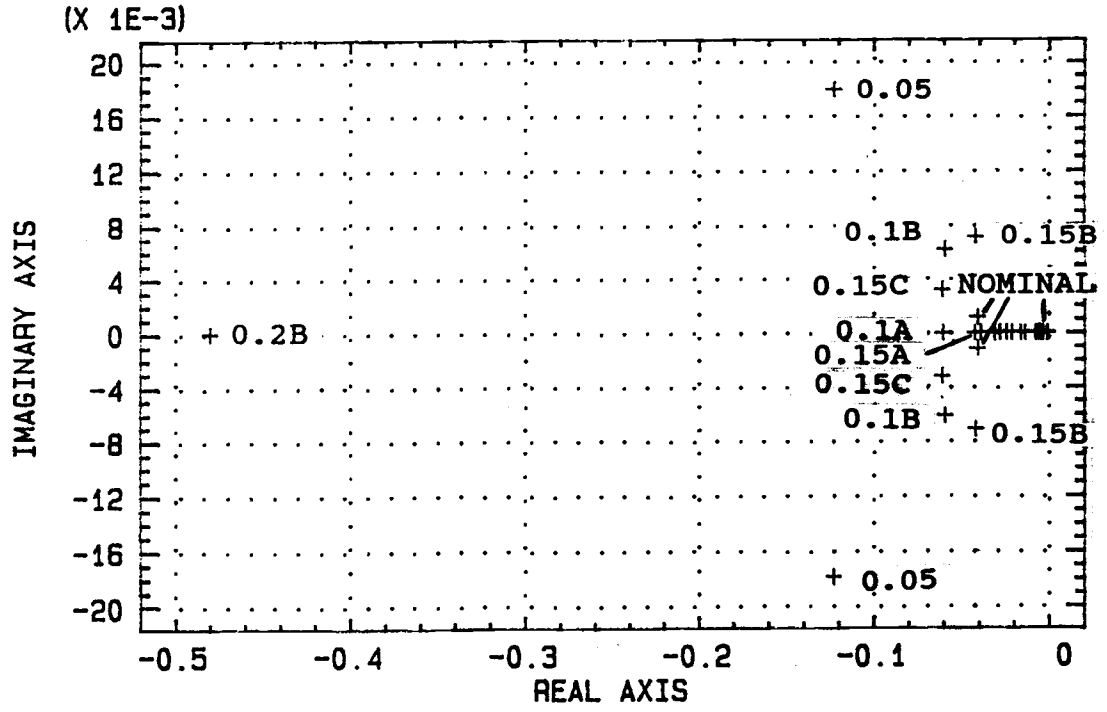

Fig. 64. Pole placement as a function of the (1,1) element of the RGA

RTS ratio values are used to achieve the same (1,1) RGA element value. From this plot it can be seen that smaller values of the (1,1) RGA element lead to faster systems. It can also be seen that fixing the (1,1) RGA element approximately fixes the pole position and that changing the RX and RTS ratios, with fixed RGA, changes the position of the zero and, therefore the RPZ. This is shown to have an effect on the shape of the response curve in Figures 67 through 70. Also, for a given degree of interaction, as specified by the value of the (1,1) RGA element, smaller RTS and RX ratios have most significant zeros placed closer to the origin.

Figure 64 is a plot of the poles of the 2 X 2 systems for the different (1,1) elements of the RGA. The only discernable pattern is that the more interactive the system, i.e., the nearer the (1,1) element of the RGA to 0.45, the slower the overall system as shown by the slowest pole.

Figure 65 is a plot of the zeros for the different (1,1) elements of the RGA. The important pattern in this plot is that the more interactive the system, the closer to the origin is the most significant zero.

Figure 66 is a plot of the RPZ ratio as a function of the (1,1) element of the RGA. This plot shows that the less interactive systems, i.e., with smaller (1,1) RGA elements, have the larger RPZ ratio. Also, for a

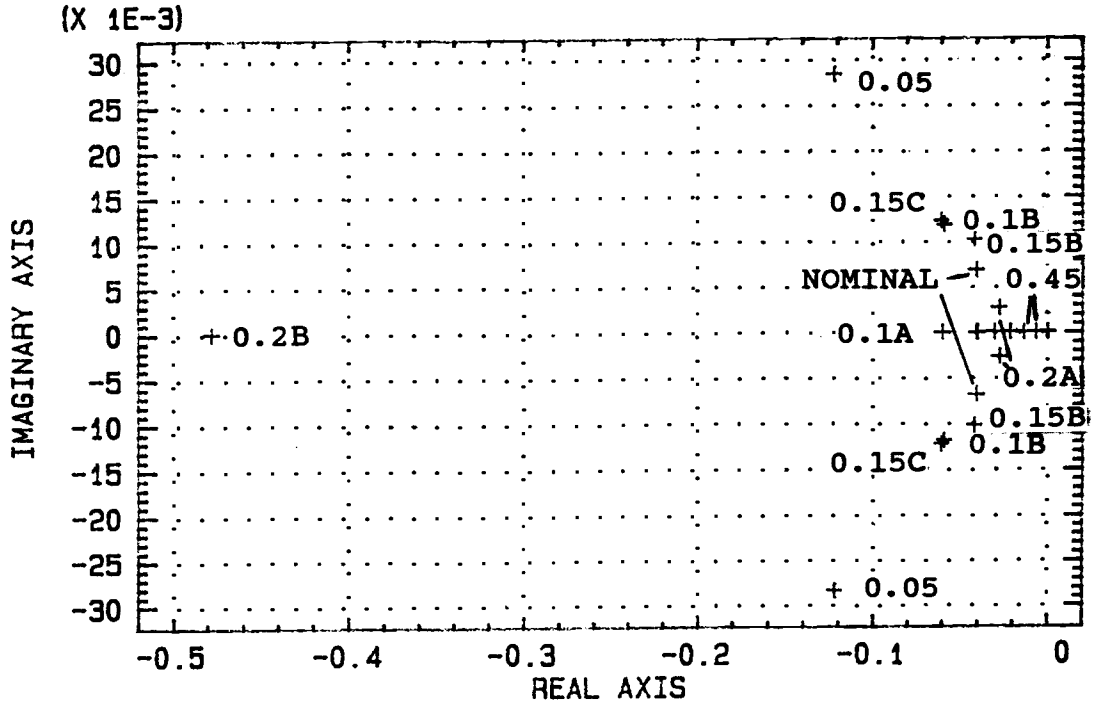

Fig. 65. Zero placement as a function of the (1,1) element of the RGA

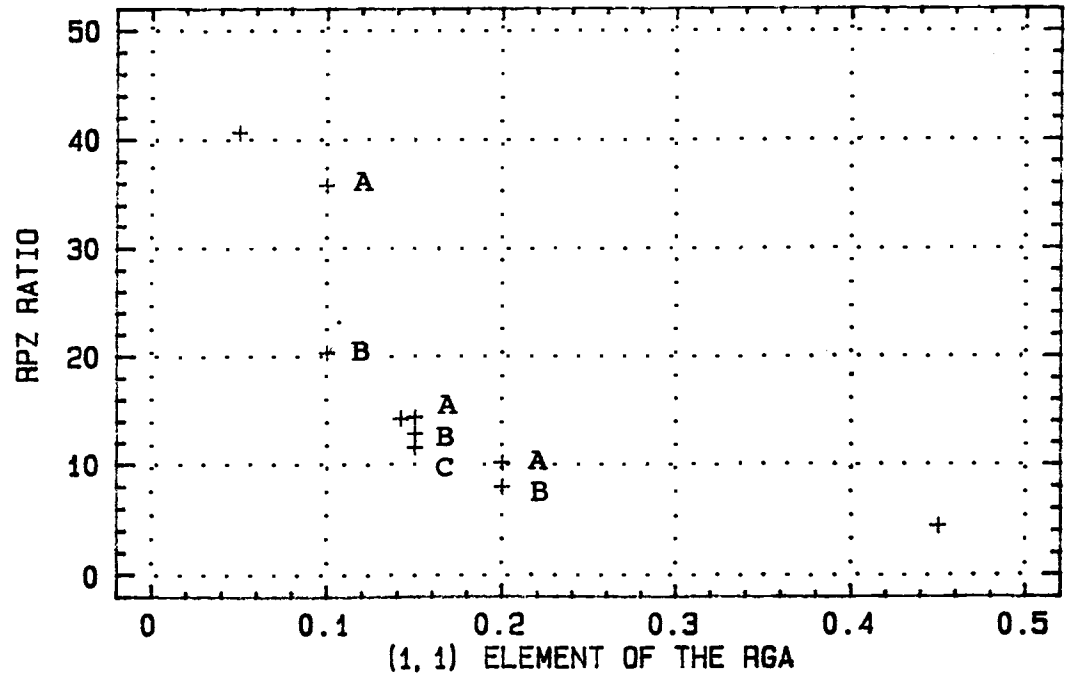

Fig. 66. RPZ ratio as a function of the (1,1) element of the RGA

given degree of interaction, the smaller RTS and RX ratios have greater values of the RPZ ratio.

Figures 67 through 70 show open-loop responses of systems with (1,1) element RGA values from 0.05 through 0.45. Each set of responses is for individual set point changes of only one manipulated variable at a time. The manipulated variable changes are a 40 % decrease in X and a 10 % increase in °C for delta TS. Notice the dramatic initial open-loop response of temperature TF for a change in the flow fraction in Figure 67. The immediate change in the temperature is due to the nature of the mixing point and the omission of dead time in the equations relating to the time it would take for the fluid to flow through pipes to the mixing point and temperature sensor. It should be noticed that there is a change in both the extent of the initial deviation from the original steady-state value and the time required to reach the new steady-state value. In general, the larger the interaction, as measured by the (1,1) element of the RGA, the slower the response. For any given value of the (1,1) element of the RGA, larger values for the RTS and RX ratios yield slightly faster open-loop responses.

Tables 35a and 35b show the values used in programs DTXFCN and DTHES2 to determine the open-loop response curves for the various (1,1) elements and RTS and RX

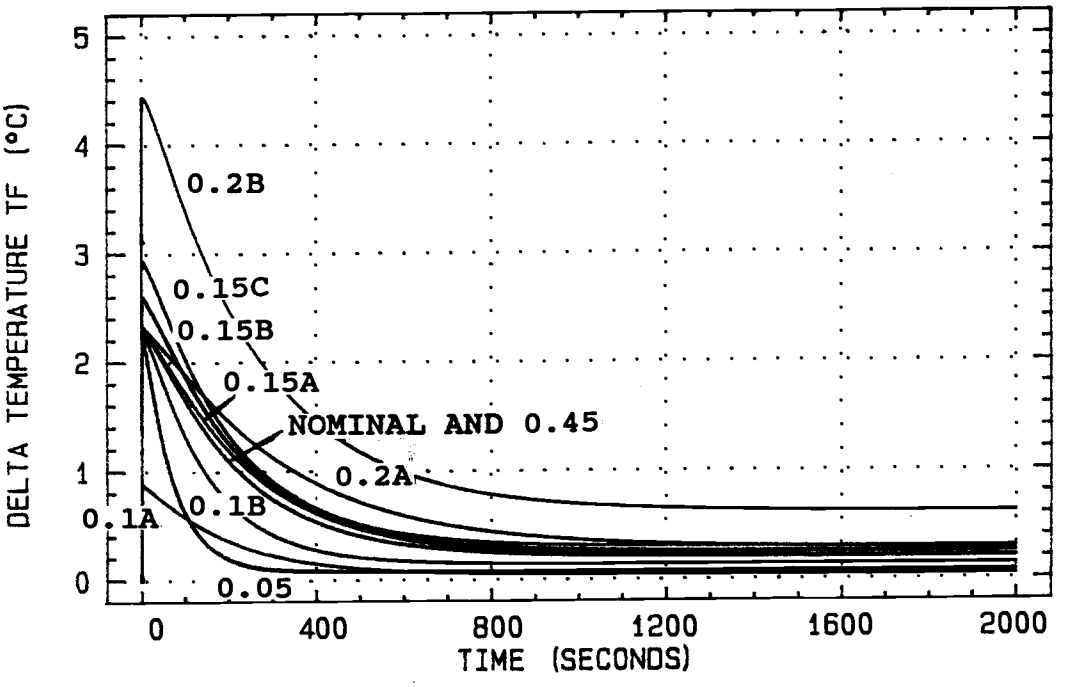

Fig. 67. Open-loop response to a 40 % decrease in the flow fraction as a function of the RGA value for TF

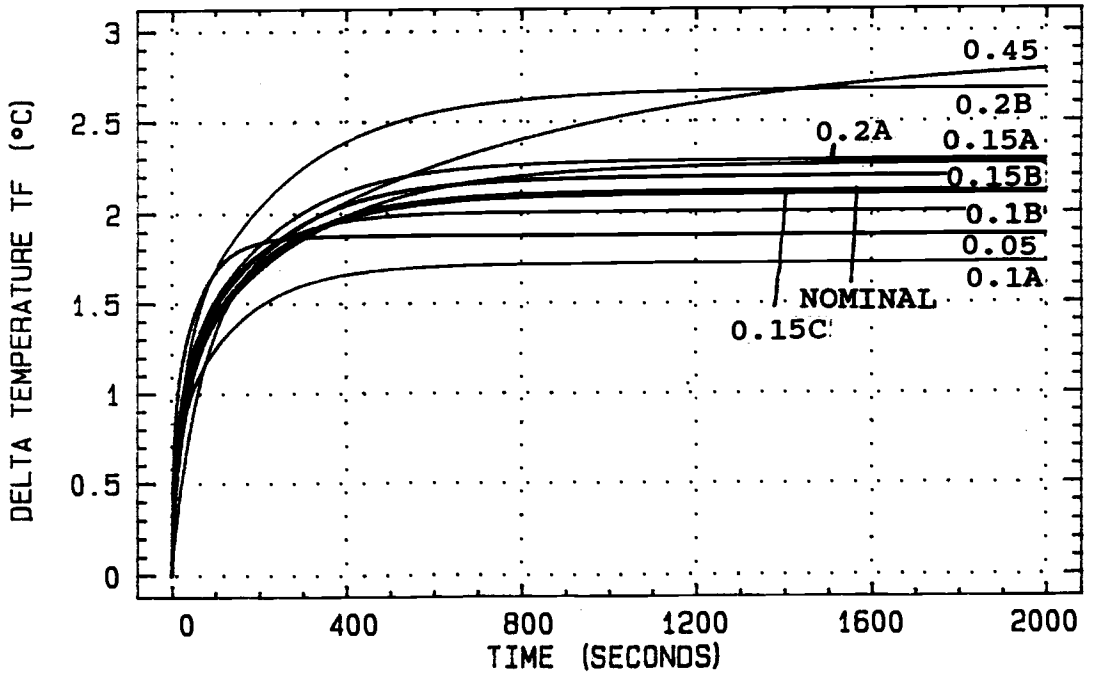

Fig. 68. Open-loop response to a 10 % increase in the steam temperature as a function of the RGA value for TF

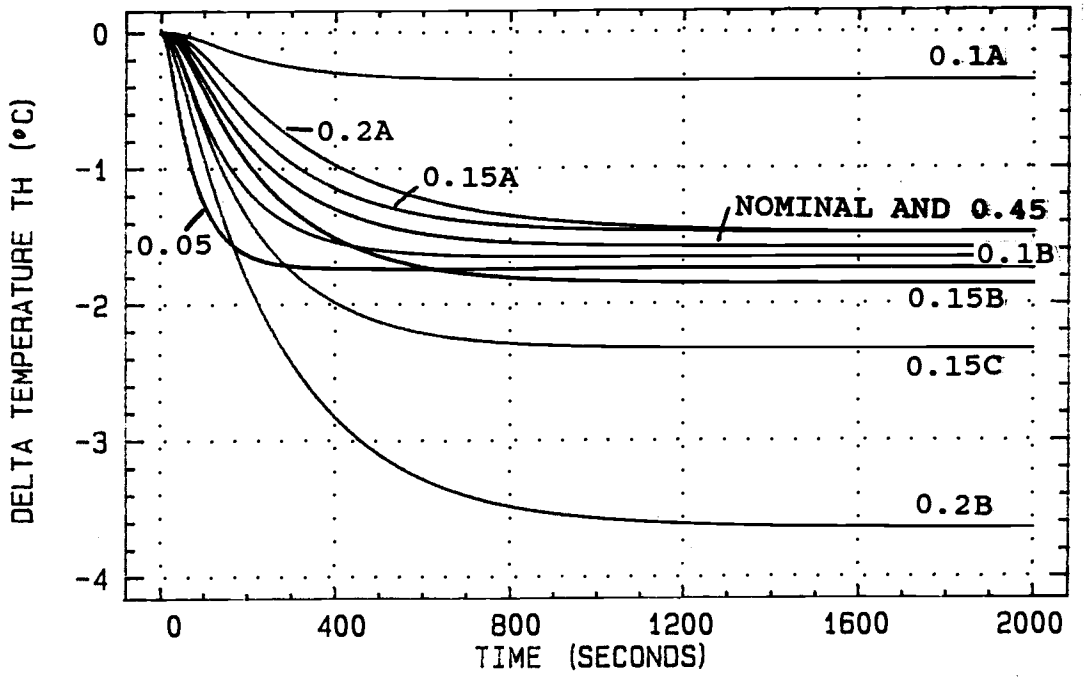

Fig. 69. Open-loop response to a 40 % decrease in the flow fraction as a function of the RGA value for TH

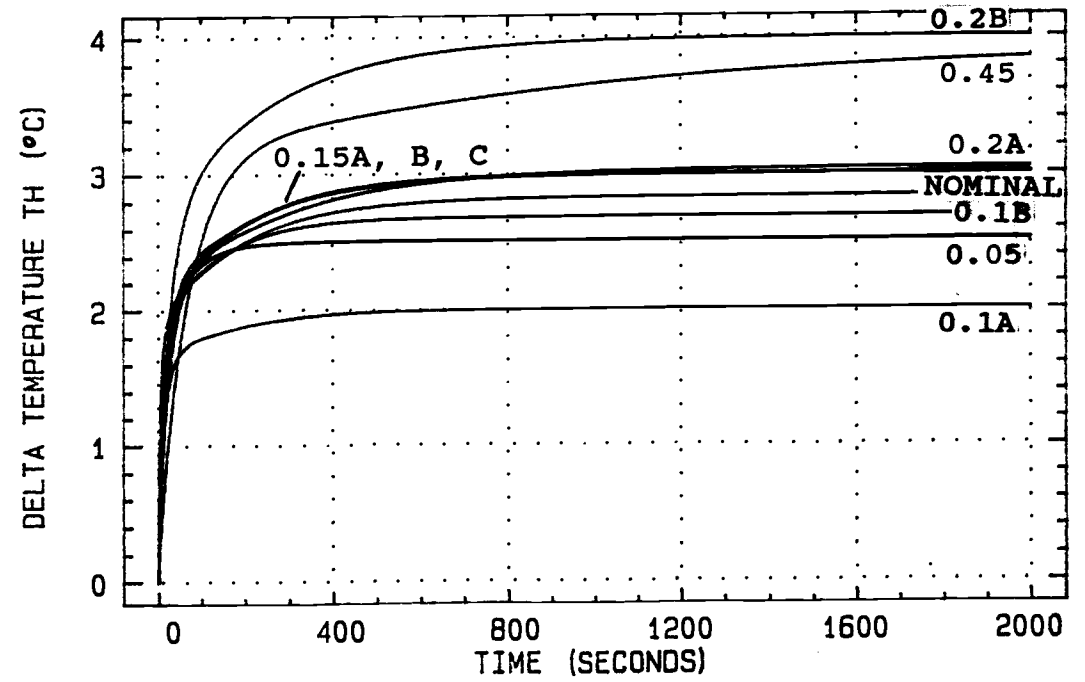

Fig. 70. Open-loop response to a 10 % increase in the steam temperature as a function of the RGA value to TH

Table 35a. Temperatures used to determine the process parameters from program DTXFCN

RGA	T1	TH	TS	TF	T2
0.05	40.99993	58.49972	503.0944	52.59979	46.7
0.1	40.99993	54.86302	200.0000	52.59979	50.34
0.1	40.99993	58.49972	269.0972	52.59979	46.7
0.15	39.42901	58.49972	200.0000	52.59979	46.7
0.15	40.99993	59.22149	200.0000	52.59979	45.98
0.15	40.99993	58.49972	200.0000	51.02887	43.56
0.2	40.99993	58.49972	152.0986	52.59979	46.7
0.2	40.99993	63.82209	200.0000	52.59979	41.38
0.45	40.99993	58.49972	87.0994	52.59979	46.7
NOM	40.99993	58.49972	200.0000	52.59979	46.7

Table 35b. RTS and RX ratios for various 1,1 RGA element values

RGA	RTS	RX
0.05	1.33714	-25.40572
0.1	1.16326	-10.46931
0.1	1.33714	-12.03429
0.15	1.30937	-7.41977
0.15	1.36340	-7.72593
0.15	1.42691	-8.08583
0.2	1.33714	-5.34857
0.2	1.49173	-5.96992
0.45	1.33714	-1.63429
NOM	1.338	-8.089

ratios.

Sensitivity of system parameters to different RTS and RX ratios with the (1,1) RGA element constant at the nominal value

This section contains the plots showing the sensitivity of the system and process parameters and the open-loop responses to several pairs of the RTS and RX ratios which have a constant (1,1) RGA element equal to the nominal value of 0.1419. That is, these processes have equivalent steady-state process interactions but different individual transfer function gains and dynamic interactions.

Table 36 shows the values of temperatures used to compute the system parameters and open-loop responses from programs DTXFCN and DTHES2. The system parameters were determined by maintaining the (1,1) RGA element and the steam temperature at their nominal values.

Figure 71 is a plot of the slowest pole position as a function of the steam temperature ratio, RTS. This plot shows that although the ratios yield valid design temperatures, designs having RHP poles require negative heat transfer area in the recycle heat exchanger.

Figure 72 is a plot of the most significant zero as a function of the steam temperature ratio, RTS. This plot shows that the same RTS ratios that have RHP poles,

Table 36. Temperatures used to determine the process parameters from program DTXFCN for the nominal 1,1 RGA element value and varying RTS and RX ratio values

TS = 200.0 TI = 35.1

	RTS	RX	TF	T1	TH	T2
R1	1.1	-6.652	56.3724	37.227	58.4996	54.2452
R2	1.3	-7.861	53.0998	40.5	58.4997	47.6999
NOM	1.338	-8.089	52.5998	41.0	58.4997	46.7
R3	1.41	-8.466	51.6955	41.904	58.4997	44.8914
R4	1.43	-8.647	51.4634	42.136	58.4997	44.4272
R5	1.45	-8.768	51.2377	42.362	58.4997	43.9758
R6	1.47	-8.889	51.0182	42.582	58.4997	43.5366
R7	1.49	-9.010	50.8045	42.795	58.4997	43.1093
R8	1.50	-9.071	50.6998	42.900	58.4997	42.8999
R9	1.70	-10.28	48.8645	44.735	58.4997	39.2294
R10	1.999	-12.09	46.7999	46.800	58.4997	35.1

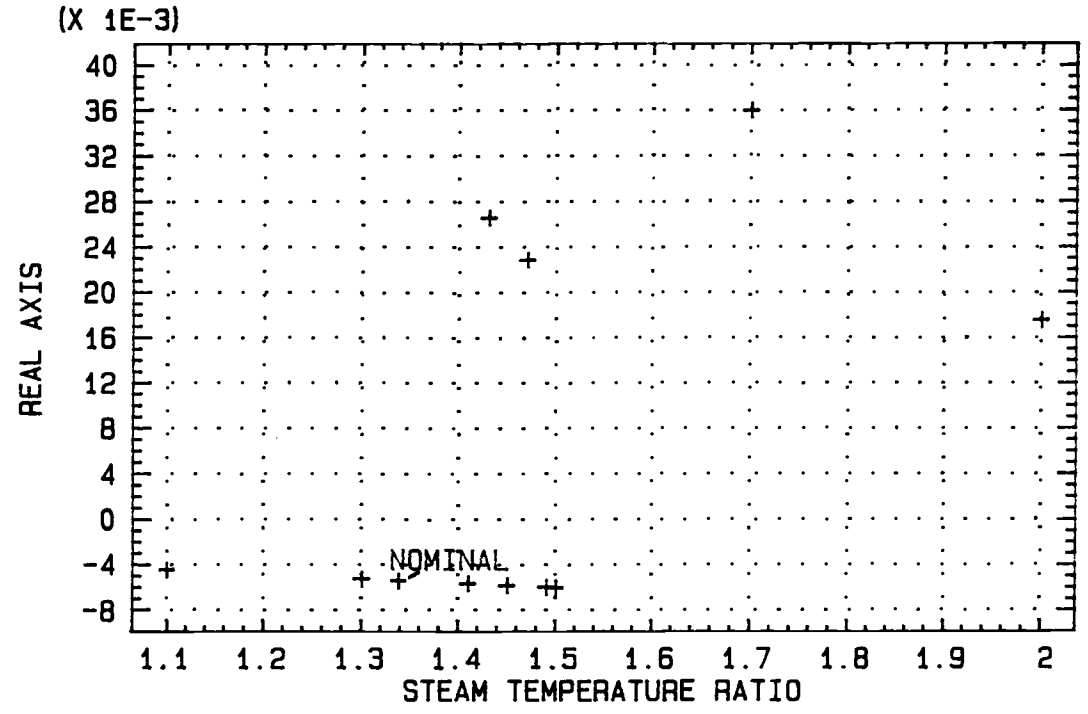

Fig. 71. Slowest pole as a function of the steam temperature ratio

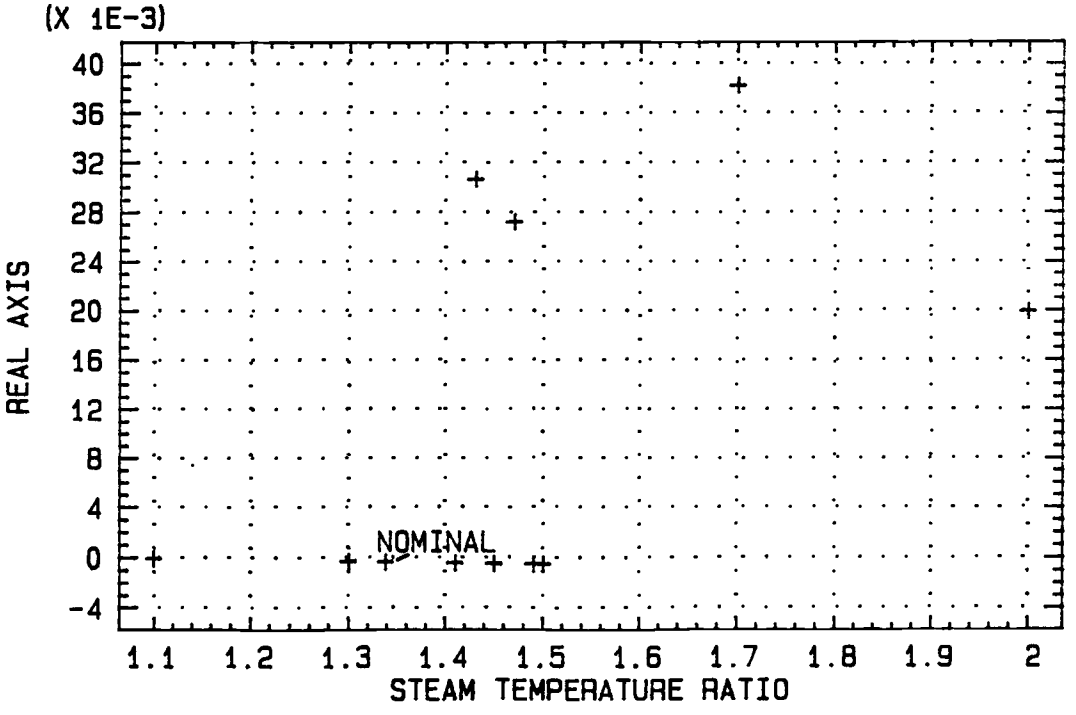

Fig. 72. Most significant zero as a function of the steam temperature ratios

also have RHP zeros.

Figures 73a and 73b show the most significant zero positions as functions of the slowest pole positions. Figure 73a shows the points for all of the RTS ratios examined. Figure 73b excludes those points in Figure 73a which require negative heat transfer area.

Figure 74 is a plot of the RPZ ratio as a function of the steam temperature ratio, RTS. This plot shows that feasible processes have RPZ ratios larger than 10.

Figure 75 is a plot of the recycle heat transfer area as a function of the steam temperature ratio, RTS. This plot shows infeasible negative heat transfer areas for those processes shown previously to have RHP poles. RTS ratios designated R7 and R8 show very large required heat transfer areas since the temperature difference between the hot and cold fluids leaving the recycle heat exchanger is very small.

Figures 76 through 79 are the open-loop responses for the processes which are shown to be feasible by their four design temperatures, ratios R1 through R8, even though the processes represented by R4 and R6 are expected to be open-loop unstable because of their RHP poles and negative heat transfer area. These figures show the open-loop responses to individual step changes in the flow fraction, delta X = -0.2 and in the steam temperature, delta TS = 20 °C. From these plots, the

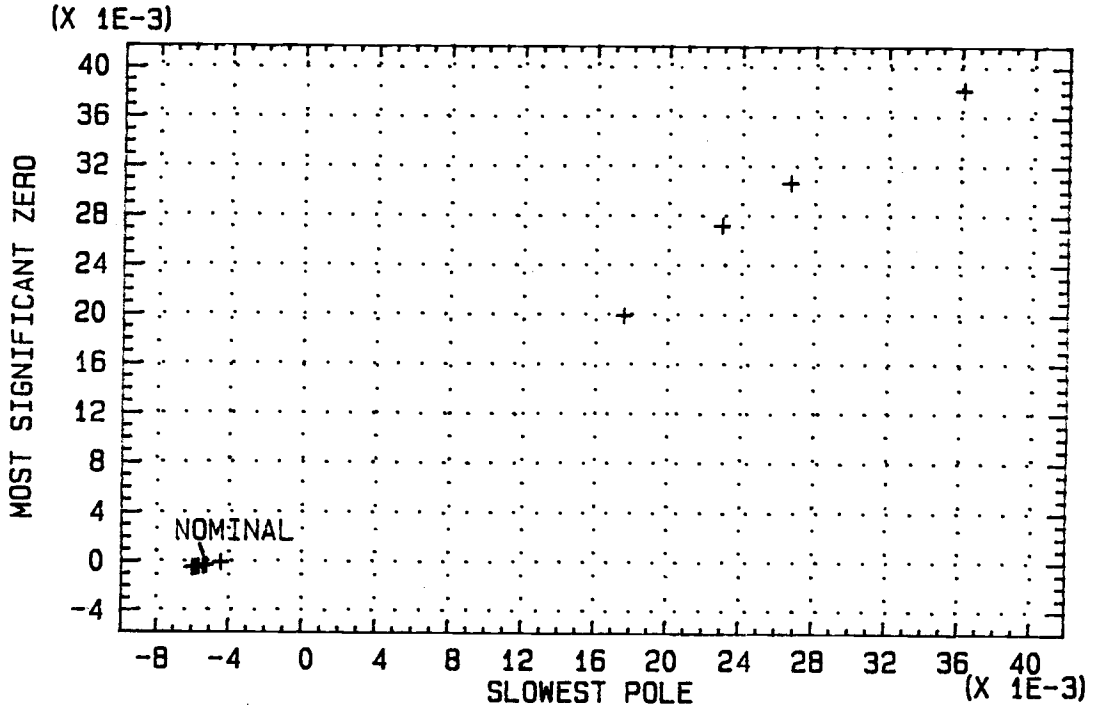

Fig. 73a. Most significant zero as a function of the slowest pole and the RTS ratio

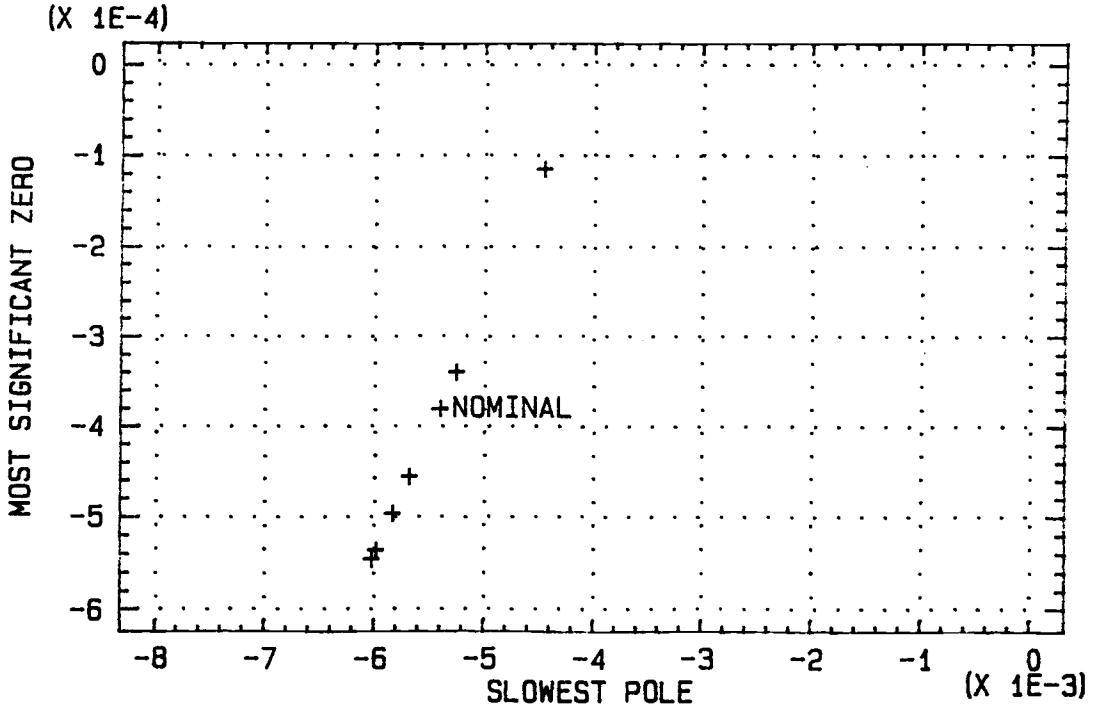

Fig. 73b. Most significant zero as a function of the slowest pole for stable RTS ratios

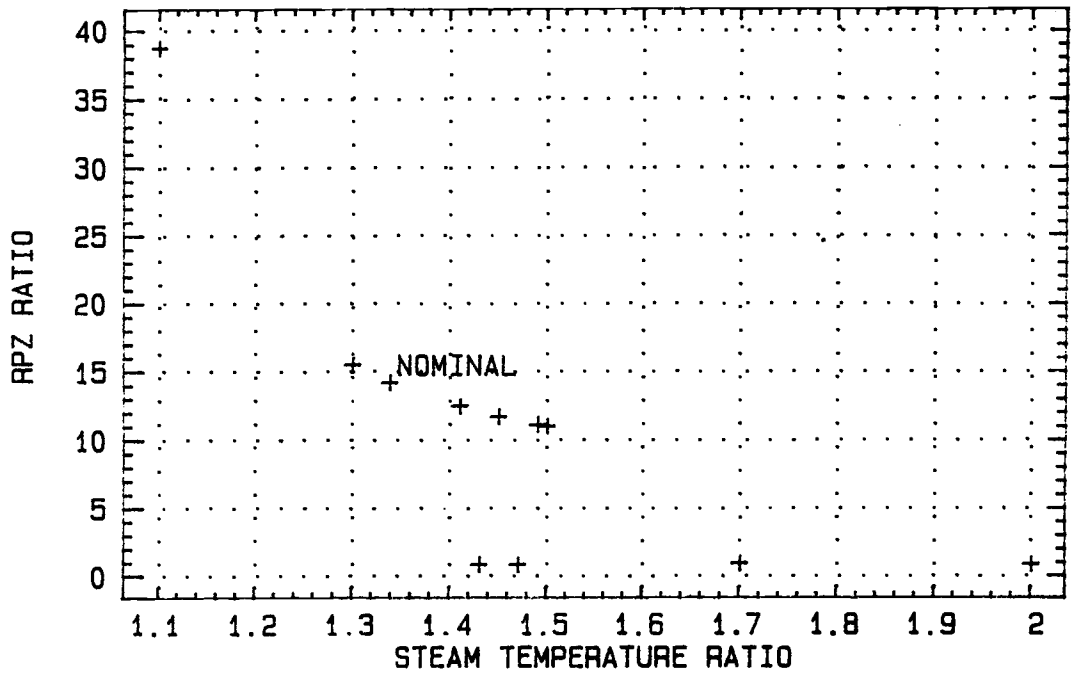

Fig. 74. RPZ ratio as a function of the steam temperature ratio

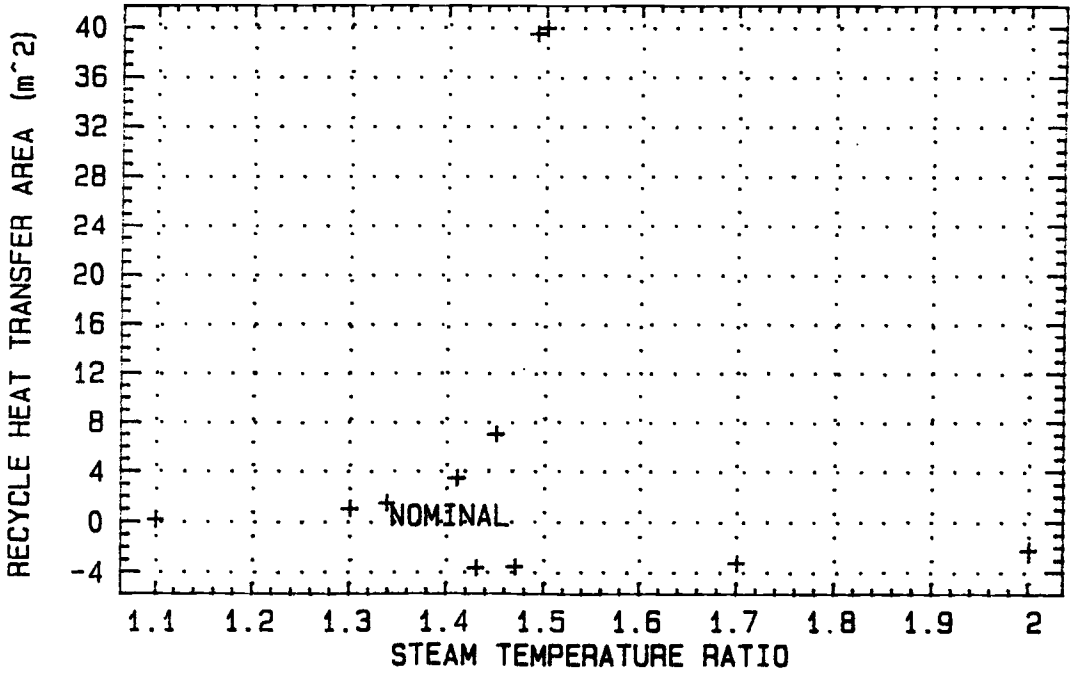

Fig. 75. Recycle heat transfer area as a function of the steam temperature ratio

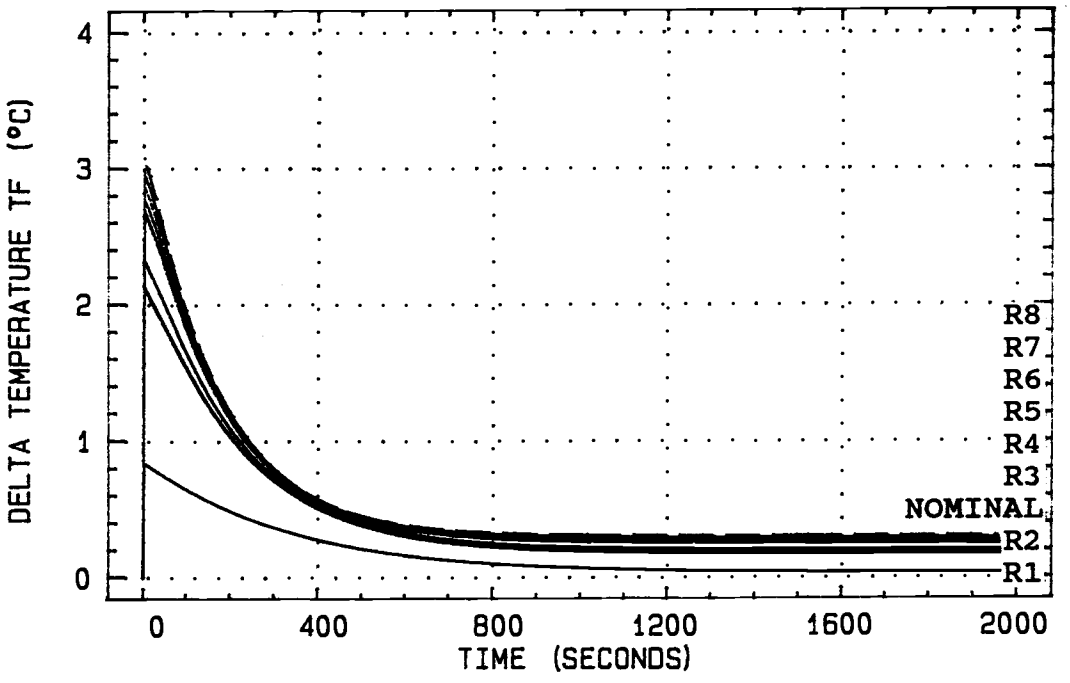

Fig. 76. Open-loop response to a 40 % decrease in the flow fracton as a function of the RTS ratio for TF

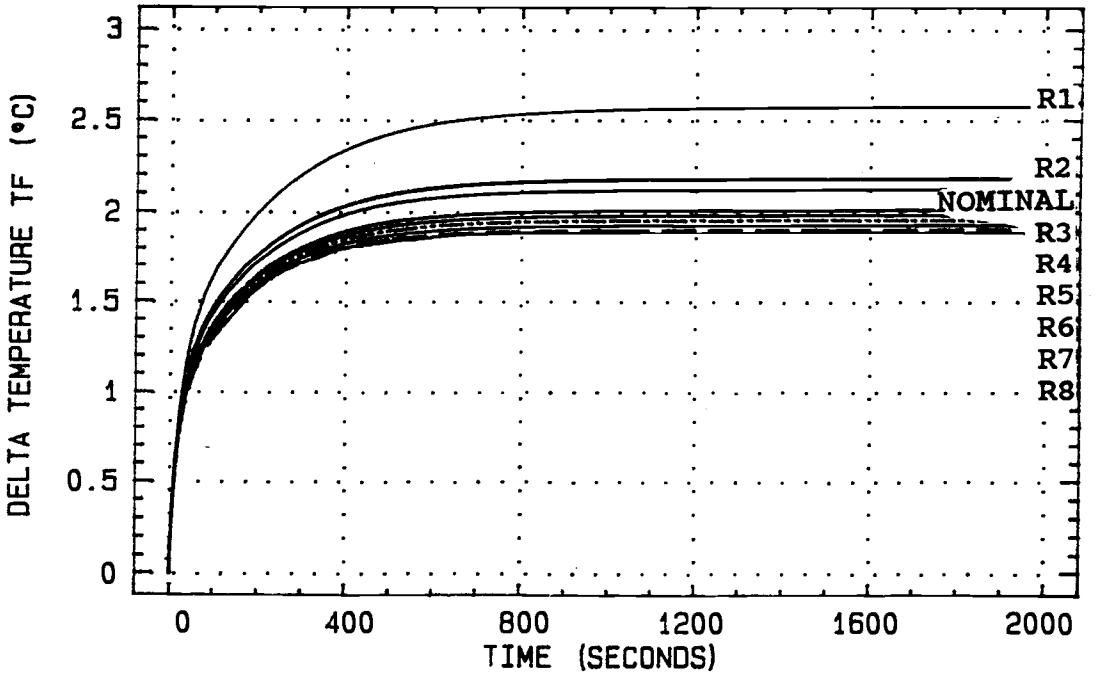

Fig. 77. Open-loop response to a 10 % increase in the steam temperature as a function of the RTS ratio for TF

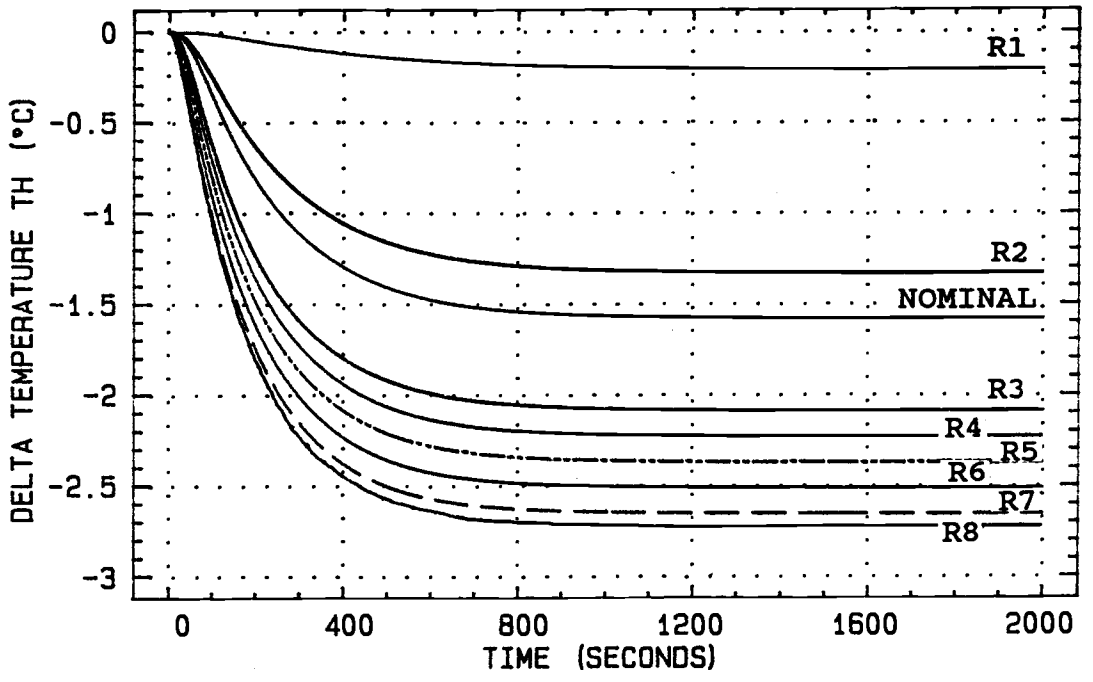

Fig. 78. Open-loop response to a 40 % decrease in the flow fraction as a function of the RTS ratio for TH

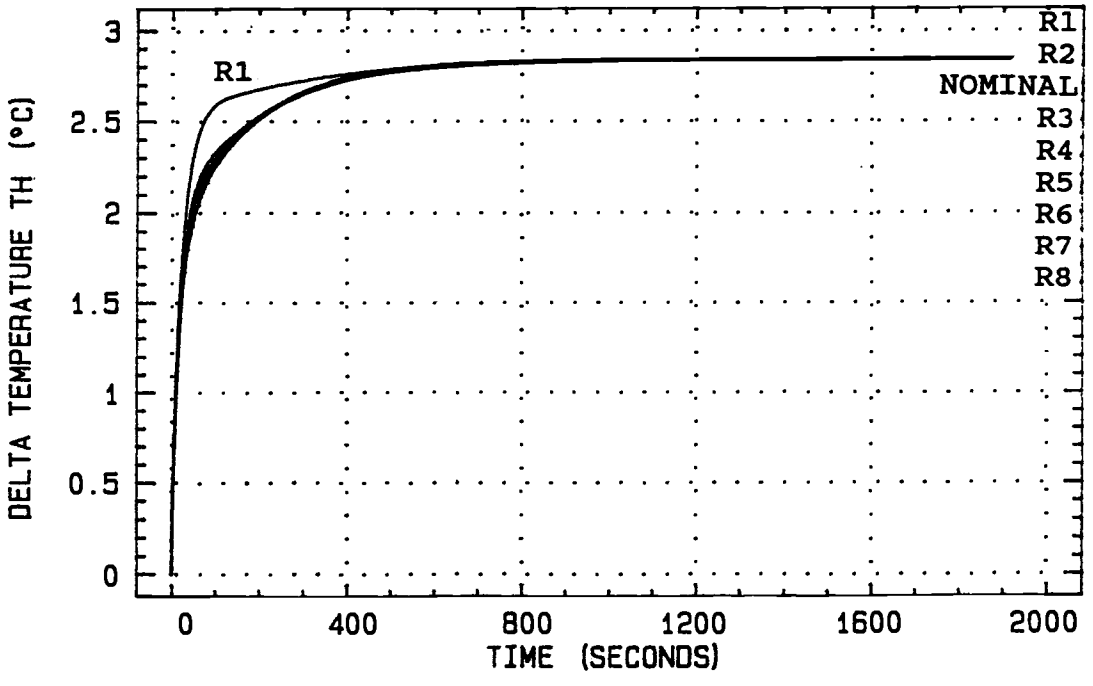

Fig. 79. Open-loop response to a 10 % increase in the steam temperature as a function of the RTS ratio for TH

response to a change in X, is slightly slower to reach smaller steady-state values for smaller values of RTS. However, the response to a change in TS, is slightly faster and reaches larger steady-state values for smaller values of RTS.

For changes in X, there are larger initial changes in the TF/X response and larger steady-state gains for increases in the RTS ratio, for both TF/X and TH/X transfer functions. For changes in TS, the steady-state gain for the transfer function TH/TS remains constant as the RTS ratio is increased. The steady-state gain of the transfer function TF/TS decreases as the steam temperature ratio is increased.

There are no open-loop responses for the processes R9 and R10 as these ratios require infeasible process temperatures.

REMARKS

1. Network system design based upon a desired set of pole positions may be roughly accomplished through the use of Figures 39 through 44. These figures show the variations in pole position by changing one process parameter at a time and using nominal values for the other system parameters.

2. Figures 45 through 50, showing the positions

of the zeros for the TF/X transfer function, should be used in conjunction with Figures 39 through 44 to design the desired open-loop responses into the network.

3. For nominal design temperatures, faster networks may be designed by using larger overall steam heat exchanger transfer coefficients, smaller recycle and steam heat exchanger volumes, larger steam heat transfer areas, higher steam temperatures and smaller flow fractions bypassing the recycle heat exchanger values.

4. If it is desired to change the RPZ ratio, only the volume of the recycle heat exchanger, the volume of the steam heat exchanger, the steam temperature and the flow fraction may be used. The other process parameters have no effect on this ratio.

5. Figures 55 through 58 can be used to check the feasibility of a design based upon the recycle heat exchanger heat transfer area. This heat transfer area needs to be checked against the recycle heat exchanger volume being used.

6. Since four parameters (in this study, the four design temperatures) must be specified to describe the network, it is possible to specify three of the design temperatures and the (1,1) element of the RGA. The effect of choosing the (1,1) element of the RGA and three of the four design temperatures is shown in

Figures 59 through 62.

7. Smaller values of the (1,1) element of the RGA yield faster networks due to less interactions. Smaller values of the (1,1) element of the RGA also have larger RPZ ratios. However, for a given (1,1) element value, larger values of the RTS and RX ratios yield faster open-loop responses to changes in the manipulated variables.

8. The extent of initial deviation for the TF/X transfer function is a function of the RTS and RX ratios more than the value of the interactions. Larger ratios lead to increased initial deviations and higher steady-state gains.

9. From the nominal value of the (1,1) element of the RGA and different RTS and RX ratios, the four design temperatures may be determined. Although the design temperatures may be valid, the network may not be physically possible. This is illustrated in ratios R4 and R6, which have ostensibly valid design temperatures yet have poles in the RHP and negative recycle heat transfer areas.

10. Those networks which are open-loop stable, as shown by having all poles in the left-half complex S-plane, also have RPZ ratios greater than 10.

11. Those networks which are open-loop unstable, as shown by poles in the RHP, also have infeasible

negative heat transfer areas.

12. As shown in Figures 76 through 79, the open-loop response is slightly slower to reach steady state for smaller RTS ratios for changes in the flow fraction. At the same time, the open-loop response to a change in steam temperature is slightly faster for smaller RTS ratios.

14. For changes in the flow fraction, there are larger initial deviations and steady-state gains as the RTS ratio increases.

15. For changes in the steam temperature, the steady-state gain of the TH/TS transfer function remains constant as the RTS ratio increases. The steady-state gain of the TF/TS transfer function decreases as the RTS ratio increases.

APPENDIX B - PROGRAM LISTINGS

```
      PROGRAM THESIS
C*****************************************************
C
C     THIS PROGRAM SIMULATES A STEP CHANGE IN ONE OR BOTH
C     OF THE MANIPULATED VARIABLES.  THE USER IS PROMPTED
C     FOR THE PROCESS PARAMETERS AND VARIABLES.  THE
C     PROGRAM USES WATER AS THE FLUID.
C
C     THIS PROGRAM NEEDS TO BE LINKED TO DEPISOD2.OBJ TO
C     BE USED.  DEPISOD2.OBJ IS THE DOUBLE PRECISION
C     VERSION OF EPISODE.
C
C     THE TEMPERATURE OUTPUTS ARE PLACED IN FILE EPI.ONE.
C
C     THIS PROGRAM IS TO BE USED AFTER DTXFCN TO VERIFY
C     THE TEMPERATURES USED ARE VALID.
C
C     WRITTEN BY JEFFREY J. PASHAK          NOVEMBER 1988
C
C*****************************************************
      INTEGER NQUSED, NSTEP, NFE, NJE, Q
      INTEGER N, MF, INDEX, IPRINT, FINAL
      DOUBLE PRECISION HUSED, YO, TO, TI, TS, TF, HINIT,
     S EPS, HO, TOUT
      DIMENSION YO(3)
      DOUBLE PRECISION F, X, Y, Z, V1, V2, V3, RHO, CP,
     S U3, A3
      COMMON/VARIAB/ F, X, Y, Z, V1, V2, V3, TI, TS, TF
      COMMON/EPCOM9/ HUSED, NQUSED, NSTEP, NFE, NJE
C
C
      OPEN (1, FILE = 'EPI.ONE', STATUS = 'NEW')
C
      N = 3
      TO = 0.
      HO = 1E-4
      EPS = 1E-4
      IERROR = 3
      MF = 21
      INDEX = 1
C
      RHO = 1000.
      CP = 4186.
      U3 = 2800.
      A3 = 0.08D0
      V1 = 0.04D0
      V2 = V1
```

```
      V3 = 0.01D0
C
      WRITE (*,*) 'T1, T2, TH = ?'
      READ (*,*) YO(1), YO(2), YO(3)
      WRITE (*,*) 'INITIAL STEAM TEMP = ?'
      READ (*,*) TSIN
      WRITE (*,*) 'INITIAL VALVE OPENING = ?'
      READ (*,*) XIN
      TF = YO(2) * XIN + (1 - XIN) * YO(3)
      TI = YO(1) + TF - YO(3)
      F = U3 * A3 * (TSIN - YO(3)) / (YO(3) - YO(1)) /
     S RHO / CP
      Y = U3 * A3 / RHO / CP
      Z = (YO(3) - YO(2)) / (YO(2) - YO(1)) * F * XIN
      WRITE (*,*) 'FINAL TIME(NUMBER OF ITERATIONS) = ?'
      READ (*,*) FINAL
      WRITE (*,*) 'USING WHAT PRINT INTERVAL?'
      READ (*,*) ENTVL
      WRITE (*,*) 'STEP CHANGE TO WHAT X VALUE?(FROM ',
     S XIN,')'
      READ (*,*) X
      WRITE (*,*) 'STEP CHANGE TO WHAT TS VALUE?(FROM',
     S TSIN,')'
      READ (*,*) TS
      WRITE (1, 100)
  100 FORMAT (1X, 'TIME', 6X, 'TEMP H', 7X, 'TEMP F')
      WRITE (1, 110) TO, YO(3), TF
  110 FORMAT (1X, F7.1, 3X, 4(F15.10, 2X))
C
      TOUT = TO + ENTVL
C
      DO 10, IPRINT = 1, FINAL
        CALL DRIVE (N, TO, HO, YO, TOUT, EPS, IERROR,
     S     MF, INDEX)
        TF = X * YO(2) + (1 - X) * YO(3)
        WRITE (1, 110) TO, (YO(Q), Q = 1,3), TF
        IF (INDEX .NE. 0) THEN
          WRITE (*,*) 'INDEX .NE. 0  OOPS!! MISTAKE!!!'
          STOP
         ENDIF
        TOUT = TOUT + ENTVL
   10  CONTINUE
       STOP
       END
C
C
C
      SUBROUTINE DIFFUN(N, T, YY, YDOT)
C*****************************************************
C
C     THIS SUBROUTINE CALCULATES THE VALUE FOR THE
C     DIFFERENTIAL EQUATIONS.
```

```
C
C*************************************************************
      INTEGER N
      DOUBLE PRECISION T, YY, YDOT
      DOUBLE PRECISION F, X, Y, Z, V1, V2, V3, TI, TS,
     S TF
      DIMENSION YY(N), YDOT(N)
      COMMON/VARIAB/ F, X, Y, Z, V1, V2, V3, TI, TS, TF
C
      YDOT(1) = F / V1 * TI + Z / V1 * YY(2) - (F + Z) /
     S V1 * YY(1)
      YDOT(2) = Z / V2 * YY(1) + F * X / V2 * YY(3) - (Z
     S + X * F) / V2 * YY(2)
      YDOT(3) = Y / V3 * TS + F / V3 * YY(1) - (F + Y) /
     S V3 * YY(3)
C
      RETURN
      END
C
C
C
      SUBROUTINE PEDERV(N, T, YY, PD, NO)
C*************************************************************
C
C     THIS SUBROUTINE CALCULATES THE PARTIAL DERIVATIVES
C     OF THE DIFFERENTAL EQUATIONS.
C
C*************************************************************
      INTEGER N, NO
      DOUBLE PRECISION T, YY, PD
      DOUBLE PRECISION F, X, Y, Z, V1, V2, V3, TI, TS,
     S TF
      DIMENSION PD(NO, NO)
      COMMON/VARIAB/ F, X, Y, Z, V1, V2, V3, TI, TS, TF
C
      PD(1, 1) = - (F + Z) / V1
      PD(1, 2) = Z / V1
      PD(1, 3) = 0.
      PD(2, 1) = Z / V2
      PD(2, 2) = - (Z + X * F) / V2
      PD(2, 3) = F * X / V2
      PD(3, 1) = F / V3
      PD(3, 2) = 0.
      PD(3, 3) = - (F + Y) / V3
C
      RETURN
      END
```

```
      PROGRAM TXFCN
C*********************************************************
C
C     THIS PROGRAM CALCULATES THE POLES, ZEROS, SYSTEM
C     ZEROS, TRANSFER FUNCTIONS, THE SLOWEST POLE TO MOST
C     SIGNIFICANT ZERO RATIO AND VARIOUS PROCESS
C     PARAMETERS AND VARIABLES GIVEN THE TARGET/DESIGN
C     TEMPERATURES.
C
C     WRITTEN BY JEFFREY J. PASHAK            OCTOBER 1988
C
C*********************************************************
      DOUBLE PRECISION NUM(4), DEN(4), COF(4), DCOF(4),
     S ROOTR(3)
      DOUBLE PRECISION ROOTDR(3), ROOTI(3), ROOTDI(3),
     S ZZN(5), ZZNI(5)
      DOUBLE PRECISION ZZP(5), ZZPI(5), SYSZERO(6),
     S SCOF(6), SROOTR(5)
      DOUBLE PRECISION SROOTI(5), THTS(3), TFTS(3),
     S NEWDEN(5), THX
      DOUBLE PRECISION T1, TH, TS, TF, TI, A3, V3, RHO,
     S CP, V1, V2, X
      DOUBLE PRECISION U3, T2, F, Y, Z, ZERO, POLE,
     S RATIO, VRATIO
      DOUBLE PRECISION VVRATIO,VVVRATIO, VV
      INTEGER IER, DIER, SIER, Q, PZ, NZ, NUMRT, DENRT,
     S II
      INTEGER I, J, K, LL, M, N, MP1, NP1, QQ, INC, INS,
     S INT, INTT
      CHARACTER*1 YY
C
C     DATA INPUT SECTION
C
      WRITE (*,*) 'CHANGES IN INPUT MAY BE MADE AT THE
     S END OF INPUT'
      WRITE (*,*) 'SECTION IF YOU MAKE A MISTAKE.'
C
      INT = 0
   10 RHO = 1000.
      CP = 4186.
      PZ = 0
      NZ = 0
      INC = 0
      INS = 0
C
      WRITE (*,*) 'TS(',TS,'), TF(',TF,') = ?'
      READ (*,*) TS, TF
      WRITE (*,*) 'T1(',T1,'), TH(',TH,') = ?'
      READ (*,*) T1, TH
      TI = T1 + TF - TH
C
```

```
      IF (INT .EQ. 1) GOTO 111
C
  11  IF (INT .EQ. 0) THEN
        V3 = 0.01D0
        U3 = 2800.
       ELSE
        WRITE (*,*) 'VOLUME 3(',V3,') = ?'
        READ (*,*) V3
        WRITE (*,*) 'OVERALL HT TX COEF (U3)(',U3,')
     S   = ?'
        READ (*,*) U3
        GOTO 111
       ENDIF
   12 IF (INT .EQ. 0) THEN
        A3 = 0.08D0
       ELSE
        WRITE (*,*) 'AREA 3(',A3,') = ?'
        READ (*,*) A3
        GOTO 111
       ENDIF
   13 IF (INT .EQ. 0) THEN
        V1 = 0.04D0
        V2 = V1
       ELSE
        WRITE (*,*) 'VOLUME OF HT EX1 COLD SIDE(',V1,')
     S   = ?'
        READ (*,*) V1
        V2 = V1
        GOTO 111
       ENDIF
   14 IF (INT .EQ. 0) THEN
        X = 0.5D0
       ELSE
        WRITE (*,*) 'FRACTION OF FLOW TO HOT SIDE OF HT
     S   EX1(',X,') = ?'
        READ (*,*) X
        GOTO 111
       ENDIF
   15 WRITE (*,*) 'DO YOU WANT TX FCNS FOR CONSYD?(Y/N)'
      READ (*,'(A1)') YY
      IF (YY .EQ. 'Y' .OR. YY .EQ. 'y') INC = 1
      IF (INC .EQ. 1) THEN
        WRITE (*,*) 'CONSTANT FOR EXTRA S IN
     S   DENOMINATOR(0 FOR SEMI', ' PROPER, 3RD/3RD
     S   ORDER SYSTEM) = '
        READ (*,*) CON
       ENDIF
      IF (INT .EQ. 1) GOTO 111
   16 WRITE (*,*) 'DO YOU WANT TO CREATE THE SYSTEM
     S ZEROS FILE? (Y/N)'
      READ (*,'(A1)') YY
```

```
      IF (YY .EQ. 'Y' .OR. YY .EQ. 'y') INS = 1
  111 WRITE (*,*) 'TS         =', TS, '  TF          =',
     S TF
      WRITE (*,*) 'T1         =', T1, '  TH          =',
     S TH
      WRITE (*,*) 'V1 , V2    =', V1, '  V3          =',
     S V3
      WRITE (*,*) 'HT TX COEF 3 =', U3, '  HT TX AREA 3
     S =', A3
      WRITE (*,*) 'FRAC FLOW TO PREHEAT EX =', X
      WRITE (*,*) 'DO YOU WANT TO CHANGE:'
      WRITE (*,*) '1)  TEMPERATURES TS, TF, T1, TH(AND
     S THEREFORE TI)'
      WRITE (*,*) '2)  VOLUME 3 OR HEAT TRANSFER
     S COEFFICIENT'
      WRITE (*,*) '3)  HEAT TRANSFER AREA 3'
      WRITE (*,*) '4)  VOLUME 1(AND THEREFORE VOLUME 2)'
      WRITE (*,*) '5)  FRACTION OF FLOW TO HEAT EX1'
      WRITE (*,*) '6)  FIGURE TX FCNS FOR
     S CONSYD(STRICTLY PROPER)'
      WRITE (*,*) '7)  DETERMINE SYSTEM ZEROS'
      WRITE (*,*) '8)  CONTINUE'
      READ (*,*) INTT
      INT = 1
      IF (INTT .GT. 8 .OR. INTT .LT. 1) THEN
        GOTO 111
       ELSE
        GOTO (10, 11, 12, 13, 14, 15, 16) INTT
       ENDIF
C
C     OPEN STATEMENTS
C
      OPEN (1, FILE = 'GREAT.NOW', STATUS = 'NEW')
      OPEN (2, FILE = 'RATIOS.NOW', STATUS = 'NEW')
      OPEN (3, FILE = 'POLES.NOW', STATUS = 'NEW')
      OPEN (4, FILE = 'ZEROS.NOW', STATUS = 'NEW')
      OPEN (6, FILE = 'NUMER.NOW', STATUS = 'NEW')
      OPEN (7, FILE = 'DENOM.NOW', STATUS = 'NEW')
      OPEN (9, FILE = 'ODDBALL.NOW', STATUS = 'NEW')
      IF (INC .EQ. 1) THEN
        OPEN (10, FILE = 'TXFCN.NOW', STATUS = 'NEW')
       ENDIF
      IF (INS .EQ. 1) THEN
        OPEN (5, FILE = 'SYSZERO.NOW', STATUS = 'NEW')
        OPEN (8, FILE = 'NSYSZER.NOW', STATUS = 'NEW')
       ENDIF
C
C     HEADER STATEMENTS FOR FILES
C
      WRITE (1,100)
  100 FORMAT (4X, 'V1', 5X, 'V2', 5X, 'V3', 5X, 'X', 4X,
```

```
     S 'GREATEST', ' POLE (R,i)', 8X, 'GREATEST ZERO
     S (R,i)')
      WRITE (2,110)
  110 FORMAT (4X, 'V1', 5X, 'V2', 5X, 'A3', 5X, 'X', 3X,
     S 'P/Z RATIO', 4X, 'V1/V2 RATIO', 2X, 'V1/V3
     S RATIO', 2X, 'V2/V3 RATIO')
      WRITE (3, 120)
  120 FORMAT (4X, 'V1', 5X, 'V2', 5X, 'A3', 5X, 'X', 8X,
     S 'POLE 1 (R,i)', 15X, 'POLE 2 (R,i)', 15X, 'POLE 3
     S (R,i)')
      WRITE (4, 130)
  130 FORMAT (4X, 'V1', 5X, 'V2', 5X, 'A3', 5X, 'X', 8X,
     S 'ZERO 1 (R,i)', 15X, 'ZERO 2 (R,i)', 15X, 'ZERO 3
     S (R,i)')
      WRITE (6, 150)
  150 FORMAT (4X, 'V1', 5X, 'V2', 5X, 'A3', 5X, 'X', 4X,
     S 'NUM CONST', 7X, 'NUM S1', 7X, 'NUM S2', 7X, 'NUM
     S S3')
      WRITE (7, 160)
  160 FORMAT (4X, 'V1', 5X, 'V2', 5X, 'A3', 5X, 'X', 4X,
     S 'DEN CONST', 7X, 'DEN S1', 7X, 'DEN S2', 7X, 'DEN
     S S3')
      WRITE (9, 180)
  180 FORMAT (4X, 'U3', 5X, 'A3', 5X, 'V1', 5X, 'X', 8X,
     S  'Z', 12X, 'Y', 11X, 'T2', 12X, 'F')
      IF (INS .EQ. 1) THEN
        WRITE (5, 140)
  140   FORMAT (4X, 'V1', 5X, 'V2', 5X, 'A3', 5X, 'X',
     S   4X, 'SYSTEM ', 'ZEROS GREATER THAN ZERO (R,i)')

        WRITE (8, 170)
  170   FORMAT (4X, 'V1', 5X, 'V2', 5X, 'A3', 5X, 'X',
     S   4X, 'SYSTEM',
     S         ' ZEROS LESS THAN/EQUAL TO ZERO (R,i)')
        ENDIF
      IF (INC .EQ. 1) THEN
            WRITE (10,190)
  190       FORMAT (4X, 'U3', 6X, 'A3', 4X, 'V1V2', 4X,
     S        'X', 5X, 'CON')
        ENDIF
C
C    THIS SECTION FINDS THE F, Y, Z, AND T2 GIVEN THE
C    ABOVE INFO
C
      F = U3 * A3 * (TS - TH) / (TH - T1) / RHO / CP
      Y = U3 * A3 / RHO / CP
      T2 = (TF - (1. - X) * TH) / X
      Z = (TH - T2) / (T2 - T1) * F * X
      WRITE (*,*) 'V1 ,   V2  = ', V1, '  V3          =
     S ', V3
      WRITE (*,*) 'FRAC FLOW  = ',  X, '  TOTAL FLOW =
```

```
S ', F
 WRITE (*,*) 'HT EX1 (Z) = ',  Z, '  HT EX3 (Y) =
S ', Y
 WRITE (*,*) 'INLET    TEMP    (TI)   =', TI
 WRITE (*,*) 'TEMP OUT OF HT EX2 (T2) =', T2
 M = 3
 N = 5
 NUM(1) = (T2 - TH) * F * Z * Y
 NUM(2) = (T2 - TH) * (V1 * Z * (F + Y) + V2 * (F +
S         Z) * (F + Y) + V3 * F * Z)
 NUM(3) = (T2 - TH) * (V1 * V2 * (F + Y) + V1 * V3
S         * Z + V2 * V3 * (F + Z))
 NUM(4) = (T2 - TH) * V1 * V2 * V3
 DEN(1) = F**3 * X + F**2 * (Y * X + Z) + F * Z * Y
S         * (1 + X)
 DEN(2) = V1 * (F * X + Z) * (F + Y) + V2 * (F + Z)
S         * (F + Y) + V3 * (F**2 * X + F * Z * (1 +
S         X))
 DEN(3) = V1 * V2 * (F + Y) + V1 * V3 * (F * X + Z)
S         + V2 * V3 * (F + Z)
 DEN(4) = V1 * V2 * V3
 IF (INS .EQ. 1) THEN
   SYSZERO(1) = F**2 * Z * Y * (F**2 * X + F * (X *
S                Y + Z) + Z * Y * (1 + X))
   SYSZERO(2) = V1 * F * Z * Y * ((F + Y) * (F * X
S               + Z * (1 + X)) + Y * (F * X + Z) + F
S               * (F * X + Z * (1 - X))) + V2 * F *
S               Y * (F + Z) * ((F + Y) * (F * X + Z
S               * (1 + X)) + Z * Y + F * Z * (1 -
S               X)) + V3 * F * Z * (F**2 * X * Y
S               + F * Z * Y * (1 + X))
   SYSZERO(3) = V1 * V2 * Y * ((F + Y) * (F**2 * X
S               + F * Z * (1 + X) + Z * (F + Z) + (F
S               + Z) * (F * X + Z)) + F**2 * Z * (1
S               - X)) + V1 * V3 * Z * Y * (F**2
S               * X + F * Z * (1 + X) + F**2 * X + F
S               * Z) + V2 * V3 * F * Y * (F + Z) *
S               (F * X + Z * (2 + X)) + V1 * V2 * V3
S               * F * Z * Y + V1**2 * Z * Y * (F +
S               Y) * (F * X + Z) + V2**2 * Y * (F
S              + Y) * (F + Z)**2
   SYSZERO(4) = V1 * V2 * V3 * Y * (F**2 * X + F *
S               Z * (1 + X) + Z * (F + Z) + (F + Z)
S               * (F * X + Z) + F * Z) + V1**2 * V2
S               * Y * (F + Y) * (F * X + 2 * Z) + 2
S               * V1 * V2**2 * Y * (F + Y) * (F
S               + Z) + V1**2 * V3 * Z * Y * (F * X +
S               Z) + V2**2 * V3 * Y * (F + Z)**2
   SYSZERO(5) = V1**2 * V2 * V3 * Y * (F * X + 2 *
S               Z) + 2 * V1 * V2**2 * V3 * (F + Z) +
S               V1**2 * V2**2 * Y * (F + Y)
```

```
         SYSZERO(6) = V1**2 * V2**2 * V3 * Y
        ENDIF
C
C     TRANSFER FUNCTION NUMERATORS AND DENOMINATOR FOR
C     CONSYD SIMULATION
C
       IF (INC .EQ. 1) THEN
         THTS(3) = Y * V1 * V2
         THTS(2) = Y * (V1 *(F * X + Z) + V2 * (F + Z))
         THTS(1) = Y * F * (F * X + Z * (1 + X))
         THX = (TH - T2) * F**2 * Z
         TFTS(3) = Y * V1 * V2 * (1 - X)
         TFTS(2) = Y * V1 * (F * X + Z - Z * X) + Y * V2
     S     * (F + Z) * (1 - X)
         TFTS(1) = F * Y * (F * X + Z)
         NEWDEN(5) = CON * DEN(4)
         NEWDEN(4) = CON * DEN(3) + DEN(4)
         NEWDEN(3) = CON * DEN(2) + DEN(3)
         NEWDEN(2) = CON * DEN(1) + DEN(2)
         NEWDEN(1) = DEN(1)
        ENDIF
       NP1 = 6
       MP1 = 4
       CALL POLRT(NUM, COF, M, MP1, ROOTR, ROOTI, IER)
       CALL POLRT(DEN, DCOF, M, MP1, ROOTDR, ROOTDI,
     S  DIER)
       IF (INS .EQ. 1) THEN
         CALL POLRT(SYSZERO, SCOF, N, NP1, SROOTR,
     S    SROOTI, SIER)
        ENDIF
       IF (ROOTDR(1) .LT. 0. .AND. ROOTDR(2) .LT. 0.
     S  .AND. ROOTDR(3) .LT. 0.) THEN
         WRITE (4,200) V1, V2, A3, X, (ROOTR(Q),
     S    ROOTI(Q), Q = 1, M)
         WRITE (3, 200) V1, V2, A3, X, (ROOTDR(Q),
     S    ROOTDI(Q), Q = 1, M)
  200    FORMAT (1X, 3(F5.3, 2X), F4.2, 3(2X, E11.5,',',
     S    1X, E11.5,'i'))
        ENDIF
       PZ = 0
       NZ = 0
       IF(INS .EQ. 1) THEN
         DO 50 II = 1, 5
           IF (SROOTR(II) .GT. 0.) THEN
             PZ = PZ + 1
             ZZP(PZ) = SROOTR(II)
             ZZPI(PZ) = SROOTI(II)
            ELSE
             NZ = NZ + 1
             ZZN(NZ) = SROOTR(II)
             ZZNI(NZ) = SROOTI(II)
```

```
          ENDIF
   50    CONTINUE
         WRITE (5,200) V1, V2, A3, X, (ZZP(Q), ZZPI(Q), Q
     S     = 1, PZ)
         WRITE (8,200) V1, V2, A3, X, (ZZN(Q), ZZNI(Q), Q
     S = 1, NZ)
         ENDIF
        WRITE (6,230) V1, V2, A3, X, (NUM(Q), Q = 1, 4)
        WRITE (7,230) V1, V2, A3, X, (DEN(Q), Q = 1, 4)
        WRITE (9,220) U3, A3, V1, X, Z, Y, T2, F
  210 FORMAT (1X, 3(F5.3, 2X), F4.2, 2(2X, E11.5,',',
     S  1X, E11.5,'i'))
  220 FORMAT (1X, F5.0, 2X, 2(F5.3, 2X), F4.2, 4(2X,
     S  E11.5))
  230 FORMAT (1X, 3(F5.3, 2X), F4.2, 4(2X, E11.5))
C
C  PRINTING TRANSFER FUNCTION VALUES
C
      IF (INC .EQ. 1) THEN
  310   FORMAT (3X, F5.0, 2X, 4(F5.3, 2X))
        WRITE (10,310) U3, A3, V1, X, CON
        WRITE (10,320)
  320   FORMAT (3X, 'THTSCON', 8X, 'THTSS', 10X,
     S    'THTSS2')
        WRITE (10,330) (THTS(QQ), QQ = 1, 3)
        WRITE (10,350)
  350   FORMAT (3X, 'TFTSCON', 8X, 'TFTSS', 10X,
     S    'TFTSS2')
        WRITE (10,330) (TFTS(QQ), QQ = 1, 3)
        WRITE (10,360)
  360   FORMAT (3X, 'THX')
        WRITE (10,330) THX
        WRITE (10,370)
  370   FORMAT (3X, 'NEWDENCON', 6X, 'NEWDENS', 8X,
     S    'NEWDENS2', 7X, 'NEWDENS3', 7X, 'NEWDENS4')
        WRITE (10,330) (NEWDEN(QQ), QQ = 1, 5)
  330   FORMAT (1X, 5(E11.5, 4X))
       ENDIF
C
C     FINDING THE GREATEST ZERO AND POLE AND THE RATIOS
C
      NUMRT = 1
      DENRT = 1
      ZERO = ROOTR(1)
      POLE = ROOTDR(1)
      IF (ROOTR(2) .GT. ZERO) THEN
        ZERO = ROOTR(2)
        NUMRT = 2
       ENDIF
      IF (ROOTDR(2) .GT. POLE) THEN
        POLE = ROOTDR(2)
```

```
          DENRT = 2
         ENDIF
        IF (ROOTR(3) .GT. ZERO) THEN
          ZERO = ROOTR(3)
          NUMRT = 3
         ENDIF
        IF (ROOTDR(3) .GT. POLE) THEN
          POLE = ROOTDR(3)
          DENRT = 3
         ENDIF
        IF (ZERO .NE. 0.) THEN
          RATIO = POLE / ZERO
         ELSE
          WRITE (*,*) 'PROBLEM IN THE RATIO SECTION'
         ENDIF
        VRATIO = V1 / V2
        VVRATIO = V1 / V3
        VVVRATIO = V2 / V3
        WRITE (1, 210) V1, V2, V3, X, POLE, ROOTDI(DENRT),

      S        ZERO, ROOTI(NUMRT)
        WRITE (2, 230) V1, V2, A3, X, RATIO, VRATIO,
      S  VVRATIO, VVVRATIO
        STOP
        END
C
C
C
       SUBROUTINE POLRT(XCOF,COF,M,MP1,ROOTR,ROOTI,IER)
C*******************************************************
C
C     THIS SUBROUTINE CALCULATES THE ROOTS OF AN
C     EQUATION.
C
C*******************************************************
       DOUBLE PRECISION XCOF, COF, ROOTR, ROOTI
       DIMENSION XCOF(MP1),COF(MP1),ROOTR(M),ROOTI(M)
       DOUBLE PRECISION XO,YO,X,Y,XPR,YPR,UX,UY,V,YT,
      S  XT,U,XT2,YT2,SUMSQ,DX,DY,TEMP,ALPHA
       INTEGER IFIT
C
       IFIT=0
       N=M
       IER=0
       IF (XCOF(N+1)) 10,25,10
   10 IF (N) 15,15,32
C
   15 IER=1
   20 RETURN
C
   25 IER=4
```

```
      GO TO 20
C
   30 IER=2
      GO TO 20
   32 IF (N-36) 35,35,30
   35 NX=N
      NXX=N+1
      N2=1
      KJ1= N+1
      DO 40 L=1,KJ1
      MT=KJ1-L+1
   40 COF(MT)=XCOF(L)
C
   45 XO=.00500101
      YO=0.01000101
C
      IN=0
   50 X=XO
C
      XO=-10.0*YO
      YO=-10.0*X
C
      X=XO
      Y=YO
      IN=IN+1
      GO TO 59
   55 IFIT=1
      XPR=X
      YPR=Y
C
   59 ICT=0
   60 UX=0.0
      UY=0.0
      V= 0.0
      YT=0.0
      XT=1.0
      U=COF(N+1)
      IF (U) 65,130,65
   65 DO 70 I=1,N
      L= N-I+1
      TEMP=COF(L)
      XT2=X*XT-Y*YT
      YT2=X*YT+Y*XT
      U=U+TEMP*XT2
      V=V+TEMP*YT2
      FI=I
      UX=UX+FI*XT*TEMP
      UY=UY-FI*YT*TEMP
      XT=XT2
   70 YT=YT2
      SUMSQ=UX*UX+UY*UY
```

```
      IF (SUMSQ) 75,110,75
   75 DX=(V*UY-U*UX)/SUMSQ
      X=X+DX
      DY=-(U*UY+V*UX)/SUMSQ
      Y=Y+DY
   78 IF (DABS(DY)+DABS(DX)-1.0D-05) 100,80,80
C
   80 ICT=ICT+1
      IF (ICT-500) 60,85,85
   85 IF (IFIT) 100,90,100
   90 IF (IN-5) 50,95,95
C
   95 IER=3
      GO TO 20
  100 DO 105 L=1,NXX
      MT=KJ1-L+1
      TEMP=XCOF(MT)
       XCOF(MT)=COF(L)
  105 COF(L)=TEMP
      ITEMP=N
      N=NX
      NX=ITEMP
      IF (IFIT) 120,55,120
  110 IF (IFIT) 115,50,115
  115 X=XPR
      Y=YPR
  120 IFIT=0
  122 IF (DABS(Y)-1.0D-4*DABS(X)) 135,125,125
  125 ALPHA=X+X
      SUMSQ=X*X+Y*Y
      N=N-2
      GO TO 140
  130 X=0.0
      NX=NX-1
      NXX=NXX-1
  135 Y=0.0
      SUMSQ=0.0
      ALPHA=X
      N=N-1
  140 COF(2)=COF(2)+ALPHA*COF(1)
  145 DO 150 L=2,N
  150 COF(L+1)=COF(L+1)+ALPHA*COF(L)-SUMSQ*COF(L-1)
  155 ROOTI(N2)=Y
      ROOTR(N2)=X
      N2=N2+1
      IF (SUMSQ) 160,165,160
  160 Y=-Y
      SUMSQ=0.0
      GO TO 155
  165 IF (N) 20,20,45
      END
```

```
      PROGRAM IMPULSE
C*************************************************************
C
C     THIS PROGRAM CALCULATES THE IMPULSE RESPONSE
C     COEFFICIENTS FROM THE PROGRAM THESIS SIMULATION
C     OUTPUT FILE EPI.ONE.
C
C     OUTPUT FILE EP.DAT IS CREATED TO HOLD THE IMPULSE
C     RESPONSE COEFFICIENTS.
C
C     WRITTEN BY JEFFREY J. PASHAK           OCTOBER 1988
C
C*************************************************************
      DOUBLE PRECISION TFX, TFX1, TFX2, THX, THX1, THX2
      DOUBLE PRECISION TFTS, TFTS1, TFTS2, THTS, THTS1,
     S THTS2
      CHARACTER AZ
C
      OPEN(1, FILE='EPISODE.ONE', STATUS='OLD')
      OPEN(2, FILE='EP.DAT', STATUS='NEW')
      READ (1,101) AZ
  101 FORMAT (1X,A)
      DO 10 I = 1, 20
         IF (I .EQ. 1) THEN
           READ(1,*) A, B, C, THX1, TFX1
           READ(1,*) A, B, C, THX2, TFX2
          ELSE
           THX1 = THX2
           TFX1 = TFX2
           READ(1,*) A, B, C, THX2, TFX2
          ENDIF
         THX = THX2 - THX1
         TFX = TFX2 - TFX1
         WRITE (2,100) THX, TFX
  100    FORMAT(1X, 2E18.8)
   10  CONTINUE
      STOP
      END
```

```
      PROGRAM LAPLCTX
C*************************************************************
C
C     THIS PROGRAM CALCULATES THE IMPULSE RESPONSE
C     COEFFICIENTS FOR THE LINEAR TRANSFER FUNCTIONS BY
C     USING THE INVERSE LAPLACE OF THE LINEAR TRANSFER
C     FUNCTIONS IN THE TIME DOMAIN.  THE OUTPUT FROM THIS
C     PROGRAM MAY BE USED IN PROGRAM EIMC.
C
C     THE OUTPUT FROM THIS PROGRAM IS PLACED IN FILES
C      X.TXF AND TS.TXF FOR USE IN EIMC.  OUTPUT.TXF IS
C      THE COMBINATION OF X.TXF AND TS.TXF.
C
C     WRITTEN BY JEFFREY J. PASHAK            OCTOBER 1988
C
C*************************************************************
      DOUBLE PRECISION A, B, C, T, TFX, TFX1, TFX2,
     S TFTS, TFTS1, TFTS2
      DOUBLE PRECISION THX, THX1, THX2, THTS, THTS1,
     S THTS2
      INTEGER TIME, FINAL
C
      OPEN (1, FILE = 'X.TXF', STATUS = 'NEW')
      OPEN (2, FILE = 'TS.TXF', STATUS = 'NEW')
      OPEN (3, FILE = 'OUTPUT.TXF', STATUS = 'NEW')
C
      WRITE (*,*) 'FINAL TIME = ?'
      READ (*,*) FINAL
      WRITE (*,*) 'INTERVAL OF ITERATIONS = ?'
      READ (*,*) INT
C
      DO 10 TIME = 1, FINAL + 1, INT
         T = DBLE(TIME) - 1.
         A = DEXP(-.54061E-2 * T)
         B = 2 * DEXP(-.040916 * T)
         C = DCOS(.1153E-2 * T)
         D = DSIN(.1153E-2 * T)
         IF (TIME .EQ. 1) THEN
           TFX2 = -.84433 - 11.244 * A + B * (.14415 * C
     S           + 6.4395 * D)
           TFTS2 = .10612 - .05899 * A + B * (-.023565 *
C
     S             + .18572 * D)
           THX2 =  6.82728 - 9.0619 * A + B * (1.1173 *
C
     S             + 18.405 * D)
           THTS2 = .1419 - .047545 * A + B * (-.047177 *
C
     S             + .53493 * D)
         ELSE
          TFX1 = TFX2
```

```
            TFTS1 = TFTS2
            THX1 = THX2
            THTS1 = THTS2
            TFX2 = -.84433 - 11.244 * A + B * (.14415 * C
     S             + 6.4395 * D)
            TFTS2 = .10612 - .05899 * A + B * (-.023565 *
C
     S              + .18572 * D)
            THX2 =  6.82728 - 9.0619 * A + B * (1.1173 *
C
     S              + 18.405 * D)
            THTS2 = .1419 - .047545 * A + B * (-.047177 *
C
     S              + .53493 * D)
            TFX = TFX2 - TFX1
            TFTS = TFTS2 - TFTS1
            THX = THX2 - THX1
            THTS = THTS2 - THTS1
           ENDIF
          WRITE (1,100) THX, TFX
          WRITE (2,100) THTS, TFTS
          WRITE (3,110) T, THX2, TFX2, THTS2, TFTS2
  100     FORMAT (1X, 2(F15.10, 2X))
  110     FORMAT (1X, F10.3, 4(2X, F15.10))
   10   CONTINUE
       STOP
       END
```

```
      SUBROUTINE PLANT(T, XP, XPALG, XPDOT, DELTA,
     S DIST, UP, YP, DISTSS, UPSS, YPSS, NP, NPALG,
     S MDIS, MIP, MOP, ISAMPL)
C*********************************************************
C
C     THIS SUBROUTINE MUST BE LINKED TO CONSYD SIMULATION
C     PROGRAM SNTEG.  IT CALCULATES THE VALUES OF THE
C     DIFFERENTIAL EQUATIONS AND CALCULATES THE OUTLET
C     TEMPERATURE ALGEBRAICALLY.
C
C     THIS SUBROUTINE IS WRITTEN USING VAX FORTRAN.
C
C     WRITTEN BY JEFFREY J. PASHAK           OCTOBER 1988
C
C*********************************************************
      IMPLICIT REAL (A-H, O-Z)
      LOGICAL ISAMPL
      DIMENSION XP(3), XPALG(1), XPDOT(3), DELTA(4),
     S DIST(1), UP(3), YP(3), DISTSS(1), UPSS(3),
     S YPSS(3)
      COMMON/PLANT/ F, Z, Y, TI, V1, V2, V3
      DO 10 I = 1, MIP
        UP(I) = UP(I) + UPSS(I)
   10 CONTINUE
C
C     EQUATION FOR dT1/dt
C
      DELTA(1) = -XPDOT(1) + F / V1 * TI + Z / V1 *
     S  ZP(2) - XP(1) * (F + Z) / V1
C
C     EQUATION FOR dT2/dt
C
      DELTA(2) = -XPDOT(2) + Z / V2 * XP(1) + F / V2 *
     S  UP(1) * XP(3) - XP(2) * (Z + UP(1) * F) / V2
C
C     EQUATION FOR dTH/dt
C
      DELTA(3) = -XPDOT(3) + Y / V3 * UP(2) + F / V3 *
     S XP(1) - XP(3) * (F + Y) / V3
C
C     EQUATION FOR TEMPERATURE TF
C
      DELTAP = UP(1) * XP(2) + (1 - UP(1)) * XP(3)
C
C     OUTPUTS
C
      YP(1) = XP(3)
      YP(2) = DELTAP
C
      DO 20 I = 1, MIP
        UP(I) = UP(I) - UPSS(I)
```

```
   20  CONTINUE
       DO 30 I = 1, MOP
         YP(I) = YP(I) - YPSS(I)
   30  CONTINUE
       RETURN
       END
C
      SUBROUTINE PPAR(NP, MPALG, MDIS, MIP, MOP, ICPNAM)
C*********************************************************
C
C     THIS SUBROUTINE INTERACTIVELY CALLS FOR THE PROCESS
C     PARAMETERS WHEN LINKED TO THE CONSYD SIMULATION
C     PROGRAM SNTEG.
C
C     THIS SUBROUTINE IS WRITTEN USING VAX FORTRAN.
C
C     THIS SUBROUTINE ASKS FOR VARIABLES FOUND IN PROGRAM
C     DTXFCN OUTPUT FILE ODDBALL.NOW
C
C     WRITTEN BY JEFFREY J. PASHAK           OCTOBER 1988
C
C*********************************************************
      IMPLICIT REAL (A-H, O-Z)
      CHARACTER* (*) ICPNAM(8)
      COMMON/PLANT/F, Z, Y, TI, V1, V2, V3
C
      WRITE (*,*) 'FROM DTXFCN, F = ?'
      READ (*,*) F
      WRITE (*,*) 'FROM DTXFCN, Y = ?'
      READ (*,*) Y
      WRITE (*,*) 'FROM DTXFCN, Z = ?'
      READ (*,*) Z
      WRITE (*,*) 'TI = ?'
      READ (*,*) TI
      WRITE (*,*) 'V1 (AND V2) = ?'
      READ (*,*) V1
      V1 = V2
      WRITE (*,*) 'V3 = ?'
      READ (*,*) V3
C
C     VARIABLE NAMES
      ICPNAM(1) = 'TEMP T1'
      ICPNAM(2) = 'TEMP T2'
      ICPNAM(3) = 'TEMP TH'
      ICPNAM(4) = 'VALVE OP'
      ICPNAM(5) = 'TEMP TS'
      ICPNAM(6) = 'TEMP TH'
      ICPNAM(7) = 'TEMP TF'
C
      RETURN
      END
```

APPENDIX C - SAMPLE PROGRAM RUNS

SAMPLE RUN FOR PROGRAM DTXFCN

This run does not calculate the transfer functions for CONSYD nor does it calculate the system zeros. There are no corrections to be made to the values shown.

```
C:\THESIS>DTXFCN
CHANGES IN IMPUT MAY BE MADE AT THE END OF INPUT
SECTION IF YOU MAKE A MISTAKE.
TS(      .00000000000000), TF(      .00000000000000) = ?
200.
52.6
T1(      .00000000000000), TH(      .00000000000000) = ?
41.
58.5
DO YOU WANT TX FCNS FOR CONSYD? (Y/N)
N
DO YOU WANT TO CREATE THE SYSTEM ZEROS FILE? (Y/N)
N
TS     =    200.000000000000   TF    =    52.60000000000
T1     =     41.000000000000   TH    =    58.50000000000
V1, V2 =  4.0000000000000E-002 V3 = 1.0000000000000E-002
HT TX COEF 3 = 2800.0000  HT TX AREA 3 = 8.00000000E-002
FRAC FLOW TO PREHEAT EX = 5.000000000000E-001
DO YOU WANT TO CHANGE:
1)   TEMPERATURES TS, TF, T1, TH(AND THEREFORE TI)
2)   VOLUME 3 OR HEAT TRANSFER COEFFICIENT
3)   HEAT TRANSFER AREA 3
4)   VOLUME 1 (AND THEREFORE VOLUME 2)
5)   FRACTION OF FLOW TO HEAT EX1
6)   FIGURE TXFCNS FOR CONSYD(STRICTLY PROPER)
7)   DETERMINE SYSTEM ZEROS
8)   CONTINUE
8
V1, V2 =  4.0000000000000E-002 V3 = 1.0000000000000E-002
FRAC FLOW = 5.00000000000E-001 TOTAL FLOW = 4.32680E-004
HT EX1 (Z) = 4.4786212023E-004 HT EX3 (Y) = 5.35117E-005
INLET TEMP (TI)  =  35.1000000
TEMP OUT OF HT EX2 (T2) = 46.70000000
Stop - Program terminated.
```

SAMPLE RUN FOR PROGRAM DTHES2

The number of iterations is 2000 and since the print interval is 1 the final time is 2000. There is a step change in the flow fraction, X, of -0.2, therefore the new X value is 0.3. There is no change in the steam temperature.

```
C:\THESIS>DTHES2
T1, T2, TH = ?
41.0
46.7
58.5
INITIAL STEAM TEMP = ?
200.0
INITIAL VALVE OPENING = ?
0.5
FINAL TIME(NUMBER OF ITERATIONS) = ?
2000
USING WHAT PRINT INTERVAL?
1.
STEP CHANGE TO WHAT X VALUE?(FROM 5.000000E-001)
0.3
STEP CHANGE TO WHAT TS VALUE?(FROM   200.00000000)
200.
Stop - Program terminated.
```

APPENDIX D - HEAT EXCHANGER SIZING TEST

These equations are based upon the internal section of the bath type heat exchanger. These equations use a minimum distance between plates of 5 cm.

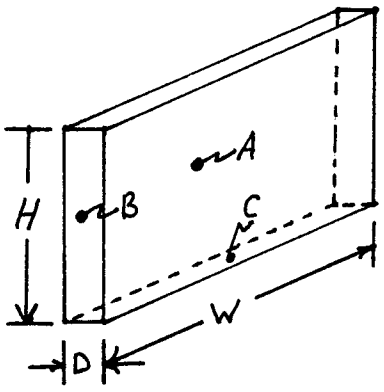

AREA A = HW
AREA B = HD
AREA C = WD

VOLUME = HWD

TOTAL AREA = 2A + 2B + C

Given D_{min} = 5 cm = 0.05 m,
W = 2H for maximum TOTAL AREA,

$$\text{MAX TOTAL AREA} = 4H^2 + 0.1H + 0.1H$$
$$= 4H^2 + 0.2H$$

Therefore,

$$4H^2 + 0.2H - \text{MAX TOTAL AREA} = 0$$

From this quadratic equation the solution for H is

$$H = \frac{-b \pm \sqrt{b^2 - 4ac}}{2a}$$

where

a = 4
b = 0.2
c = MAX TOTAL AREA (area from design specifications)

Substitute this H value into the following equation to yield the volume for this maximum heat transfer area, for the given D_{min}.

$$\text{VOLUME} = 0.1H^2$$

If the volume is smaller than the design volume, the value of D can be increased. Conversely, if the volume is larger than the design volume, the value of $D = D_{min}$ is too small. This creates an infeasible heat

exchanger, that is, a heat transfer area that is too large for the designed heat exchanger volume.